Characterization of nuclear segregation of RNA as a potential novel marker and regulation mechanism of quiescence in neural stem cell

Coum, Antoine

Awarding institution:
King's College London

CHARACTERIZATION OF NUCLEAR SEGREGATION OF RNA AS A POTENTIAL NOVEL MARKER AND REGULATION MECHANISM OF QUIESCENCE IN NEURAL STEM CELL

ANTOINE F. COUM

Institute of Psychiatry, Psychology and Neuroscience

King's College London

A thesis submitted for the degree of

Doctor of Philosophy

January 2019

ABSTRACT

Characterization of quiescent stem cells is a crucial step in manipulating quiescence in tissue regeneration and repair, and cancer treatment. Through the characterization of a *Drosophila melanogaster* mutant, I uncovered a potential novel regulation mechanism of neural stem cell quiescence. I observed that downregulation of Nucleoporins and karyopherins induces quiescence in *Drosophila melanogaster* neural stem cells. Nucleocytoplasmic transport components appeared altered *in vivo* in *Drosophila* neural stem cell and *in vitro* in a cell culture model of mouse adult hippocampal neural stem cell. I thus hypothesized that transport of particular cargo should be altered in quiescent neural stem cells, and demonstrated that polyadenylated RNA is segregated to the nucleus in quiescent neural stem cells in both models. I also started to characterize targets linked to this segregation mechanism, and showed that nuclear segregation of polyadenylated RNA occurred in mouse muscle satellite cells. Although much characterization of this novel mechanism in stem cell quiescence still has to be done, I offer a view of a potential novel regulator as well as a potential novel marker of quiescence.

ACKNOWLEDGEMENTS

To Rita Sousa-Nunes for the opportunity given. To François Guillemot, Noelia Urban, and Isabelle Blomfield for providing the mouse cell culture model and for their precious input.

Thank you to Rachel Shaw for her invaluable technical help and insight. Thank you to Andrea Chai for her support through the tedious times and for reading this thesis while caring for Sammy.

Thank you to Anthony Graham and Esther Bell for opening their door and guiding me through these last years.

Thank you to Darren Williams for reminding me that nothing matters in the end, leading me to pull through hard patches.

Thank you to Alina Miedzik for her relentless work and her eye opening honesty. Thanks to Andrea Borreguerro, Agnes Wong, and Hania Fiaz for taking over some experiments and for being so easy to manage.

Thank you to Rita Chaouni for her kindness and comforting words, even through her own hardships. Thank you to Sinzi Pop for her friendship and joyfulness, as well as for our failed campaign.

Merci à ma famille pour leur soutien inconditionel. Merci Gwen, Mamy et Pépère d'avoir été là pour moi, physiquement et mentalement. Merci Maman, Aurore et Amandine d'avoir été là malgré mes absences et la distance. Merci Papa pour tes conseils et ton amitié.

Enfin, merci Alix, sans qui je ne me serai lancé dans cette voie.

TABLE OF CONTENTS

TABLE OF FIGURES

TABLE OF TABLES

ABBREVIATIONS

Argonaute (Ago)

Adult hippocampal NSC (AHNSC)

A plasmid editor (ApE)

Protein basic local alignment search tool (BLASTp)

Bone morphogenic protein 4 (BMP4)

Bromodeoxyuridine (BrdU)

Cyclin dependent kinase (CDK)

Central nervous system (CNS)

Death caspase 1 (Dcp1)

DEAD-box helicase 6 (DDX6)

Deformed (dfd)

Dominant mutation (DM)

Deadpan (Dpn)

Drop (Dr)

Extensor digitorum longus (EDL)

5-ethynyl-2'-deoxyuridine (EdU)

Epidernal growth factor (EGF)

Extracellular-regulated kinase (ERK)

Fetal bovine serum (FBS)

Phenyl-glycine (FG)

Fibroblast growth factor (FGF)

Fluorescein-5-isothiocyanate (FITC)

Fluorescence loss in photobleaching (FLIP)

Forkhead box O3 (FoxO3)

Fluorescence recovery after photobleaching (FRAP)

Genomic DNA (gDNA)

Green fluorescent protein (GFP)

Gene ontology (GO)

Immunohistochemistry (IHC)

Inscuteable (Insc)

Kyoto Encyclopedia of Genes and Genomes (KEGG)

1st larval instar (L1)

2nd larval instar (L2)

3rd larval instar (L3)

Larval hatching (LH)

Mosaic analysis with a repressible cell marker (MARCM)

Miranda (Mira)

Muscle satellite cell (MSC)

Nuclear export signal (NES)

Nuclear factor 1 (Nfix)

Nuclear localization signal (NLS)

Nuclear pore complex (NPC)

Neural Stem Cell (NSC)

Nucleoporin (Nup)

Phosphate buffer saline (PBS)

Triton X-100 PBS (PBT)

Polymerase chain reaction (PCR)

Phosphohistone h3 (PH3)

Polyadenylated (polyA)

Pore membrane protein (Pom)

Ras-related nuclear protein (Ran)

Retinoblastoma (Rb)

RNA-binding protein fox (Rbfox)

Ribonucleic acid interference (RNAi)

Room temperature (RT)

Scutoid (Sco)

Small nuclear ribonucleoprotein (snRNP)

Snuportin 1 (Snupn)

Snorlax (Snx)

Simian virus 40 (SV40)

Tubby (Tb)

T-cell restricted intracellular antigen 1-related protein (TIAR)

Melting temperature (Tm)

Target of rapamycin (TOR)

Upstream activation sequence (UAS)

Unkempt (Unk)

Wheat germ agglutinin (WGA)

Wandering 3rd larval instar (WL3)

White prepupae (WPP)

Wild-type (WT)

Yellow fluorescent protein (YFP)

1 GENERAL INTRODUCTION

1.1 STEM CELLS UNDERGO PERIODS OF QUIESCENCE

Stem cells are defined as self-renewing cells that can give rise to a multitude of different cell types. Stem cells can be totipotent and differentiate into any type of cell in an organism; multipotent and differentiate into several types of cells in an organism; or unipotent and differentiate in a single cell type (Dottori & Pera, 2008; Smith, 2006). Regulated proliferation of stem cells is required for the growth, repair and homeostasis of tissues during development, as well as during adulthood where they replenish damaged or aging cells (Bergmann, Spalding, & Frisén, 2015; Eriksson et al., 1998; Götz, Nakafuku, & Petrik, 2016; Jin, 2016).

In the central nervous system (CNS), neural stem cells (NSCs) give rise to the variety of neurons, astrocytes, oligodendrocytes and ependymal cells mostly during development, but, importantly, also during adult stages in many species. In humans, adult NSCs contribute to the functional plasticity of the CNS by generating cells that impact tissue repair, cognition and mood (Jessberger, 2016; Kheirbek & Hen, 2011; Kriegstein & Alvarez-buylla, 2011; Spalding et al., 2013).

A common property of stem cells is the ability to enter a state of transient cell cycle arrest, called cellular quiescence or G0, which is controlled by both intrinsic regulatory mechanisms and extrinsic signals (Lin & Scott, 2012). Quiescence is defined as a reversible state, where cells exit the cell cycle in response to either growth inhibiting signals or absence of growth-promoting signals (Coller, Sang, & Roberts, 2006; Egger, Chell, & Brand, 2008; Valcourt et al., 2012). Cellular

quiescence was originally characterized by a G1 DNA content, an altered cellular metabolism, and distinct morphological changes such as decreased cell size and increased nucleus to cytoplasm ratio (Laporte et al., 2011; Lemons et al., 2010), and

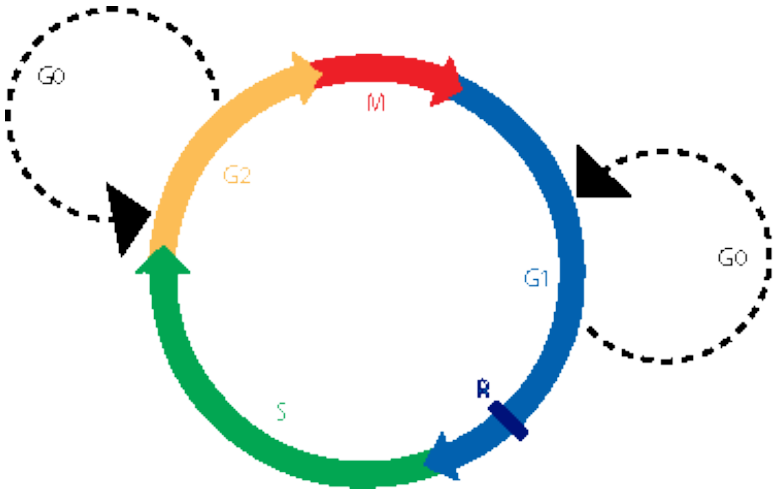

G0 was considered by some as a prolonged G1 phase in slow-cycling cells (Patt & Quastler, 1963) (Figure 1.1).

FIGURE 1.1. SCHEMATIC PRESENTATION OF THE CELL-CYCLE AND QUIESCENT STATES.

Quiescence has recently been described as a non-homogeneous state, as cells remain quiescent for longer durations they enter a deeper state of quiescent and become less sensitive to growth signals. Quiescence depth is regulated by Retinoblastoma (Rb)-E2F, as a higher level of Rb-E2F leads to a deeper quiescent state and a slower re-entry in the cell-cycle in quiescent SCs (Kwon et al., 2017). More recently, *Drosophila melanogaster* NSCs have been described as being arrested in either G1 or G2, the G2 NSCs appearing to re-enter the cell cycle faster than the ones arrested in G1 (Otsuki & Brand, 2018). Reversibility of the quiescent state is the principal difference with permanent irreversible growth arrest states of terminally differentiated or senescent cells (Sang, Coller, & Roberts, 2008; Subramaniam et al., 2013).

Adult NSCs spend the majority of their time in quiescence, one of the reasons it took a long time to identify them in mammals (Conover & Notti, 2008). Several studies support the notion that quiescence is important for preventing stem cell exhaustion (Furutachi, Matsumoto, Nakayama, & Gotoh, 2013; Nakamura-Ishizu, Takizawa, & Suda, 2014; O'Farrell, 2011) as disrupting the balance between quiescent and activated NSCs leads to a premature depletion or silencing of long-lasting NSCs (Codega et al., 2014; Encinas et al., 2011; Furutachi et al., 2013; Hsieh, 2012).

Quiescence also contributes to the resistance of cancer cells to chemotherapy and radiotherapy, which usually target proliferating cells (L. Li & Bhatia, 2011; Saito et al., 2010; Vidal, Rodriguez-Bravo, Galsky, Cordon-Cardo, & Domingo-Domenech, 2014). Awakening of these dormant cells can lead to tumour relapse following treatment, hence detection of quiescent cells in tumour resections may be of diagnostic and prognostic value (Kreso & Dick, 2014; Meacham & Morrison, 2013).

Altogether, understanding quiescence regulation should benefit regenerative therapies, neuropsychiatric interventions and cancer treatments (Wells, Griffith, Wells, & Taylor, 2013). To this day, no molecular marker has been uncovered for quiescence. This state is characterized by a low metabolic rate (Laporte et al., 2011; Valcourt et al., 2012), low RNA content (Fukada et al., 2007a), low transcription rate (Pearce & Pearce, 2013) and lack of proliferation markers (Gerdes, Schwab, Lemke, & Stein, 1983). Hence, quiescent cells have traditionally been identified by the absence of markers associated with proliferation. Identification relies on functional assays such as failure to incorporate or retain nucleotide analogs such as bromodeoxyuridine (BrdU) or 5-ethynyl-2'-deoxyuridine (EdU) (Venezia et al., 2004); or through endogenous proliferation markers such as proliferating cell nuclear antigen (a DNA polymerase accessory protein which is expressed in S-phase), Ki67 (a protein associated with ribosomal RNA transcription expressed in all phases

except G0), minichromosomemaintenance-2 (a protein that functions in replication origins and expressed in S phase), and phosphohistone H3 (PH3, an M-phase-specific histone modification) (Iatropoulos & Williams, 1996; Whitfield, George, Grant, & Perou, 2006). Hence, a concerted understanding of what is common and distinctive about quiescence of different stem cell types remains lacking. The topic has gained momentum in recent years and a few pathways have been implicated in the regulation of quiescence.

1.2 Stem Cell quiescence is actively regulated

Initially seen as a dormant state with very low basal activity, recent advances in adult stem cell quiescence studies revealed insights suggesting quiescence is an actively maintained state. Molecularly, quiescent SCs present altered expression of cell cycle regulatory genes: downregulation of positive regulators of cell proliferation such as cyclins and cyclin dependent kinases (CDKs); and upregulation of negative regulators of cell cycle such as CDK inhibitors (Cheung & Rando, 2013; Fukada et al., 2007a; Ladha, Lee, Upton, Reed, & Ewen, 1998). Quiescent cells display unique expression profiles, including upregulated genes involved in transcriptional regulation and stem cell fate decisions such as forkhead box O3 (FoxO3) (Gopinath, Webb, Brunet, & Rando, 2014; Kops et al., 2002); as well as downregulated genes involved in DNA replication and cell cycle progression such as cyclins (Blanpain, Lowry, Geoghegan, Polak, & Fuchs, 2004; Forsberg et al., 2010; Fukada et al., 2007), demonstrating that this is an actively maintained state (Cheung & Rando, 2013). Several signaling pathways appear involved in a perfectly balanced 'dormant' state allowing fast reactivation. p53, regulator of several cellular processes involved in genome integrity, plays an important role in quiescence regulation (Itahana et al., 2002; McConnell et al., 2016); similarly, the tumour suppressor RB, involved in cell

cycle progression inhibition, triggers over-proliferation of SCs when downregulated (Hosoyama, Nishijo, Prajapati, Li, & Keller, 2011; Jacques et al., 2010). At the cell autonomous level, the Target of Rapamycin (TOR) pathway is emerging as a possible common feature of quiescence regulation in all eukaryotic cells, from yeast to invertebrate and mammalian NSCs (Paliouras et al., 2012; Sousa-Nunes, Yee, & Gould, 2011a; Yanagida, 2009). Downstream of TOR, components of the forkhead transcription factor family play a prominent role in regulation of NSC quiescence from flies to rodents as FoxO-deficient mice show initial increased brain size and proliferation of NSCs during early postnatal life, followed by precocious significant decline in the NSC pool and accompanying neurogenesis in adult brains (Paik et al., 2009; Sousa-Nunes et al., 2011a). In adult zebrafish and rodent NSCs as well as in mammalian muscle cells, cell fate is determined by the levels of Notch activity, and quiescence is promoted by high Notch activity (Bjornson et al., 2012; Chapouton et al., 2010). In muscle, another potentially key quiescence regulator is a member of the extracellular-regulated kinase (ERK) family (Ebisuya, Kondoh, & Nishida, 2005). The Salvador/Hippo/Warts signaling maintains the quiescent state of *Drosophila* NSCs (Ding, Weynans, Bossing, Barros, & Berger, 2016) and implication of this pathway in regulation of quiescence had previously been shown for mouse liver and skin (Mira et al., 2010; Y. Sun, Hu, Zhou, Pollard, & Smith, 2011). Replacing the mitogen epidermal growth factor (EGF) with BMP4 in the culture medium of a mouse NSC model induced characteristic features of quiescent cells (Martynoga et al., 2013). Through this model of quiescent NSCs they were able to identify active enhancers in quiescent and proliferating NSCs and predicted a major role for the nuclear factor one (Nfix) family in the gene regulatory network controlling NSC quiescence (Martynoga et al., 2013).

1.3 *Drosophila* NSCs as a model for quiescence regulation

Drosophila NSCs have played a major role in our understanding of fundamental principles and mechanisms of neurogenesis, including asymmetric cell division (Betschinger & Knoblich, 2004; Januschke & Gonzalez, 2008; Sousa-Nunes, Cheng, & Gould, 2010) and tumour formation(Egger et al., 2008; Jennings, 2011; Potter, Turenchalk, & Xu, 2000). *Drosophila* presents the advantages of having a clear spatiotemporal segregation between cycling and quiescent NSCs, and a conveniently short transition time between these states during development (Fernández-Hernández, Rhiner, & Moreno, 2013) (Figure 1.2). *Drosophila* NSCs undergo quiescence during a period of about 24 hours that intervenes between embryonic and postembryonic neurogenesis (Truman & Bate, 1988).

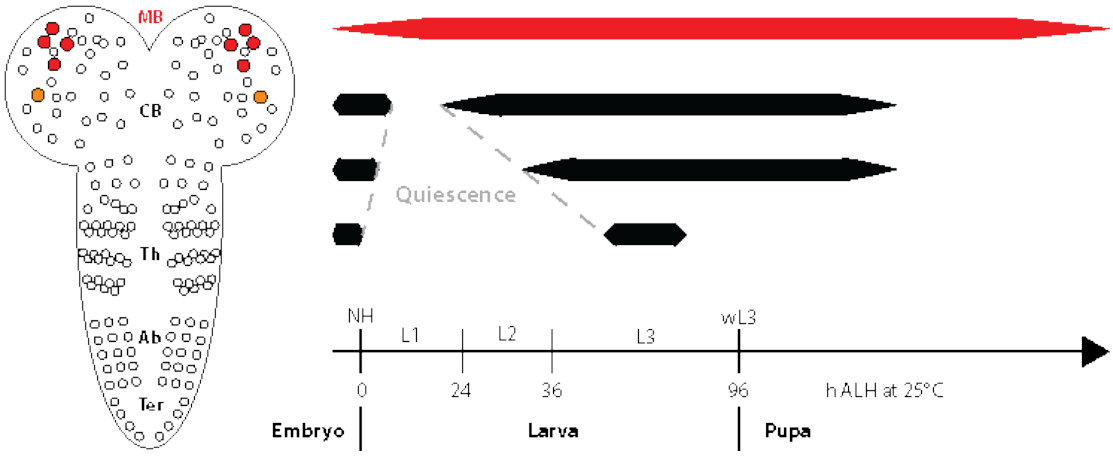

Figure 1.2. *Drosophila* NSCs undergo quiescence in a stereotypical spatiotemporal pattern during development.

Schematic representation of a larval CNS, in which circles represent NSCs. MB: Mushroom Body; CB: Central Brain; Th: Thoracic, Ab: Abdominal, Ter: Terminal neuromeres; NH: newly hatched larval stage, L1: first instar larval stage, L2: second instar larval stage, L3: third instar larval stage, wL3: wandering phase of third instar; ALH: after larval hatching. Red and black lines represent proliferating state. MBs

never enter quiescence (red), whilst all other NSCs enter and exit quiescence in a specific spatiotemporal pattern. Adapted from (Truman & Bate, 1988).

In *Drosophila*, quiescent NSCs present a cellular extension, hereafter referred as "fiber". This morphology is characteristic of their quiescent state (Ding et al., 2016) since NSCs actively cycling or blocked in the cell cycle by numerous mutations do not present it. Therefore, whilst studying its function is beyond the scope of this project, the presence of a fiber indicates *Drosophila* NSC quiescence. Intriguingly, the morphology of *Drosophila* quiescent NSCs is reminiscent of that of adult mammalian NSCs (Kriegstein & Alvarez-buylla, 2011) and for these a correlation between radial fiber length and proliferation has been observed, longer fibers correlating with quiescence (Suh et al., 2007).

1.4 HYPOTHESES AND AIMS

In this project, we are employing *Drosophila melanogaster* in parallel with a mammalian NSC model of quiescence to test the following hypotheses:

- Nucleocytoplasmic transport is altered in quiescent versus active NSCs.
- This alteration is mediated by a different nuclear pore complex (NPC) and/or transportin composition.
- Distinct nuclear pore composition and transport play a causal role in regulating the active versus quiescent state of NSCs.
- Causality is mediated by differential nuclear permeability between the 2 states leading to compartmentalization of cargo.
- The novel mechanism of NSC quiescence regulation by nuclear permeability is evolutionarily conserved in mammals.

Towards testing the above hypotheses, the specific objectives of this project are:

- To determine Nucleoporin (Nup) expression profiles in quiescent versus active NSCs.
- To establish causality between Nup levels and NSC quiescence.
- To establish causality between karyopherins levels and NSC quiescence.
- To uncover potential correlation between Nups, karyopherins and previously uncovered regulators of NSCs quiescence.
- To assess nuclear permeability in quiescent versus active NSCs.
- To identify altered compartmentalization of cargo during quiescence.
- To confirm results in different mammalian models.

2 MATERIALS AND METHODS

2.1 *DROSOPHILA* REARING

All *Drosophila* stocks used through this thesis are listed in (Appendix Table 1).

2.1.1 DROSOPHILA HUSBANDRY

Drosophila were raised on our standard R1 medium (8 % (m/v) glucose, 2 % (m/v) cornmeal, 5 % (m/v) Brewer's yeast, 0.8 % (m/v) agar, 2 % (v/v) ethanol, 0.24 % (v/v) methyl-4-hydroxybenzoate, 0.37 % (v/v) propionic acid). Stocks were kept at 18 °C or room temperature (RT; which in our laboratory was 22 °C). Virgin female collection was performed as described in Greenspan 2004.

For timed larval collections crosses were set-up in cages with grapefruit juice plates (25 % (v/v) grape-juice, 1.25 % (m/v) sucrose, 2.5 % (m/v) agar in water) supplemented with yeast paste, which were changed daily. Other crosses were set-up on standard cornmeal medium supplemented with dry live yeast.

2.1.2 DROSOPHILA STAGING

Drosophila melanogaster has four distinct stages of its lifecycle: embryo, larvae, pupae and adult. At 25 °C embryogenesis lasts for ~24 h after which the larva hatches. Larval development can be subdivided in 3 stages, separated by two moults: first instar (L1), second instar (L2) lasting for ~24 h each, and third instar (L3) lasting for ~48 h at 25 °C in our food. During the final ~8 h L3 larvae start leaving the food in preparation for pupariation; this is referred to as the wandering L3 (WL3) stage. Finally, the larva immobilizes and becomes white pre-pupae (WPP) for ~20 min before developing into a pupae. The pupal stage lasts ~96 h at 25 °C before eclosion of the adult.

Larvae can be staged through morphological changes they undertake after larval hatching (LH), namely in their tracheal system and mouth hooks (Park, Filippov, Gill,

& Adams, 2002). One clear distinction between L1 and L2 is due to the inflation of the dorsal longitudinal trunks, the major tracheal vessels, visible as lines or tubes, respectively, at each of these stages. L2 and L3 were distinguished by a thickening and branching of the anterior spiracles at L3 and WL3 was identified by the wandering behaviour.

2.1.3 Timed larval collection

Adult *Drosophila* crosses were setup at room temperature in cages onto which new plates were transferred onto every 24 h with fresh yeast paste. The old plate was cleared of yeast paste and all hatched larvae and placed at 25 °C or 29 °C for a set time. Larvae were then picked and dissected.

2.2 Mosaic analysis with a repressible cell marker

CNS clones were generated by mosaic analysis with a repressible cell marker (MARCM) (Slack, Somers, Sousa-Nunes, Chia, & Overton, 2006). Unless otherwise stated the parental F0 generation was allowed to lay for 24h at 25 °C, their first generation progeny F1 larvae were heat-shocked at 37 °C for 20 min to 1 h and 30 min depending on experimental needs 48 and 72 h after larval hatching. Larvae were then reared until dissection at 25 °C unless otherwise stated.

2.3 Gal4/UAS system

The Gal4/UAS system is a binary expression system primarily used in *Drosophila*, although it has also been applied to mice and zebrafish. In one construct, a cell-specific promoter drives the expression of the gene encoding Gal4, a transcription factor normally expressed in yeast. In a second construct, a transgene of interest is regulated by a promoter sequence called an upstream activation sequence (UAS). The Gal4 protein binds to the UAS sequence and efficiently drives expression of the transgene. Thus, the transgene will only express in cells defined by the promoter regulating Gal4 (Brand & Perrimon, 1993). For simplicity and following convention,

enhancer-GAL4, UAS-X expression will be referred to as enhancer>X. GAL4 activity is optimal at 30°C and reduced at lower temperature (Wilder, 2000). Additionally, Gal4/UAS can also be used in combination with another yeast protein, Gal80. The Gal80 protein binds to and inhibits the activity of Gal4. Thus, a second promoter element can drive expression of Gal80 to further restrict the cells expressing the transgene. Furthermore, Gal80 can be made temperature sensitive: the Gal80ts protein is active at 19 °C but not 30 °C. Therefore, it is possible to express a transgene in specific cells using the Gal4/UAS system and to regulate the timing of transgene expression by controlling the temperature, and thus the expression of Gal80ts.

As an example, Ribonucleic Acid interference (RNAi) was carried out in *Drosophila* NSCs using the GAL4/UAS system where GAL4 was driven by nab, a NSC specific driver. RNAi experiments included UAS-Dcr2, known to promote efficiency (Q. Liu et al., 2013). Unless otherwise stated, RNAi crosses were set up at 25°C and the F0 was transferred to new vials daily. F1 was transferred to the desired temperature until dissected.

2.4 *DROSOPHILA* GENETICS

2.4.1 STOCK GENOTYPING AND REBALANCING

Stocks carrying lethal mutations were maintained with so-called balancer chromosomes, which prevent recombination (Greenspan 2004). Balancers also carry dominant mutations (DM) that allow chromosome tracking in adults. Since balancer dominant markers may not be suitable for genotyping at all stages, strains with lethal mutations were rebalanced with a newer generation of balancers marked with Yellow Fluorescent Protein (YFP) under the control of the deformed (dfd) enhancer. To rebalance a mutation on the second chromosome, flies were crossed with Scutoid (Sco)/CyO,dfd-YFP, and when rebalancing a lethal mutation on the third

chromosome with Drop (Dr)/TM6B,Sb,dfd-YFP. Male and virgin progeny carrying the desired balancer were selected to generate rebalanced stocks. In addition to YFP, L3 animals balanced on chromosome III could also be genotyped by the presence or absence of the marker Tubby (Tb), carried by the TM6B balancer, and which is characterized by shorter and stockier animals.

2.4.2 GENERATION OF RECOMBINANT STOCKS

In *Drosophila*, meiotic recombination only occurs in females (Greenspan, 2004). The following crossing scheme was used to generate a stock with multiple components of interest on the same chromosome ('F' refers to generation):

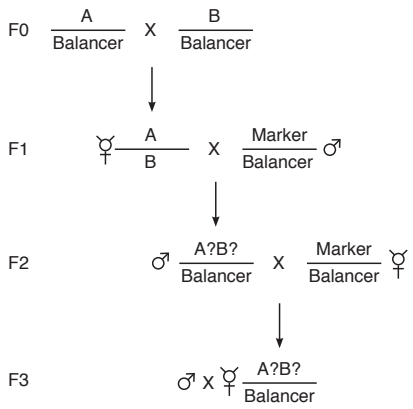

For the II chromosome, the Marker/Balancer stock used was Sco/CyO,dfd-YFP. For the III chromosome, the Marker/Balancer stock used was Drop/Tm6B,Tb,Sb,dfd-YFP. Tests were then performed to determine the presence of the component of interest.

2.4.3 GENERATION OF COMPOUND STOCKS ON II;III CHROMOSOMES

The following crossing schemes were used to generate a stock with multiple components of interest on separate chromosomes (if multiple generations required setting up in parallel then they are indicated by multiple crosses of the same generation):

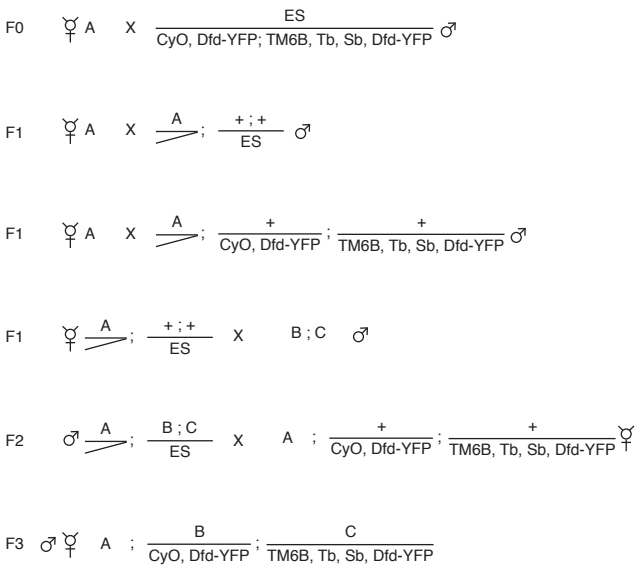

2.5 LARVAL BRAIN DISSECTIONS

Dissections were performed in phosphate-buffered saline (PBS) or DEPC-treated PBS accordingly to experimental needs. L1 and L2 dissections were performed using forceps (no. 5) and tunsgten needles (0.5 mm diameter tungsten wire from Goodfellow Cambridge Ltd. bent to be held in 1 ml syringe and 5G needle holders, wire was electrolytically sharpened with a 3-12 V AC current passing through 2M NaOH). CNSs were immobilized on poly-L-lysine coated slides for all further steps; L3 larvae were dissected using forceps only and placed in 1.5 mL eppendorf tubes for all further steps.

2.6 POLY-L-LYSINE SLIDES PREPARATION

Poly-L-Lysine slides were made in house. Slides with ground edges (Fisher Scientific, 12383118) were incubated for 10 min at RT in 5 g/L poly-L-Lysine hydro-bromide (Sigma, P1524) with 0.0025 % Professional Photo-Flo concentrate (Kodak, 153-879W). Slides were then dried for 10 minutes at 60 ºC. Incubation/drying cycle was repeated 4 times before leaving the slides to further dry at RT for 2 hours.

2.7 IMMUNOHISTOCHEMISTRY (IHC)

2.7.1 ANTIBODY STAINS

CNSs were immediately fixed in freshly prepared methanol-free 4 % (v/v) formaldehyde (Thermo Scientific, 28908) in PBS for 15 min at RT (L1 and L2 CNSs were dissected and placed on poly-L-lysine coated slides immediately, whilst L3 CNSs were fixed and stained in 1.5 ml microcentrifuge tubes). Once fixed, the tissues were rinsed once in PBS then washed 4x15 min with 0.1 % (v/v) Triton-X in PBS (PBT), blocked in normal goat serum 5 % (v/v) in 0.1 % PBT for at least 1hour at RT (or overnight at 4 °C) and incubated in primary antibody in blocking solution overnight at 4 °C. Tissues were then washed 4x20 min with 0.1 % (v/v) PBT, followed by incubation with secondary antibody diluted in blocking solution for 2 h at RT. Samples were then incubated with DAPI (Sigma, D9542) diluted 1:10^4 in PBS for 15 min if needed. Finally, samples were washed 4x20 min with PBT at RT and mounted in Vectashield (Vector laboratories, H-1000).

Table 2.1. Primary antibodies for *Drosophila.*

Target	Species	Source	Reference	Dilution
Miranda	Mouse	F. Matzusaki		1:50
Deadpan	Guinea Pig	J. Skeath		1:1000
Deadpan	Guinea Pig	R. Sousa-Nunes	Shaw et al. 2018	1:5000
Deadpan	Rat	S. Thor		1:200
Snorlax (CG14712)	Guinea Pig	R. Sousa-Nunes	CSI 1.9	1:100
Snorlax (CG14712)	Guinea Pig	R. Sousa-Nunes	CGT 1.7	1:100
GFP	Rabbit	Life Technologies	A-11122	1:1000
GFP	Chick	Life Technologies	A10262	1:1000
GFP	Mouse	Life Technologies	A-11120	1:1000
Elav	Rat	DHSB	7E8A10	1:100
PhosphoHistone H3	Rabbit	Upstate	06-570	1:400
Nup50	Guinea			1:50
Nup62	Mouse			1:100
Nup98	Rabbit			1:1000
Nup358	Mouse	Abcam	MAB414	1:500
Unk	Rat	J. Bateman	-	1:500
Lamin	Mouse	DHSB	ADL195	1:1000
WGA	-	Biotum	29027-1	1:1000
Elav	Rat	DHSB	7E8A10	1:100

2.7.2 5-ethynyl-2'-deoxyuridine (EdU) incorporation and staining

EdU is a Thymidine analogue, used to label replicating DNA. CNSs were dissected in PBS and transferred immediately into fresh 10 mM EdU (Click-iT EdU Imaging Kit, Life Technologies, C10337) diluted in PBS for 2 h, fixed with 4 % Formaldehyde in PBS for 15 min then permeabilised for 20 min with 0.1 % PBT. EdU was developed in colour reaction buffer according to manufacturer's instructions followed by addition of Alexa Fluor Azide colour reaction mix according to the manufacturer's instructions, after which samples were washed 4x30 min in 0.1 % PBT at RT.

If EdU staining was combined with IHC, samples were incubated with primary and secondary antibodies after the fixing step and fixed again before the colour reaction.

2.7.3 In situ hybridization

All buffers were made from DEPC-treated water. Brains or cells were fixed in methanol-free 4 % formaldehyde in DEPC-PBS pH 7.4 for 15 min, incubated in cold methanol for 10 min and rehydrated in 70 % ethanol in DEPC-treated PBS for 10 min minimum. Samples were incubated in 1 M Tris PH 8.0 for 5 min before hybridization with Cy3-Oligo-dT(50) (Genelink, 26-4322-02) in hybridization buffer (2xSSC (0.3 M NaCl, 0.03 M sodium citrate, pH 7.0), 1 mg/ml Yeast tRNA, 0.005 % BSA, 10 % dextran sulfate, 25 % formamide deionized) accordingly to experimental needs. When needed, samples were incubated in 2xSSC with 0.1 % Triton X-100 with antibodies or DAPI.

2.8 Mouse cell culture

2.8.1 Mouse Adult Hippocampal Neural Stem Cells (AHNSCs) culture

AHNSCs were generated in the laboratory of François Guillemot (Urbán et al., 2017). Cells were cultured in DMEM/F-12 medium (Gibco, 11320-033) supplemented with N-2 max (R&D Systems, AR009), 5 % Penicillin/Streptomycin (Sigma, P4333), 5 % L-Glutamine (Sigma, G7513), 10 ng/ml EGF (Peprotech, 315-09), 10 ng/ml FGF

(Peprotech, 450-33), 10 ng/ml Heparin (Fischer Scientific Ltd, 10429693). Flasks were coated with 10 μg/ml Laminin (Sigma, L2020) for 30 min at 37 °C prior to seeding. Cells were passaged twice a week using Acutase (Sigma, A6964) before they reached 80 % confluency.

Quiescence was induced by replacing EGF with BMP4 (R&D Systems, 5020-BP-010) in culture media. Cells reached quiescence after 72 hours (Urbán et al., 2017). Cells were counted with a Malassez cell counter (VWR, 631-0975).

2.8.2 Mouse Muscle Satellite Cells (MSCs) culture

Culture of single fibers was performed according to previously described strategies (Moyle & Zammit, 2014). Briefly, dissected extensor digitorum longus (EDL) muscles were digested in a filtered solution of 0.2 % collagenase (Sigma-Aldrich, C0130) in DMEM High Glucose (1 %) L-Glutamine (1 %) Penicillin/Streptomycin (Life Technologies, 11965092) (isolation medium). After 2 h of connective tissue digestion, EDLs were mechanically dissociated fiber by fiber. Quiescent satellite cells on the isolated myofibers were activated by a solution of 10 % horse serum (0.5 %) chicken embryo extract in filtered isolation medium. Contracted fibers were removed.

2.8.3 Immunohistochemistry

AHNSCs were seeded at 105 cells/ml on Laminin (Sigma, L2020)-coated round coverslips inserted into 24-well plates. Cells were left to attach for 24 hours before any further procedures. Cells were fixed in 4 % methanol-free formaldehyde for 10 min, rinsed in PBS then washed twice in 0.1 % (w/v) PBT. Stainings were carried out as above but cells were mounted in Aqua PolyMount (Polysciences Inc, 18606-20).

Table 2.2. Primary antibodies for mouse cells.

Target	Species	Source	Reference	Dilution
Ran	Rabbit	Novus	NB100-91945	1:200
Nup188	Rabbit	Novus	NBP1-28717	1:1000
Nup53	Rabbit	Novus	NB100-93322	1:2000
TPR	Rabbit	Novus	NB100-2867	1:2000
Nup98	Rabbit	Novus	NBP1-58188	1:500
Nup37	Rabbit	Novus	NBP1-74146	1:1000
Sec13	Rabbit	Novus	NBP2-20278	1:500
Rae1	Rabbit	Novus	NBP1-57186	1:200
TMEM48	Rabbit	Novus	NBP1-91603	1:1000
Nup p62	Rabbit	Novus	NBP1-31381	1:1000
Nup50	Rabbit	Novus	NBP2-19610	1:1000
Nup160	Rabbit	Novus	NBP1-76928	1:500
Nup88	Rabbit	Novus	NBP1-31796	1:200
Nupl2	Rabbit	Novus	NBP2-31666	1:500
HIV-1 Rev binding	Rabbit	Novus	NBP1-91991	1:500
Agfg2	Rabbit	Novus	NBP1-83213	1:2000
Nup54	Rabbit	Novus	NBP1-85899	1:1000
Nupl1	Rabbit	Novus	NBP2-13684	1:100
Nup153	Rabbit	Novus	NBP1-81725	1:1000
AAAS	Rabbit	Novus	NBP1-89424	1:500
Seh1l	Rabbit	Novus	NBP1-80773	1:1000
Nup43	Rabbit	Novus	NBP1-88792	1:500
Lamin C	Mouse	Novus	NBP1-50051	1:200
Nup133	Mouse	Novus	H00055746-	1:500
Nup53	Rabbit	Novus	NBP2-24637	1:2000
Nup205	Rabbit	Novus	NBP1-91247	1:1000
RanBP2/Nup358	Mouse	Novus	NB100-74480	1:500
Nup210	Rabbit	Novus	NB100-93336	1:500
RanGAP1	Goat	Novus	NB100-1384	1:1000
Nestin	Rat	Millipore	MAB353	1:200
Ki67	Mouse	BD Bioscience	550609	1:100
Rbfox1	Rabbit	Abcam	AB154490	1:1000
Rbfox1	Guinea	M. Busczock	-	1:5000
Rbfox3	Mouse	Chemicon	MAB8377	1:500
TIAR	Mouse	BD Bioscience	610350	1:200
DDX6	Rabbit	Genetex	GTX102795	1:1000
Unk	Rabbit	Atlas	HPA027962	1:500

Other immunohistochemistry stains (EdU and in situ PolydT) were carried out as specified in 2.7.

Myofibers were fixed in 4% paraformaldehyde for 10 min, treated with 0.5% triton and blocked in 10% Fetal Bovine Serum (FBS). Primary antibodies used are the following: Pax7 (Rabbit, Abcam, MAB1675, 1:200) and Caveolin-1 (Mouse, Abcam, ab17052, 1:100). Nuclei were counterstained with DAPI.

2.8.4 Cell loading with fluorescein-5-isothiocyanate (FITC) conjugated dextrans

Cells were incubated with freshly prepared permeabilization buffer (20 mM HEPES, pH 7.4, 10 mM EGTA, 140 mM KCl, 50 µg/mL saponin (Sigma 47036), 5 mM NaN3, and 5 mM oxalic acid dipotassium salt) for 20 min. The cells were then incubated for 30 min with 20 µg/ml 8 kDa, 20 kDa, 40 kDa or 70 kDa FITC-Dextrans (Sigma, FD8S, FD20S, FD40S and FD70S) diluted in fresh medium. Dextran-containing medium was then aspirated and cells were washed twice with ice-cold PBS before fixation with 4 % methanol-free formaldehyde.

2.9 Molecular biology

2.9.1 Genomic DNA (gDNA) preparation

30 flies of the desired genotype were collected into a microcentrifuge tube and frozen for at least 30 minutes then grinded using pellet pestles (Sigma, Z359947) in 200µl of Buffer A (100mM Tris-HCl (pH 7.5), 100mM EDTA, 100mM NaCl, 0.5% SDS). A further 200µl of Buffer A was added and maceration was carried out until only cuticles remained. Samples were then treated with 10µl of Proteinase K (10mg/ml) and incubated at 55°C for 1 hour, the enzyme was then inactivated by an incubation at 95°C for 1 minute. The mixture was next incubated at 65°C for 30 minutes before RNA, proteins and polysaccharides were precipitated with 800µl of LiCl/KAc solution (286µl of 6M LiCl an 114µl of 5M KAc) and incubation of 10 mintues on ice. Samples were then centrifuged for 15 minutes at 13000rpm, supernatants were transferred into new microcentrifuge tubes and 600µl of isopropanol were added to precipitate DNA. Samples were mixed by inverting the tubes and centrifuged for 15 minutes at

13000rpm. Supernatants were aspirated and discarded, and tubes were centrifuged for further 2 minutes to remove the remaining supernatant. Pellets were washed from residual salt with 1 ml of 70 %(v/v) ethanol and centrifugation for 10 minutes at 13000rpm. Subsequently, the supernatants were removed and the pelleted DNA was air dried. Finally, the pellets were resuspended in 150µl of TE buffer (10 mM Tris-HCl, 0.1 mM EDTA (pH 8.0), Sigma, 93283). DNA samples were stored at -20 °C.

2.9.2 PRIMER DESIGN

Primers were designed using A Plasmid Editor (ApE) with the following characteristics: length of 18-24 nucleotides, melting temperature (Tm) between 55 and 65 °C, GC content between 50 and 70 %. Annealing temperature was deifined to be 5 °C below Tm. Designed primers were analyzed using OligoAnalyzer 3.1 (Integrated DNA Technologies) for more accurate characteristics predictions, homo and heterodimer and hairpin fornation. Primers were BLASTed (NCBI) to assess their specificity. Primers utilized in this study were generated by Eurofins Genomics.

Table 2.3. Primer list.

Sequence	Length (bp)	Tm (°C)	GC%
2V327			
ACACGTCTGCCCGAAACTTCC	21	61	57
CTGGCCGCCGGACGATTGT	19	64	68
GCAGCATGGAGCGTCGTCG	19	62	68
GATTGCTGGCGGACATGCTGC	21	63	62
CTCTGCCACATCGTCCAGTACC	22	60	59
CACGCTTCTAGTTGGCTCGCTC	22	61	59
GTGCCAAAGACCACCGAACAGG	22	62	59
GACGTTTGGCTACCTGCTCCG	21	61	62
CTTTGTCGGCTGCTTCTCCTGC	22	62	59
GAATGGCAGGAGCCGAAATGGC	22	63	59
ATGCCCGTCGTGACTGTGG	19	61	63
GGTGGACGTAACGGTCGTAGT	21	60	57
ACGCTTCCTACTCCCGTCAAAC	22	60	55
GTGGGACCATTGGCAGGC	18	60	67
CACAGCAGCACCATCATTCTCG	22	60	55
GCAGCGGGCTGAGTGGTG	18	62	72
CCGACAACAAATGGCAGCGATG	22	61	55
GCTGCTGCTCCTCCGAATGC	20	62	65
AAAGGCAGCGGAACCAGCTC	20	62	60
GATGCTGGAGATGCTGACGGT	21	61	57
CAACGCAACAGTCTTCGACACC	22	60	55
CTGCTGGAGCACCGAATCCG	20	61	65
AAGGAGGACTCAGCAAGCACC	21	61	57
GGTTGGATTGCTTGCTGGCG	20	61	60
CGCCGCCCAGCAATCAGG	18	63	72
CGCGGTGATTAAAGGAGGGCAG	22	62	59
3' UTR UAS-CG14712			
CCCACACCGGAGAGTCGTC	19	60	68
CCCTCACAAACACACATCCACG	22	60	54

2.9.3 Polymerase chain reaction (PCR) and sequencing

Fragment amplification was performed by PCR using Fast Start High Fidelity PCR System, dNTPack (Roche, 11581295001). Each PCR reaction was prepared according to manufacturer's indications. Samples underwent an initial denaturation (5 minutes at 95 °C), followed by 30 cycles of: denaturation (30 seconds at 95 °C), annealing (30 seconds at a primer specific temperature), extension (1 minute per 1000 base pairs fragment at 72 °C), and then a final extension (5 minutes at 72 °C).

Products were electrophoresed using TAE (40 mM Tris, 20mM acetic acid, 1 mM EDTA) as a running buffer. Samples were run in a 1 % (m/v) agarose gel with GelRed (Cambridge Bioscience, BT41003) DNA stain at 1/100,000 in TAE. Fragments were purified using the QIAquick PCR Purification Kit (Qiagen).

DNA concentration was determined by optical density on a Nanodrop2000 (ThermoScientifica) and sequencing was outsourced to Eurofins Genomics.

2.9.4 PROTEIN EXTRACTION

Media was aspirated from confluent AHNSCs and cells were washed twice with ice cold PBS. Cells were then incubated with RIPA buffer (Sigma, R0278) on ice for 5 minutes. Cells were then scraped from the flask using a plastic cell scraper (Fisher Scientific, 11597692) and collected in a tube. Contents of the tube were agitated at 4 °C for 30 minutes then centrifuged at 16,000 G for 15 minutes. Supernatant was collected to be used straight away or frozen.

Protein extraction from *Drosophila* was carried out as in (Emery, 2007).

2.9.5 WESTERN BLOTTING

Western blots were carried out with Mini-PROTEAN Tetra-Cell apparatus (Bio-rad Laboratories, 1658033FC). Stacking and separating gels were prepared as described by Biorad (Acrylamide/Bis-acrylamide 30 % Solution (Bio-rad Laboratories, 1610124), 10 % ammonium persulfate (Sigma, A3678), 1.5 M Tris (pH 8.8), 0.5 M Tris (pH 6.8), 10 % (w/v) SDS, TEMED (Sigma, T9281). Separating gel was made in a percentage appropriate to the proteins considered.

Table 2.4. Acrylamide percentage used for target molecular weight.

Acrylamide %	M.W Range of Target
7	50-500 kDa
10	20-300 kDa
12	10-200 kDa
15	3-100 kDa

Protein samples and buffers were prepared as described in manufacturer's manual. Electrophoresis and wet transfer using Mini-PROTEAN Tetra-Cell apparatus were carried out as specified in manufacturer's manual.

Table 2.5. HRP conjugated antibodies for western blotting.

a-Mouse HRP conj	Rabbit	Novus Biological	NBP1-75249
a-GP HRP conj	Goat	Novus Biological	NBP1-74871
a-Rabbit HRP conj	Donkey	Novus Biological	NBP1-75276

2.9.6 RNA EXTRACTION

All solutions used during RNA isolation steps were DEPC (Sigma, 40718) treated.

Drosophila tissues were homogenized in 1 ml of TRIZOL reagent (ThermoFischer Scientific, 15596026) per 50 mg of tissue with plastic pellet pestles (Sigma, Z359947).

AHNSCs were washed twice with ice cold DEPC-PBS and lysed by adding 1 ml of TRIZOL per 10 cm^2 and scraping. The cells were passed through a pipette several times and vortexed.

All samples were then processed in the same fashion. 250 μl of chloroform (Sigma, 2888306) were added per ml of TRIZOL, samples were shaken vigorously for 30 seconds and incubated at RT for 5 min before being centrifuged at 10,000 rpm for 15 minutes. Aqueous phase was collected and mixed with 550 μl of isopropanol (Sigma,

190764). Samples were incubated overnight at -20 °C then vortexed and centrifuged at 13,000 rpm for 15 minutes. Pellet obtained was washed with 70 % Ethanol (Sigma, 51976) and dissolved in TE buffer (Sigma, 93283).

2.9.7 CELL FRACTIONATION

Nuclear and cytoplasmic fractions of AHNSCs were obtained as follow. Confluent AHNSCs were washed twice with ice cold PBS then rotated at 4 °C for 5 min with 500 µl of N40E-CSK buffer (50 mM Tris-HCl pH 6.5, 100 mM NaCl, 300 mM Sucrose, 3 mM MgCl2, 0.15 % NP40, 4 mM DTT, 40 mM EDTA) per 10 cm^2. Cells were centrifuged at 3,000 g at 4 °C for 3 minutes. Supernatant was collected and centrifuged at 10,000 g at 4 °C for 10 minutes. The supernatant was the cytoplasmic fraction. The pellet was resuspend in 500 µl of N40E-CSK buffer and rotated at 4 °C for 3 minutes. Lysates were centrifuged at 3000 g for 3 minutes and supernatant was discarded. 500 µl of CLIP lysis buffer (50 mM Tris-HCl, pH 7.4, 100 mM NaCl, 1 % Igepal CA-630, 0.1 % SDS, 0.5 % sodium deoxycholate, 4 mM DTT) was added to the pellet. Samples were then sonicated 5 x 30 sec in a waterbath sonicator and centrifuged at 13,000 g at 4 °C for 10 minutes. The supernatant was the nuclear fraction.

Fractions were then processed as needed by experiments.

2.10 BIOINFORMATICS

CLC Sequence Viewer 7 software (CLC Bio) was used to align multiple amino acid sequences in this study.

Protein Basic Local Alignment Search Tool (BLASTp) was used to predict a function for CG14712 and to search for related nucleoporin sequences in the *Drosophila* genome. Gene Ontology terms and protein family were searched using AmiGO 2 and Panther Classification System v13.1 (The Gene Ontology).

Sequencing results were analysed with ApE v2.0.53 (M. Wayne Davis) and 4Peaks v1.8 (Nucleobytes).

2.11 Image acquisition and processing

2.11.1 Acquisition and presentation

Confocal images were acquired using a Zeiss LSM 510 and Zeiss LSM 800 with Airyscan and the Zen Blue software. Z-series scans were obtained using steps ranging from 0.1 µm to 2 µm accordingly to experimental needs. Images were processed using ImageJ and Fiji (National Institute of Health), Adobe® Photoshop® and Adobe® Illustrator®.

2.11.2 Fiji scripts

Fiji scripts and plugins were used to analyze and present images. Cell counts in *Drosophila* CNSs were carried out with the ImageJ cell counter plugin (NIH). Masking, projecting and reformatting scripts can be found online at:

https://bit.ly/2se2mjs

Or by scanning the following QR code:

2.11.3 CellProfiler scripts

Total and differential intensity analyses, mouse AHNSCs cell counts as well as IHC analysis were processed with CellProfiler 3.0.0. All scripts were checked for

efficiency and proper data analysis before use. All Project files can be found online at:

https://bit.ly/2AEXubx

Or by scanning the following QR code:

2.12 Statistics

Each experiment was repeated with at least 3 biological and technical replicates.

Graphpad Prism® software was used to carry out all significance tests and graphs. A parametric test for normal distribution was performed on all data sets and normal distributions were analyzed through an unpaired student t-test.

3 PERTURBATION OF NUCLEOCYTOPLASMIC TRANSPORT COMPONENTS IN *DROSOPHILA* NSCS CAN INDUCE QUIESCENCE

3.1 CHAPTER AIM

This chapter will:

- Characterize the 2V327 mutant and its phenotype,
- Study the function of CG14712.
- Introduce components of the nucleocytoplasmic machinery as potential regulators of NSC quiescence.

3.2 INTRODUCTION: NUCLEOCYTOPLASMIC TRANSPORT OF MACROMOLECULES

Tight regulation of nucleocytoplasmic transport is critical for both cell physiology and pathology (Beck & Medalia, 2008; Ibarra & Hetzer, 2015; Sloan, Gleizes, & Bohnsack, 2015). In eukaryotic cells, the movement of macromolecules between the nucleus and cytoplasm occurs through the NPC, a large gatekeeper protein complex spanning the nuclear envelope. This aqueous channel is generated from a complex network of around 30 largely conserved proteins known as Nups. Nups are organized into sub-complexes that are defined by the biochemical affinity of their components (Hurt & Beck, 2015), and can be subdivided into two groups according to whether their position in the NPC is symmetric or not with respect to the cytosolic and nuclear surfaces of the pore (Cautain, Hill, de Pedro, & Link, 2015). Symmetric and asymmetric groups can be further subdivided into different functional sub-groups (Figure 3.1 and Table 3.1).

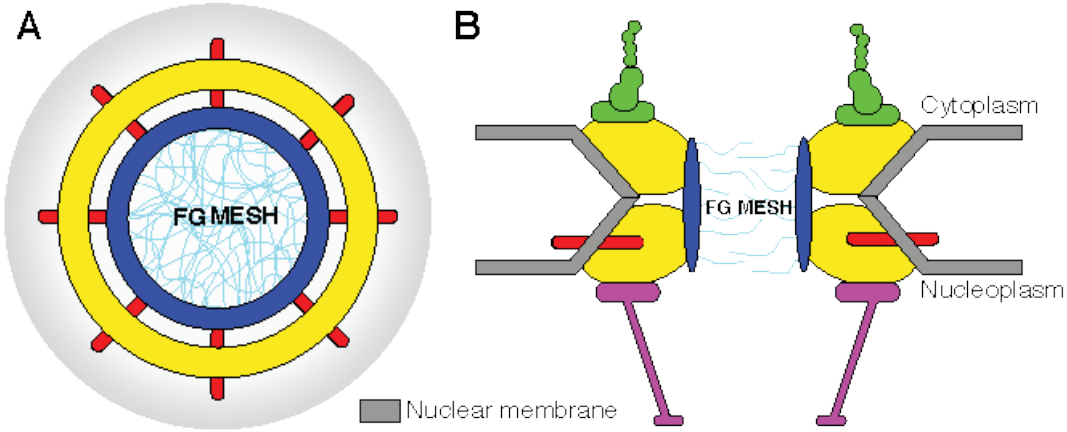

FIGURE 3.1. ARCHITECTURE OF THE NPC.

(A) Top view depicting only symmetric Nups, the barrier created by the FG mesh limits passive diffusion of macromolecules. (B) Cut-open view, depicting also asymmetric Nups (green and pink, in the cytosolic and nuclear faces of the pore, respectively). Colour coding is according to functional subgroups and matches that used in (Table 3.1).

Table 3.1. Classification of human Nups and their *Drosophila* homologs.

Symmetric				Asymmetric			
Scaffold Nups				Cytoplasmic FG Nups and Filaments		Nuclear FG Nups and Basket	
Coat Nups		Adaptor Nups					
Human	*Drosophila*	Human	*Drosophila*	Human	*Drosophila*	Human	*Drosophila*
SEH1	Nup44A	NUP93	Nup93-1/2	RANBP2	Nup358	NUP153	Nup153
NUP75/85	Nup75	NUP205	Nup205	NUP88	Mbo	NUP50	Nup50
NUP160	Nup160	NUP188	CG8771	NUP214	Nup214	Tpr	Mtor
Sec13	Sec13	NUP155	Nup154	CG1/Nlp1	NA	GLE1	Gle1
NUP96	Nup98-96	NUP35	Nup35/53	RAE1	Rae1		
NUP107	Nup107	NUP53	Nup35/53	NUP98	Nup98-96		
NUP133	Nup133			ALADIN	CG16892		
NUP37	Nup37			GLE1	Gle1		
NUP43	Nup43						

Poms		Barrier FG Nups	
Human	*Drosophila*	Human	*Drosophila*
NDC1	Ndc1	NUP62	Nup62
Gp210	CG7897	NUP54	Nup54
POM121	NA	NUPL1	Nup58

The symmetric group corresponds to the Nups present in the actual pore. Within this group can be found:

- Structural or scaffold Nups that form the skeleton of the NPC connecting integral membrane Nups to the so-called barrier Nups. Scaffold Nups can be further classified as coat Nups, which directly bind membrane Nups; and adaptor Nups, which link coat Nups to barrier Nups.
- Integral membrane proteins, also called pore membrane proteins (Poms), which anchor the NPC to the nuclear envelope, where the inner and outer nuclear membranes fuse to form the nuclear pore.
- Barrier phenyalanine-glycine (FG) rich Nups forming the innermost part of the NPC channel. Their intrinsically disordered FG sequences float in the central channel and create a hydrophobic mesh gatekeeping the passive transport of macromolecules bigger than 40kDa. On the other hand, their FG repeats can interact with carrier proteins (see below), thus facilitating the active transport of macromolecules through the mesh.
- The asymmetric group corresponds to the Nups present exclusively on the nuclear or cytoplasmic sides. Within this group can be found:
- Filament Nups extending on the cytoplasmic side.
- Nuclear basket Nups present on the nuclear side.

A subset of asymmetric Nups is also FG rich and can interact with transport complexes thus playing an important role in cargo-NPC interactions. Indeed, asymmetric Nups are key components in establishing the directionality of nucleocytoplasmic transport (Devos et al., 2006). In mammals, cytoplasmic and filaments Nups contain FG rich fibrils that extend several micrometers into the cytoplasm and might facilitate transport by guiding bound cargo-carrier complexes to the transport channel (Richardson, Mills, Dilworth, Laskey, & Dingwall, 1988;

Stewart, 2007). Nuclear basket Nups are critical for efficient mRNA/mRNP export from the nucleus and it has been shown that silencing of nuclear basket Nups Nup153 and Megator negatively deregulates the expression of thousands of genes (Vaquerizas, Suyama, Kind, Miura, & Luscombe, 2010).

While passive transport of macromolecules is a size-dependent process, active import and export through the NPC rely, respectively, on the presence of nuclear-localization (NLS) or nuclear export (NES) signals on cargo or carrier proteins. These signals consist of amino acid residues within the primary protein sequence that bind carrier proteins (soluble transport receptors of the karyopherin family known as importins and exportins) either directly or via adaptor molecules (Table 3.2).

Table 3.2. Human karyopherins and their *Drosophila* homologs.

Human	*Drosophila*
CSE1L	Cas
IPO4	CG32164/CG32165
IPO7/8	Msk
IPO9	RanBp9
IPO11	RanBP11
IPO13	Cdm
TNPO3	Trn-SR
KPNB1	FS(2)KET
RANBP5/6	Karyß3
TNPO1/2	Trn/CG8219
XPO1	Emb
XPO4	/
XPO5	RanBP21
XPO6	Exp6
XPO7/RANBP17	RanBP16
XPOT	/

The classic nucleo-cytoplasmic transport mediated by nuclear signals and their nuclear transport receptors requires metabolic energy to load and unload cargo. This energy is brought by GTP hydrolysis of the Ras-like GTPase Ran (D'Angelo & Hetzer, 2008; Steggerda & Paschal, 2002) (Figure 3.2).

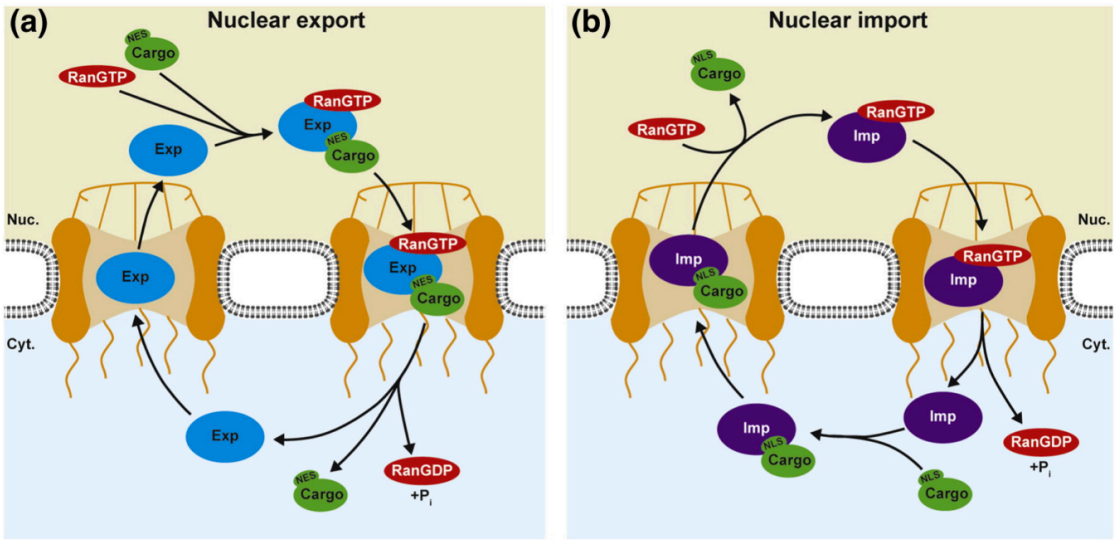

FIGURE 3.2. SCHEMATIC OVERVIEW OF RAN-DEPENDENT NUCLEOCYTOPLASMIC TRANSPORT.

(A) RNA/RNP cargos containing NES associated with exportins and RanGTP in the nucleus. After translocation through the NPC, hydrolysis of RanGTP to RanGDP and inorganic phosphate releases the cargo into the cytoplasm and the exportin is recycled back to the nucleus. (B) Cargos containing NLS bound importins at low RanGTP concentrations in the cytoplasm and translocate to the nucleus as a dimeric complex. Association of RanGTP with the importin in the nucleus releases the cargo and the importin-RanGTP complex is re-exported. Reproduced from (Sloan et al., 2015).

The transport signals interacting with Importin-α, Importin-β, Exportin-1 and Transportin-1 are well described (Cautain et al., 2015; Xu, Farmer, & Chook, 2011), but much remains to be described for the remainder. The currently known NLSs can be classified as classical or non-classical. Classical NLSs are associated with the

first uncovered nuclear import pathway, when a nuclear targeting signal in the simian virus 40 (SV40) large T antigen was characterized more than 30 years ago (Colledge, Richardson, Edge, & Smith, 1986). They can be further divided into monopartite (containing a single cluster of basic residues like the SV40 large T antigen NLS) and bipartite (containing two stretches of basic amino acids separated by 10-12 amino acids linker) (Lange et al., 2007). Classical NLSs are associated with Importin-α which in turn binds members of the Importin-β family (Lange et al., 2007). Non classical NLSs are directly associated with Importin β family members, including Importins β1 and β2 which bind to NLS-cargos directly, a pathway historically referred to as non-classical transport (Stewart, 2007).

While Nups have a defined role within the NPC, there is increasing evidence of their involvement in processes outside this structure. Nup levels have been shown to modulate cell fate in several cases and Nup98, Nup62 and Nup50 have been shown to directly stimulate the expression of developmental genes (Kalverda, Pickersgill, Shloma, & Fornerod, 2010); Nup98-96 mediates the transport or transcription of targets required for the developmental timing between amplification and differentiation in *Drosophila* germ lines (Parrott et al., 2011); and high level of Nup96 leads to a significant delay in G1/S progression in HeLa cells (Chakraborty et al., 2008). Most Nups have been shown to be involved in regulating mitosis at the cytoskeletal level. For example, in the absence of ALADIN, the mitotic kinase Aurora A spreads from centrosomes onto spindle microtubules, which affects the distribution of a subset of microtubule regulators and slows spindle assembly and chromosome alignment (Carvalhal et al., 2015); knockdown of Nup62, a barrier FG Nup, induced mitotic arrest in G2/M and mitotic cell death as well as defective centrosome segregation and centriole maturation during G2, resulting in multinucleated cells (Chieko Hashizume et al., 2013); knockdown of RanBP2/Nup358, a cytoplasmic FG

Nup that partially localizes at the centrosome during mitosis, induces G2/M phase arrest, impaired chromosomal segregation, metaphase catastrophe and mitotic cell death (C Hashizume, Kobayashi, & Wong, 2013). Furthermore, Nup358, another cytoplasmic FG Nup, has been shown to be important during metaphase for correct microtubule-kinetochore attachment, and to interact with interphase microtubules through its N-terminal region, increasing their bundling and stability (Jomon & Mary, 2008). Thus components of the nucleocytoplasmic transport machinery appear to be relevant candidates for quiescence regulators.

3.3 2V327 MUTANT NSCS SHOW ANACHRONIC CELL-CYCLE ARREST WITH MORPHOLOGICAL FEATURES OF QUIESCENCE

In a forward genetic ethylmethanesulfonate screen, a mutant (*2V327*) presenting lethality at wL3 accompanied by delayed CNS development was recovered (Rita Sousa-Nunes, unpublished data). Notably, late larval NSCs in *2V327* mutant, normally actively cycling in wild-type (WT) animals, anachronically undergo cell-cycle arrest whilst extending a fiber – features of a quiescent NSC that are absent in an active NSC (Figure 3.3A-B). 2V327 homozygous mutants are lethal at undergrown late larval stage wL3. wL3 *2V327* mutants' CNS present on average 31.7 NSCs stained with the NSC nuclear marker Dpn -corresponding to a 70% decrease in NSC number compared to wild-type- of which 6.3% stain positively for the mitotic marker PH3 –compared to 20.5% in WT. An average of 17.5 (55.3%) NSCs in *2V327* mutant CNSs present a fiber -a feature absent in WT CNSs- none of which is positive for the mitotic marker PH3. This led me to define these NSCs to be in a quiescent-like state according to their quiescent-like fiber and cell cycle arrest. It is yet too early to describe this state as quiescent as I have yet to show these NSCs can re-enter the cell-cycle, a defining feature of quiescence. Interestingly, all (100%) NSCs in *2V327* mutants present cytoplasmic Mira, which allowed me to observe fibers, opposed to 9.8% in NH CNSs in which Mira levels are very low and localized to the nucleus.

Hemizygous *2V327* mutants have very similar NSC phenotype to homozygous mutants albeit a number of Dpn positive NSCs decreased by 27.7% (Figure 3.3B-C and 3.4).

The clonal technique employed to label the *2V327* NSC shown in Figure 3.3D - MARCM (Lee & Luo, 1999)- can only lead to mutation homozygosis and reporter expression in cells born of mitotic recombination. Therefore, by inducing clones at early larval stages and since clones originate from a dividing parental cell, the *2V327* clones do not present a simple arrest in a quiescent-like state; the absence of proliferation accompanied by *de novo* fiber extension in MARCM clones suggests a cell-autonomous re-entry in a quiescent-like state.

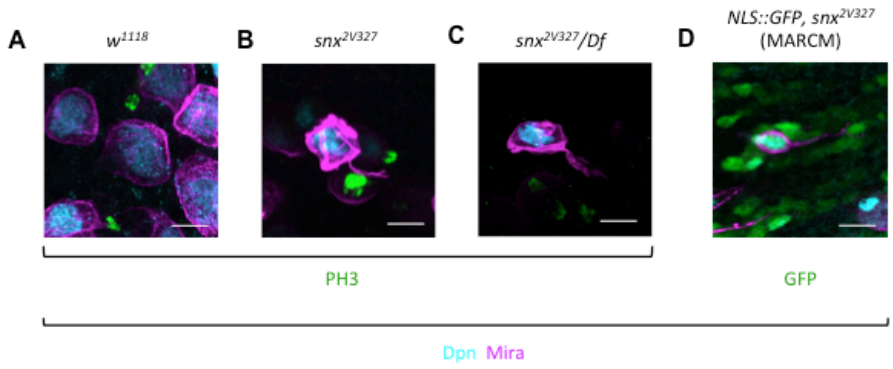

FIGURE 3.3. *2V327* PHENOTYPE.

Whole late larval brains were stained with Miranda (Mira, magenta), Deadpan (Dpn, cyan) and PH3 (green). (A) Wild-type NSC stained with NSC markers Miranda and Deadpan shows a rounded morphology, while both homozygous (B) and hemizygous (C) *CG14712*^{2V327} mutants present smaller brain lobes with fewer NBs staining for Dpn and extend a fiber characteristic of quiescent NSCs. (D) MARCM induced *snx*^{2V327} induced clones are smaller and also present a fiber characteristic of quiescent NSCs. (E) Nab>Dcr2 driven RNAi against *CG14712* phenocopy the *2V327* mutants. Scale bars: 10 μm.

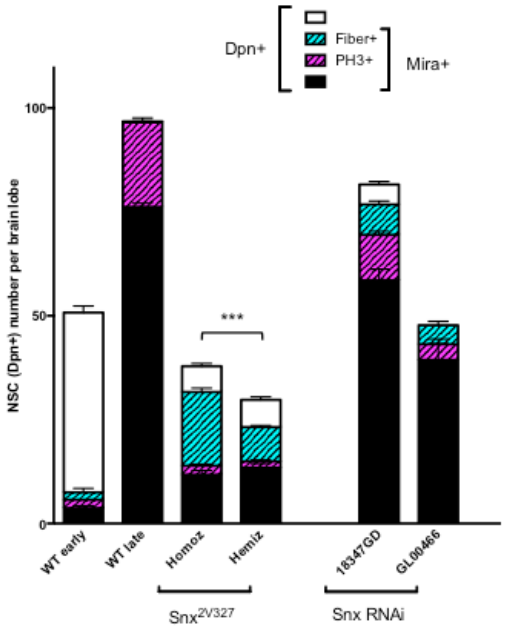

FIGURE 3.4. QUANTIFICATION OF PHENOTYPES.

NBs in each brain lobe were counted and defined following the stain they presented; WT brain lobes present around 100 NBs staining for Mira and Dpn, around 20% of which are PH3 positive. These numbers rapidly decrease in *CG14712*^{2V327} mutants and RNAis.

3.4 *2V327* IS A NULL ALLELE OF THE NOVEL NUP CG14712

After deficiency mapping, RNAi knockdown was performed on 7 candidate genes (Rita Sousa-Nunes, unpublished data) but only one phenocopied the mutant. Driving *CG14712* RNAis with *nab>Dcr2* phenocopied *2V327* mutants (Figure 3.5A). I then sequenced the coding region of CG14712 and identified the genetic lesion in 2V327 as a premature STOP codon in position 254 (Figure 3.5B). *CG14712* encodes a putative FG Nup. It is still unclear what subtype of FG Nup CG14712 corresponds to; but primary sequence comparisons through BLASTp (NCBI) indicate that the only similarity found is to *Drosophila* melanogaster Nup98-96 isoforms A and C at 32% and Homo Sapiens Nup98-96 isoform 9 at 30%. In both species, Nup98-96 is an

asymmetric Nup found on both the nuclear and cytoplasmic sides of the NPC. I named this novel Nup Snorlax (Snx) after a sleepy Pokemon that blocks passers-by as it naps (Nintendo, 1996).

Rescue of *snx*^{2V327} was attempted by expressing *UAS-snx* ubiquitously using *da-GAL4,* and in NSCs only using *nab-GAL4*. I was unable to rescue lethality or the NSC phenotype with either driver. Overexpression of snx both ubiquitously and specifically in NSCs in a WT background did not lead to any phenotype (Figure 3.5C**)**, excluding the hypothesis of a dominant negative phenotype during Snx overexpression. Furthermore, a *snx::GFP* FOSMID transgene (Sarov et al., 2016) did not rescue either lethality or the quiescent-like phenotype. Snx::GFP overexpression did not lead to any phenotype; nevertheless, snx::GFP is able to associate in the NPC despite its C-ter GFP as shown by its colocalization with wheat germ agglutinin (WGA; which in flies labels specifically Nup58; Onischenko et al., 2004**) (**Figure 3.5D**)**, further confirming the Nup characteristics of Snx.

Antibodies raised against peptides in regions either upstream or downstream of the mutated codon (CSI and CGT, respectively; Figure 3.5A) co-localize with WGA around the nuclear periphery, and also stain patches in the nucleoplasm, in NSCs and surrounding cells (Figure 3.6A**)**. This reinforces the fact that snx is indeed a Nup. Surprisingly, CGT still stained *snx*^{2V327} animals (Figure 3.6B**)**. This could be due to a lack of specificity of our antibody (hopefully ruled out in Figure 3.6C) or due to perdurance of maternal protein. The later is plausible in light of the similar signal obtained with both antibodies, their co-localization with WGA, and the long half-life and high stability of Nups in the NPC (Savas, Toyama, Xu, Yates, & Hetzer, 2012). Interestingly, Snx antibodies showed the protein localizes on the nuclear membrane in WT animals, while it appeared to be nuclear in the mutants, suggesting that the truncated Snx might be unable to assemble in the NPC. I therefore performed

immunoblots to see if Snx levels were decreased from *snx*^{2V327} homozygous mutants and test the specificity of the in-house antibody. Unfortunately, the antibody appeared unsuitable for western blots, hence specificity could not be assessed.

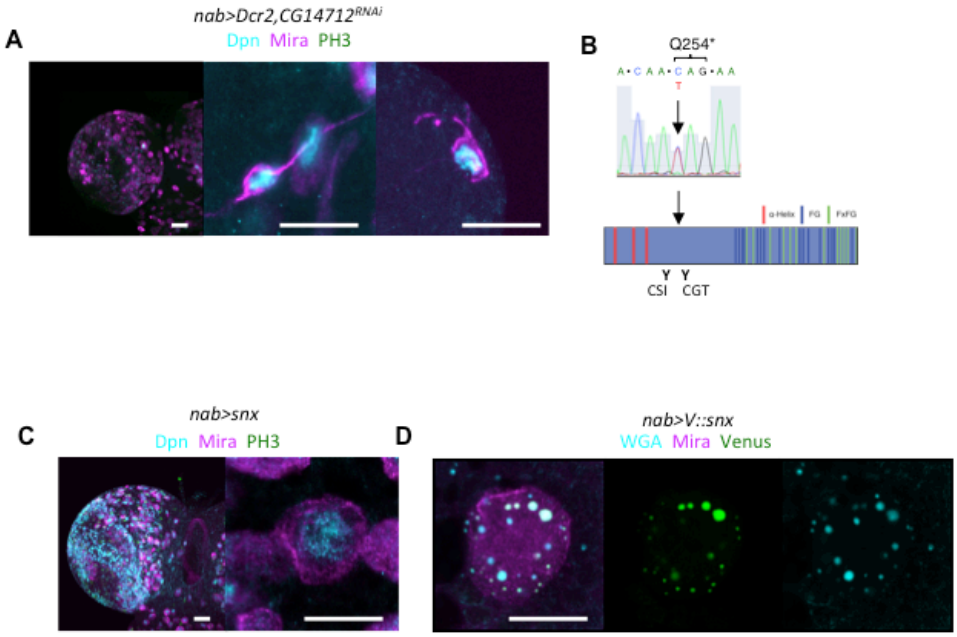

FIGURE 3.5. SNX PRESENTS A PREMATURE STOP CODON THROUGH A T TO C MUTATION (Q254*).

(A) *CG14712* RNAis phenocopy *2V327*. *Nab>Dcr2>CG14712*^{RNAi} larvae were dissected at wL3 and stained for Mira (magenta), Dpn (cyan) and PH3 (green). (B) Schematic of Snx amino acid sequence. CSI and CGT bind epitopes before and after the STOP codon respectively. (C) Overexpression of *snx* driven by *nab* or *da* did not lead to any phenotype. (D) V::Snx overexpression does not lead to a dominant negative phenotype. V::Snx (green), Mira (magenta), WGA (grey). Scale bars: 15 μm.

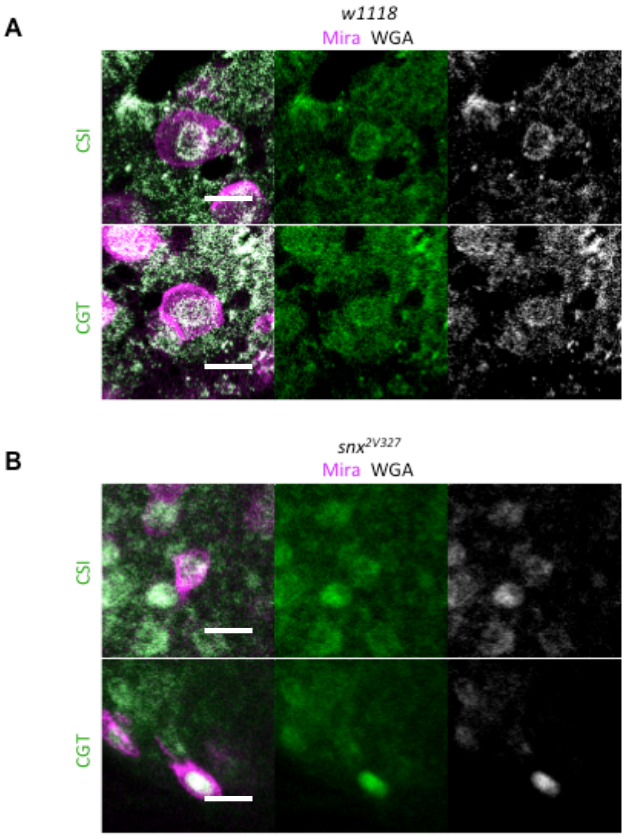

FIGURE 3.6. SNX ANTIBODIES COLOCALIZE WITH WGA.

(A) WT, (B) *snx*^{2V327} homozygous. Mira (magenta), WGA (grey), Snx (green). Scale bars: 10 μm.

3.5 DOWNREGULATION OF NUPS LEADS TO ANACHRONIC NSC CELL-CYCLE ARREST WITH MORPHOLOGICAL FEATURES OF QUIESCENCE

In order to obtain functional data on Nups and their link to NB quiescence, we expressed RNAis through *nab>Dcr-2* flies. RNAi was chosen as the method to screen for loss-of-function phenotypes as null animals would most probably be lethal, and it also allows us to specifically induce the downregulation on NSCs without perturbing the whole organism. Phenotypes were then quantified as previously carried out in 3.3. Quantifications are presented in (Figure 3.7).

Out of 28 Nups screened:

- 15 presented a quiescent-like phenotype with at least one RNAi line. This phenotype is characterized by a fewer number of NBs staining for Dpn, presence of fibers and a lower number of PH3 positive NBs.
- 2 presented a proliferation phenotype with a least one RNAi line. This phenotype is characterized by lower number of PH3 positive NBs.

Phenotypes are spread across all localization groups (Table 3.1**)** and no particular pattern is revealed. It is crucial to remember that RNAis can be unspecific and not efficient, thus a negative result does not mean the target Nup has no involvement in quiescence regulation.

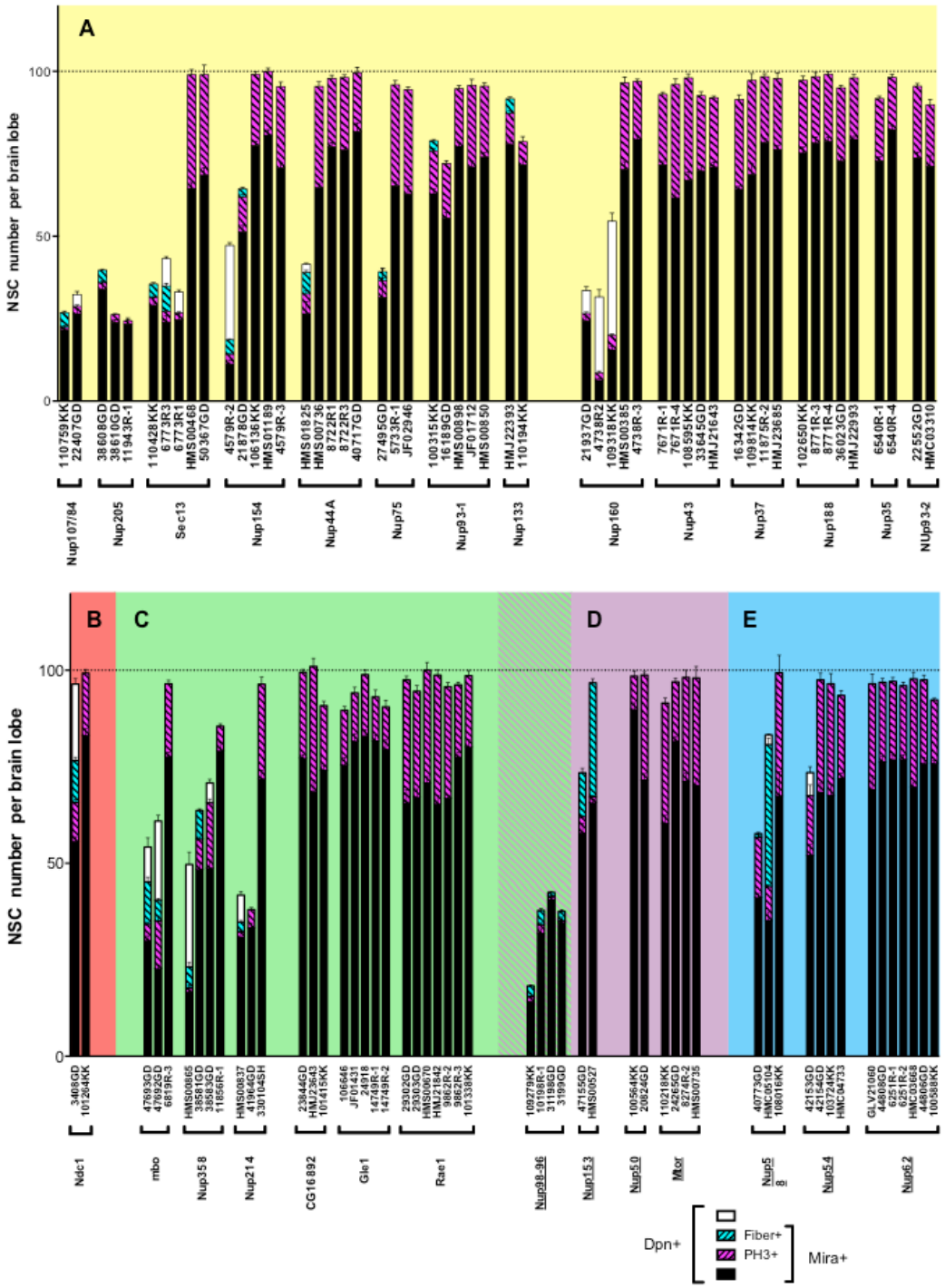

FIGURE 3.7. RNAI DOWNREGULATION OF SEVERAL NUPS IN *DROSOPHILA* NSCS LEADS TO QUIESCENT PHENOTYPE.

Colour coding follows the localization groups defined in Table 3.1. (A) Scaffold (B) Anchor (C) Cytoplasmic filaments (D) Nuclear basket (E) Central channel.

3.6 QUIESCENT-LIKE NSCS CAN RE-ENTER THE CELL-CYCLE

The quiescent-like phenotype in *Snx*^{2V327} mutants and in the previous RNAi experiment leads to a lower number of Dpn positives NSCs as well as Dpn positive but Mira negative NSCs. This suggested that NSCs might expand physiologically, then go through apoptosis or differentiation.

To rule out that the quiescent-like phenotype leads to cell death, homozygous and hemizygous *snx*^{2V327} as well as *snx*^{RNAi} were stained against the apoptotic marker Death caspase 1 (Dcp-1) (Figure 3.8). No NSC appeared positive for Dcp-1, suggesting that the lower number cells positive for NSC markers (Mira, Dpn) is not due to apoptosis.

To rule out the hypothesis that Snx and Nup downregulation leads to NSC differentiation, I needed to show that NSCs entering the quiescent-like phenotype could then re-enter the cell-cycle. A relatively simple time-point experiment using a temperature sensitive GAL80 coupled with the UAS/GAL4 system resolved the issue. The following cross was set-up: *tub-GAL80ts;nab-GAL4,UAS-Dcr2xUAS-Nup*^{RNAi}. At high temperature (31°C), the GAL4/UAS overcomes the GAL80 inhibition and the RNAi is expressed, leading the NSCs to the quiescent-like phenotype; when the temperature is low (18°C) the GAL80 takes over and the RNAi expression is stopped, giving the NSCs a chance to recover from the quiescent-like phenotype. After leaving the cross to lay at 25°C for 24h, I induced RNAi expression for different amounts of time before stopping it (Figure 3.9A**)**. I then dissected siblings before stopping the RNAi expression at WPP and quantified the phenotypes obtained. I carried out the experiment with both snx and nup98-96. The *snx*^{RNAi}-induced phenotype appeared reversible (Figure 3.9B**)**, confirming the hypothesis that Snx downregulation causes NSCs to enter quiescence as opposed to apoptosis or differentiation.

Furthermore, the *nup98-96*^{RNAi} induced phenotype also appeared reversible (Figure 3.9C**)**, suggesting that not only snx, but other Nups can induce NSC quiescence.

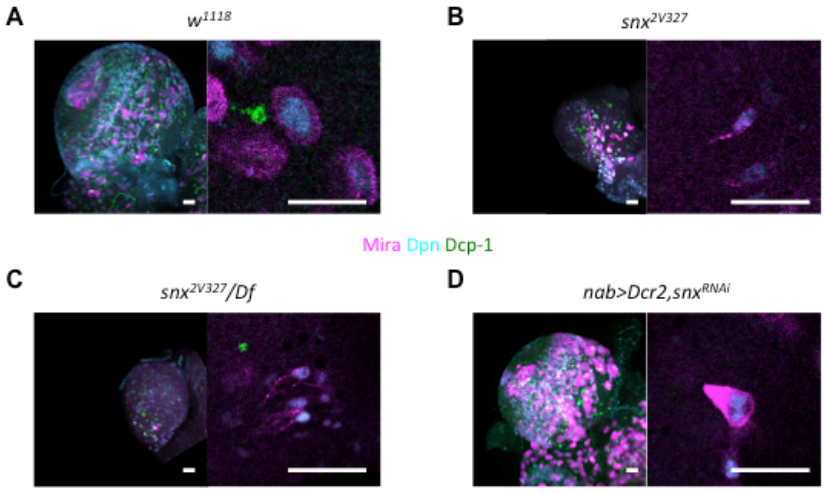

FIGURE 3.8. 2V327 MUTATIONS DOES NOT LEAD TO CELL DEATH.

Brains were stained for Mira (magenta) Dpn (cyan) and Dcp-1 (gey). No NB stains positive for Dcp-1. (A) WT. (B) Homozygous *snx*^{2V327}. (C) Hemizygous *snx*^{2V327}. (D) *snx*^{RNAi}. Scale bars: 15 μm.

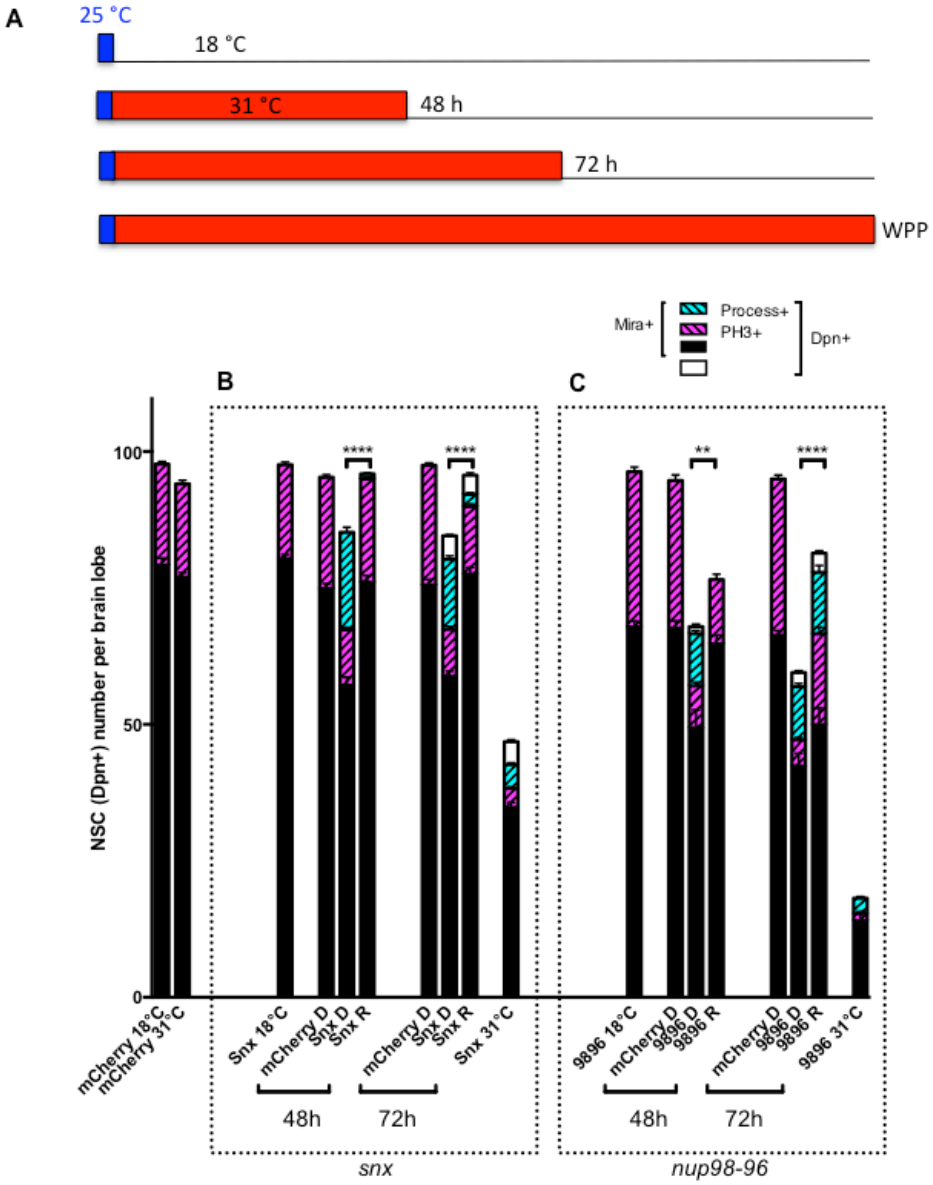

FIGURE 3.9. THE QUIESCENT-LIKE PHENOTYPE IS REVERSIBLE.

(A) Schematic of the reversibility experiment. *nab>Dcr2,GAL80^{ts}* was used to drive RNAis with a spatiotemporal control. Crosses were left to lay for 4 hours at 25ºC, progeny was placed at either 18ºC where *GAL80^{ts}* stopped the expression of the RNAi or at 31ºC where GAL4 induced the expression of the RNAi. Progeny was left for 48 or 72 hours at 31ºC then placed at 18ºC to attempt to reverse the phenotype. CNSs were dissected at white prepupae (WPP) and CNSs from siblings were dissected before temperature change. (B) Quantification of Snx reversibility experiment. (C) Quantification of Nup98-96 reversibility experiment.

3.7 DOWNREGULATION OF KARYOPHERINS INDUCES NSC QUIESCENCE

Nups are known to have functional roles outside of the NPC, Nup98 has notably been shown to act as a transcription regulator (Parrott et al., 2011). To enquire whether nucleocytoplasmic perturbation alone could lead to NSC quiescence, RNAi against karyopherins and nucleocytoplasmic transport components were expressed using *nab>Dcr2* and phenotypes induced were quantified as previously described (Appendix Figure 1**,** Hania Fiaz, partially**)**.

Out of 30 targets:

- 9 presented a quiescent-like phenotype with at least one RNAi line.
- 2 presented a proliferation phenotype with a least one RNAi line.

This confirmed that the quiescent phenotypes induced by Nups downregulation is due to their role in nucleocytoplasmic transport, and not to their roles independently of the NPC.

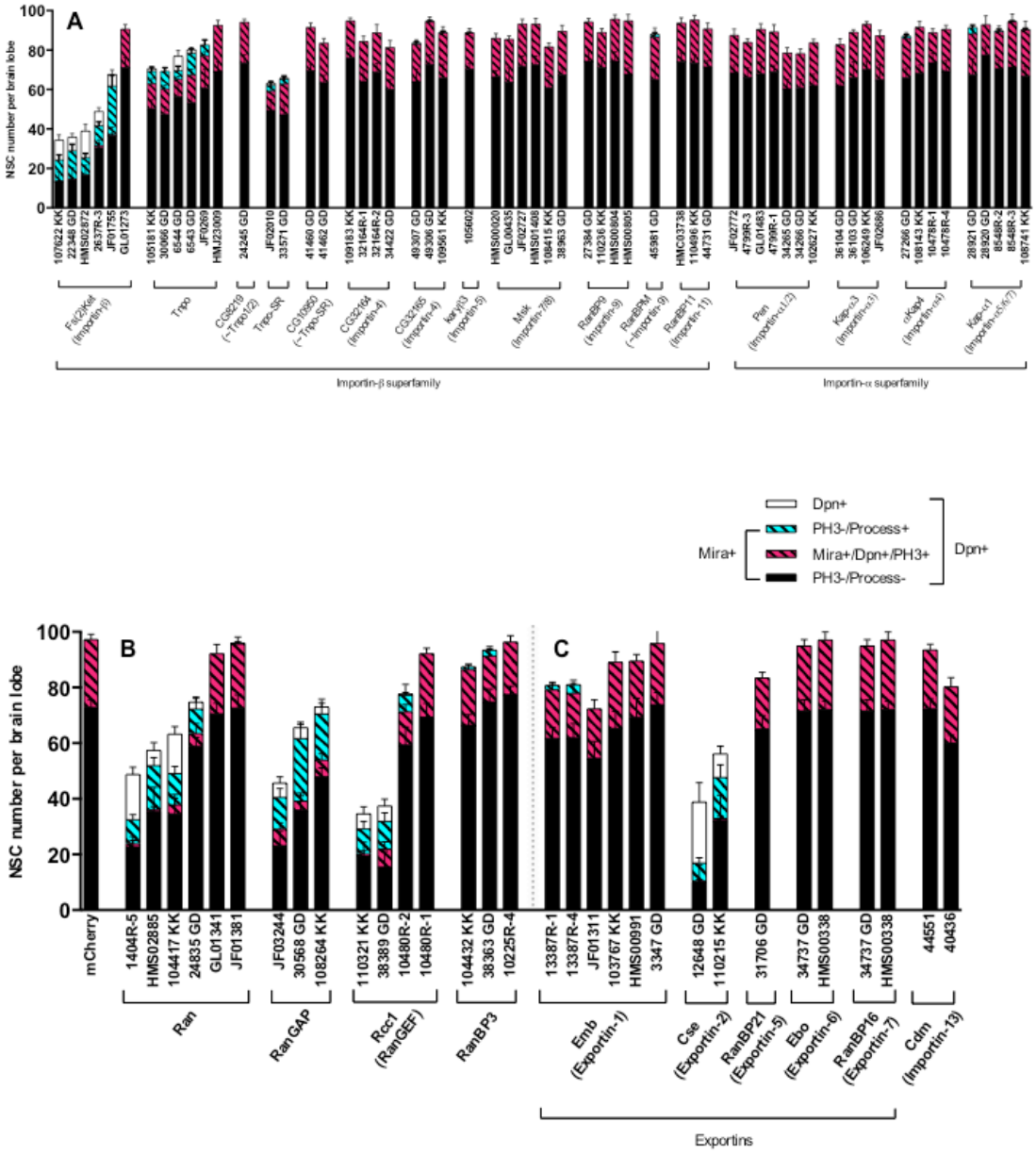

APPENDIX FIGURE 3.10: RNAI DOWNREGULATION OF SEVERAL KARYOPHERINS IN *DROSOPHILA* NSCS LEADS TO QUIESCENT PHENOTYPE.

(A) Importins. (B) Ran and RanGTPase. (C) Exportins.

3.8 DOWNREGULATION OF CELL-CYCLE COMPONENTS DOES NOT NECESSARILY INDUCE NSC QUIESCENCE

To further show our quiescent phenotype is specific to nucleocytoplasmic transport alteration, RNAi against key cell-cycle regulators were expressed through *nab>Dcr2* (Figure 3.10A-E**)**. The phenotypes observed presented developmental delays, and while CycE downregulation occasionally presented a quiescent phenotype (2 cells out of approximately 1000), downregulation of other cell-cycle components did not induce any quiescent phenotype.

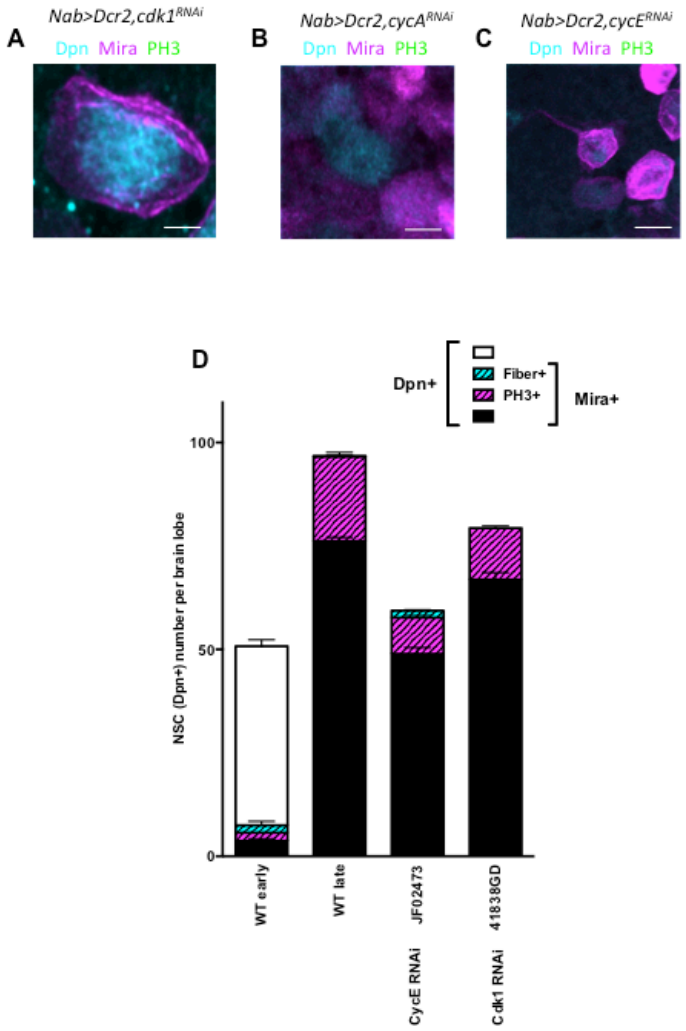

FIGURE 3.11. DOWNREGULATION OF CELL-CYCLE COMPONENTS LEADS TO VARIOUS PHENOTYPES.

Mira (magenta), Dpn (grey), PH3 (green). (A) Cdk1. (B) CycA. (C) CdycE. (D) Quantification of phenotypes. CycA downregulation lead to NBs up to 5 times larger than WT, hence the phenotype could not be quantified. Scale bars: 10 μm.

3.9 DISCUSSION

In this chapter:

- I characterized the *2V327* mutation in the Snx gene and showed that it lead to anachronic cell-cycle arrest in *Drosophila* NSCs reminiscent of quiescence.
- I showed that Snx belongs to the Nup family and is involved in *Drosophila* NSC quiescence regulation.
- I showed that several components of the nucleocytoplasmic transport machinery appear to be involved in *Drosophila* NSC quiescence regulation.

3.9.1 2V327 MUTANT PRESENTS ANACHRONIC NSC QUIESCENCE

I showed that the *2V327* mutant presents a premature STOP codon in the *Snx* gene, which leads to anachronic cell cycle arrest in NSCs with features of quiescence. Mapping of the *2V327* mutation as well as phenocopy of the mutant by Snx^{RNAi} strongly suggests that the quiescent phenotype obtained in NSCs is due to a faulty Snx. However, I was unable to rescue the *2V327* phenotype or lethality, be it ubiquitously through da>snx or locally through nab>snx in a homozygous mutant background. This could be explained by a dominant negative phenotype when overexpressing Snx as the UAS/GAL4 system does not permit the expression of protein at a physiological level. Overexpression of Snx ubiquitously or locally in a WT background did not lead to a dominant negative effect (data not shown). I then tried to create an independent gene knockout through imprecise P-element excision (Brochta, Sheilachu, & Handler, 1991; Ou, 2013), but was unable to generate another mutant (data not shown). Looking back on these results, it is impossible to conclude that the phenotype obtained in NSCs in the *2V327* mutant is due to a faulty Snx. However, it cannot be ruled out that another mutation exists in *2V327*. A Snx FOSMID is available and might be able to rescue the *2V327* phenotype and/or

lethality, confirming that the premature STOP codon in Snx is indeed responsible for the quiescent-like phenotype.

Being unable to rescue the *2V327* phenotype also means it is impossible to conclude if this very phenotype corresponds to quiescence, as I did not show that NSCs could re-enter the cell cycle in the mutant. I showed that the phenotype corresponds to a re-entry into quiescence, and the lack of Dcp-1 stain in NSCs shows the mutation does not lead to cell death. However I am unable to tell if the NSCs are not reaching a depth of quiescence from which they may no longer be able to exit (Kwon et al., 2017). Another concern is that fiber positive NSCs in *2V327* mutants stain strongly for Mira, with an intensity much higher than in proliferating NSCs, and infinitely higher than in physiologically quiescent NSCs in which Mira stain is negative (S.-L. Lai & Doe, 2014). This discrepancy in the quiescent-like phenotype when compared to physiological quiescence amplifies the concerns about the *2V327* phenotype. Hence the need for a rescue of the *2V327* phenotype through a FOSMID is strongly needed.

3.9.2 SNX ENCODES A NOVEL FG NUP

I showed that *Snx* encodes a FG Nup as shown by its amino acid sequence and its co-localization with WGA. It is however impossible to classify Snx further without knowing its exact localization in the NPC as all Nup subtypes can present FG repeats (Lemke, 2016).

Importantly, both Snx antibodies were not suited for western blotting, I thus could not confirm their specificity. Moreover, both antibodies positively stained in *2V327* homozygous mutants, when I expected to observe a staining only with the antibody binding upstream of the STOP codon. This leads me to be cautious with results brought by the in-house Snx antibodies; these experiments should be confirmed with a fully tested, potentially commercial, antibody when one is made available.

Nevertheless, and as stated previously, BLASTp of Snx shows a strongest match with human and mouse NUP98-96. However, true orthologs also called Nup96-98 are already annotated for *Drosophila*. No clear mammalian ortholog has yet been defined for the *Drosophila* Nup Snx. The Gene Ontology (GO) (Ashburner et al., 2000) classifies Snx as a central channel or nuclear basket Nup, which is in agreement with the homology to Nup98-96. The Kyoto Encyclopedia of Genes and Genomes (KEGG) (Kanehisa & Goto, 2000) defines Snx as an homolog of Pom121, an anchor Nup. Both GO and KEGG agree on Snx being involved in nuclear import of proteins, and RNA export. KEGG suggests that Snx might be involved in both RNA transport and biogenesis. Interestingly, GO also notes the interactions of Snx with kap-alpha3, a karyopherin.

The predicted 3-D structure of CG14712 protein reveals similarity to the yeast Nup47-Nup59-Nsp1 complex (Figure 3.11**)**.

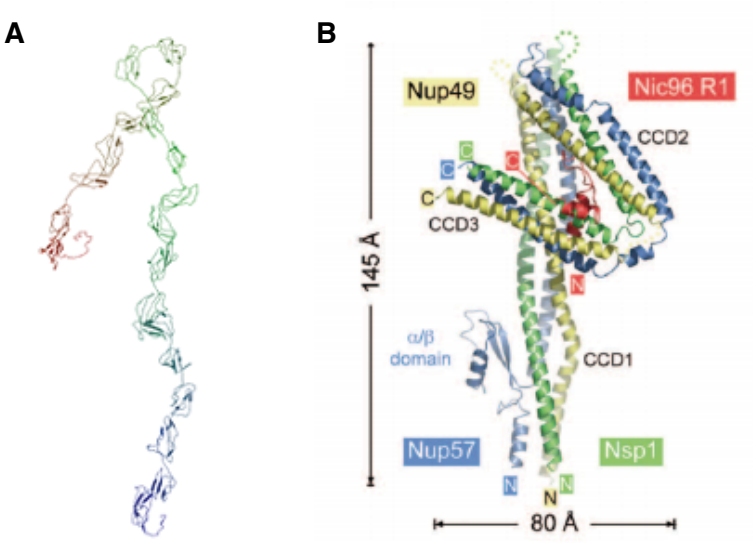

FIGURE 3.11. CG14712 AND YEAST NUP47-NUP59-NSP1 3D STRUCTURES ARE SIMILAR.

(A) Predicted 3D structure obtained by I-TASSER (Zhang, 2008). (B) 3D structure of the yeast Nup47-Nup59-Nsp1 complex. From (Stuwe et al., 2015).

The human homologs of yeast Nup49, Nup57 and Nsp1 are NUPL1, NUP54 and NUP62 respectively, which are central channel FG Nups, and are in turn homologs of *Drosophila* Nup58, Nup54 and Nup62. A look at the predicted 3D structures of these human and *Drosophila* Nups reveals a similarity with Snx. Nonetheless, predicted 3D structure alone cannot let us conclude on the subtype of Snx.

To be able to conclude on the classification of Snx as a Nup, we would need to know its exact localization within the NPC, as well as the factors it interacts with. This might be uncovered by high-resolution electron microscopy, co-immunoprecipitation with other components of the nucleocytoplasmic transport machinery, or by interactome analysis.

3.9.3 *Components of the nucleocytoplasmic transport machinery regulate NSC quiescence*

I chose RNAi as the method to screen for loss-of-function Nup phenotypes as null animals would be lethal, and because it allows me to specifically induce the downregulation on NSCs without perturbing the whole organism. I screened at least two independent RNAi lines per Nup and when both lead to analogous phenotypes I considered their effect to be specific; if the results were disparate, further RNAi lines were tested whenever possible. Obtaining a phenotype with two different lines targeting the same protein was considered sufficient to conclude on the specificity of the RNAis. However, it is more difficult to be confident about negative results, as RNAi is not always efficient (Heigwer, Port, & Boutros, 2018).

Employment of RNAi has another advantage. Through the system used to show the reversibility of the phenotypes obtained by RNAi, I could tune the RNAi levels and possibly the severity of the NSC phenotype obtained. If I can tune RNAi levels to achieve reversible cell-cycle arrest accompanied by the characteristic morphology of quiescent NSCs, I could then apply this to specific lineages for which we have some characterization of neuronal types generated at specific time points (Isshiki, Pearson, Holbrook, & Doe, 2001). It would be extremely interesting to see if neurons born after this artificial quiescence-reactivation will be of the type expected from the time of arrest or from the time of reactivation.

The data indicates that not all Nups lead to the same phenotype when downregulated in NSCs. In this case, it appears that there is an underlying pattern when looking only at the localization of Nups in the NPC. Coupled with the data obtained on karyopherin involvement in NSC quiescence regulation, it appears reasonable to consider that the quiescent phenotype is due to altered nucleocytoplasmic transport, and not to a potential role of Nups outside of the NPC -

e.g. the role of Nup98 as a transcription factor (Parrott et al., 2011). Looking closer at the positive results obtained in both Nups and karyopherins screen, three groups appear:

- A group involving targets in cell cycle and proliferation regulation: Nup93-1, Nup205, Nup44A, Nup154, Sec13, Rcc1, CSE1, Ranbp3, RanBPM and ketel (Baeg, Zhou, & Perrimon, 2005; Brinkmann, Brinkmann, Gallo, Scherf, & Pastan, 1996; Chen & Xu, 2010; Colozza et al., 2011; Dai, Lin, Chang, & Feng, 2009; Kurisaki et al., 2006; Ohtsubo et al., 1987).
- A group including targets involved in RNA export regulation: Nup358, Nup214, Nup153, Nup107, Nup98-96, Nup133, mbo, trn, trn-sr (Allemand, Dokudovskaya, Bordonné, & Tazi, 2002; Bi et al., 2005; Bonifaci, Moroianu, Radu, & Blobel, 1997; Köhler & Hurt, 2007; Kusano, Staber, & Ganetzky, 2001; Kutay, Ralf Bischoff, Kostka, Kraft, & Görlich, 1997; M. Lai, Kuo, Chang, & Tarn, 2003; Roth et al., 2003; Tekotte et al., 2002).
- A group including targets for which involvement is yet to be clearly defined, or for which involvement is too broad to be relevant: Nup58, ndc1, kap-alpha1, Ran.

Cell cycle components have already been shown to be involved in SC quiescence regulation (Cheung & Rando, 2013; Hao, Chen, & Cheng, 2016; L. Li & Bhatia, 2011; Rocheteau, Vinet, & Chretien, 2015; Terzi, Izmirli, & Gogebakan, 2016), hence the appearance of the first group could be expected, and is reassuring that Nup and karyopherin downregulation might indeed lead to NSC quiescence. While SC quiescence regulation through RNA-binding proteins, small RNAs, microRNA biogenesis and translation control has been previously reported (Galloway et al., 2016; Joh et al., 2016; Martinez et al., 2017; Zismanov et al., 2016), regulation of RNA export from the nucleus has never been linked to SC quiescence. In light of this

data, I hypothesized that RNA might be segregated differently in quiescent NSCs when compared to proliferating NSCs, and that they might show a different composition of RNA-binding proteins as well as stress related proteins as both RNA-binding and stress response proteins would potentially be able to stabilize RNA in quiescent NSCs.

4 DIFFERENTIAL NUCLEAR PERMEABILITY IN QUIESCENT VERSUS ACTIVE NSCS LEADS TO RNA SEGREGATION

4.1 CHAPTER AIM

This chapter will:

- Assess Nup composition of quiescent and active *Drosophila* NSCs.
- Assess differential compartmentalization of classical NLSs in quiescent and active *Drosophila* NSCs.
- Assess differential compartmentalization and levels of RNA, RNA-binding proteins, and stress-related proteins in quiescent and active *Drosophila* NSCs.

4.2 INTRODUCTION: ALTERED PROTEIN COMPARTMENTALIZATION IN QUIESCENT SCS

Compartmentalization of key factors in quiescence regulation has already been described. The absence of FoxO3 has been shown to lead to the proliferation of NSCs and lead the NSCs to lose their ability to re-enter a state of relative quiescence after they divide, which may lead to the amplification of progenitors and the exhaustion of the pool of NSCs *in vivo*. Hence FoxO3 is necessary to maintain NSCs quiescence, and, interestingly, is nuclear in quiescent mouse adult NSCs (Renault et al., 2009).

More recently, miR-9, along with Argonaute (Ago) proteins, was shown to be present in the nucleus of adult quiescent NSCs where it maintains NSC quiescence, notably through permitting efficient Notch signaling (Katz et al., 2016), which is involved in quiescence regulation in NSCs (Chapouton et al., 2010). Active nucleo-cytoplasmic

shuttling of miR-9/Ago appears to impact NSCs quiescence status, and miR-9 seems to highlight a state of heterogeneity among adult quiescent NSCs, making it a potential marker for re-entry of these cells in the cell cycle.

In our collaborator's in vitro mouse model of NSC quiescence, the transcription factor Nfix, a member of the nuclear factor I family, was found to be strongly induced upon quiescence. Genome-wide analyses, as well as overexpression and silencing experiments, demonstrated that Nfix plays a major role in the induction of quiescence in cultured mouse NSCs (Martynoga et al., 2013). Nfix is partially excluded from the nucleus of proliferating cultured mouse NSCs whereas it appears exclusively nuclear in quiescent ones. This suggests that Nfix activity might be regulated not only by levels but also by differential nucleocytoplasmic partitioning in cycling versus quiescent mammalian NSCs. Moreover, it suggests that specialized nucleocytoplasmic partitioning during quiescence does not necessarily assume the form of nuclear exclusion but can also take the form of increased nuclear localization.

ERK (Ebisuya et al., 2005) has been shown to be mostly cytoplasmic in quiescent cells, and to be able to shuttle in and out of the nucleus although neither a NES nor NLS has been identified in ERK1/2 (Matsubayashi, Fukuda, & Nishida, 2001). ERK is able to bind to the NPC regardless of these transport signals (Whitehurst et al., 2002), which suggest that NPC components might be able to induce nucleocytoplasmic transport and compartmentalization of factors out of the usual karyopherin-mediated transport.

4.3 LEVELS OF NUPS ARE ALTERED IN QUIESCENT NSCS

Following the observation that Nup downregulation lead to NSC quiescence in *Drosophila*, I assessed if Nup levels are altered in physiologically quiescent NSCs compared to active or reactivating NSCs. A Grh>insc::GFP background was used to label NSCs intrinsically (inscuteable (insc) is a NSC cytoskeleton adaptor protein mediating asymmetric cell division in *Drosophila* NSCs) (Kraut, Chia, Yeh Jan, Nung Jan, & Knoblich, 1996). As previously stated in 1.3, *Drosophila* NSCs are quiescent from 0 to 24 hr ALH, after which time point they start reactivating. Hence larval CNSs were dissected 0-4 hr ALH and 24-29 hr ALH and stained for Snx, Nup98, Nup96, Nup62 and Nup358. The choice of Nup antibodies was limited by availability, and was targeted to Nups presenting similarities to snx. Nup98 and Nup96 were chosen because of their similarity to snx according to pBLAST results presented in 3.2, Nup62 was chosen for its similarity as a FG Nup as well as its negative result obtained during the RNAi screen, Nup358 was chosen for its similar localization on the cytoplasmic side of the NPC as well as for it involvement in CRM-1-mediated transport of cargo (Bernad, van der Velde, Fornerod, & Pickersgill, 2004). Quantification of total intensity per volume in NSCs showed that both Nup98 and Nup96 present higher levels per volume (concentration) in quiescent NSCs when compared to active ones (Figure 4.1A-B), while Nup62 present a higher concentration in active NSCs compared to quiescent ones (Figure 4.1C**)**. Nup358 did not show any alteration of concentration between quiescent and active NSCs (Figure 4.1D).

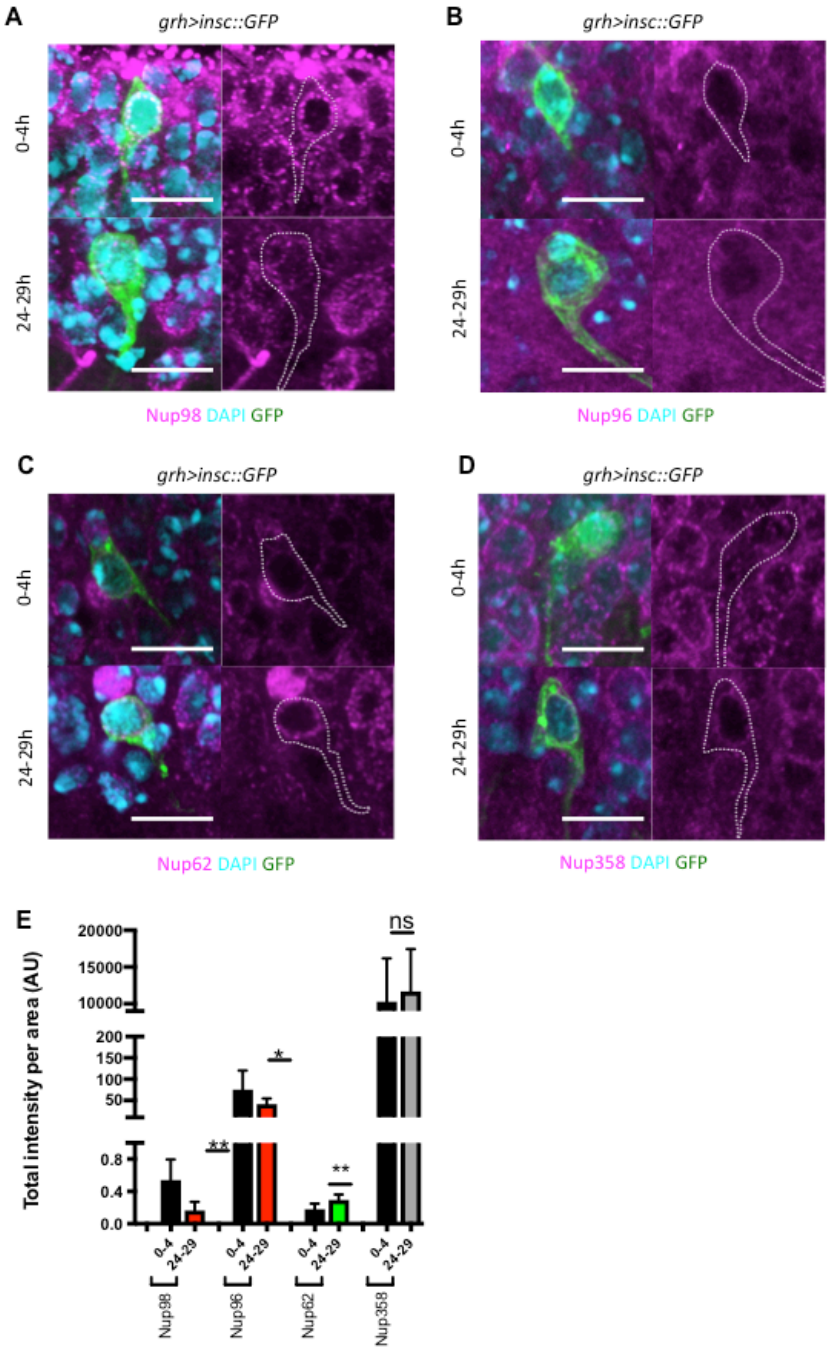

FIGURE 4.1. QUIESCENT *DROSOPHILA* NSCS PRESENT A DIFFERENT NUP COMPOSITION COMPARED TO ACTIVE NSCS.

IHC stains of isolated *Drosophila* NSCs, (Cyan) DAPI, (Green) insc::GFP and (Magenta) (A) Nup98 (B) Nup96 (C) Nup62 (D) Nup358 (E) Quantification of total intensity per area in isolated NSCs at 0-4 hr or 24-29 hr ALH (n=18). Scale bars: 10 μm.

4.4 CLASSICAL NLS LOCALIZATION IS UNALTERED IN QUIESCENT *DROSOPHILA* NSCS

An altered Nup composition, and a potentially altered karyopherin composition, in quiescent *Drosophila* NSCs lead me to hypothesize that cargo transport might be altered. Nup and karyopherin mediated transport of cargo relies on the recognition of NLS. I thus assessed the compartmentalization of two classical NLSs in active and quiescent NSCs; NLS2::GFP (monopartite) and NLS5::GFP (bipartite) expression were driven by *grh* in NH and wL3 larvae. Both NLS2 and NLS5 appeared to be present in the cytoplasm and nucleus of both quiescent and active NSCs (Figure 4.2A-B); no nuclear exclusion of NLS was observed. This experiment was repeated three times in the same conditions, and in different conditions: expression of NLS::GFP was driven at RT, 25°C, 29°C or 31°C; NLS::GFP was switched to NLS::RFP; *grh* driver was switched to *nab* driver. In all conditions NLS compartmentalization was unaltered in quiescent NSCs when compared to active ones.

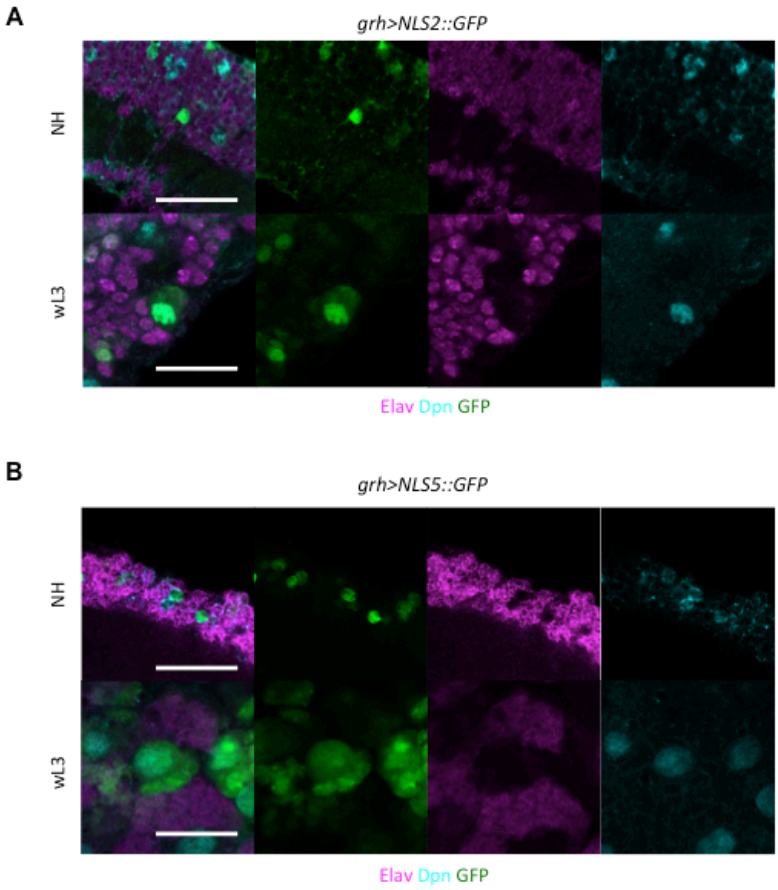

FIGURE 4.2. NLS2 (MONOPARTITE) AND NLS5 (BIPARTITE) LOCALIZATIONS ARE UNALTERED IN QUIESCENT VERSUS ACTIVE *DROSOPHILA* NSCS.

IHC stains of quiescent and active NSCs, (Cyan) Dpn, (Magenta) Elav and (Green) (A) NLS2::GFP (B) NLS5::GFP. Experiment was repeated 3 times on n=10 brains of each condition. Scale bars: 50 μm.

4.5 RNA LEVEL AND LOCALIZATION ARE ALTERED IN QUIESCENT *DROSOPHILA* NSCS

Analysis of positive hits from RNAI screens (1.3 and 1.5) as well as data mining lead me to consider RNA as one interesting cargo which transport might be altered in quiescent *Drosophila* NSCs. I carried out *in situ* hybridization of PolydT probes at 0-4, 24-29 and 29-34 hr ALH in *grh>insc::GFP* background (Figure 4.3A). Polyadenylated (polyA) RNA appeared to be retained in the nucleus of quiescent NSCs as shown by the presence of speckles or 'flowers' in the nucleus of NSCs in 0-4 hr ALH animals. Nucleocytoplasmic ratio of total intensity per volume was quantified (Figure 4.3B) showing a clear difference in RNA repartition in quiescent versus active *Drosophila* NSCs: polyA RNA is 16,7 more nuclear in 0-4 ALH quiescent NSCs than in 0-4 hr MBs; 2,4 more nuclear than at 24-29 hr; and 2,9 more nuclear than at 29-34 hr. PolyA RNA transport thus appears to be altered during quiescence in *Drosophila* NSCs.

In situ hybridization of PolydT probes was carried out in *nab>Dcr2,snx*^{RNAi}, *nab>Dcr2,nup98*^{RNAi}, and *nab>Dcr2,ketel*^{RNAi} backgrounds. (Figure 4.3C) presents phenotypes obtained in *nab>Dcr2,snx*^{RNAi} as a representation of all backgrounds. PolyA RNA appeared to concentrate more in the nucleus of NSCs as the quiescent phenotype got more pronounced (longer fiber, smaller cell body, absence of Mira stain), presenting a similar result to the one obtained in physiological quiescence. Nucleocytoplasmic ratio of intensity per volume was not quantified in RNAi backgrounds because of the broad range of phenotypes, which would lead to non-representative data.

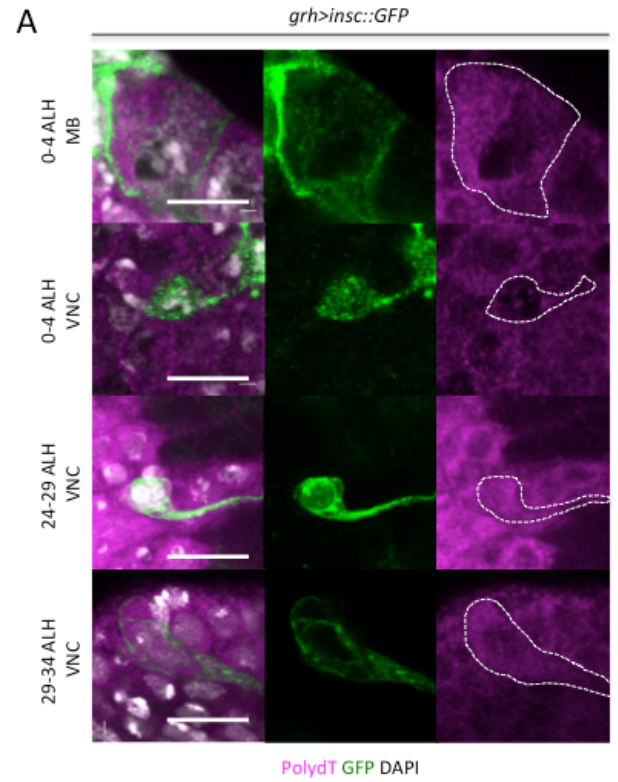
A
grh>insc::GFP
0-4 ALH MB
0-4 ALH VNC
24-29 ALH VNC
29-34 ALH VNC
PolydT GFP DAPI

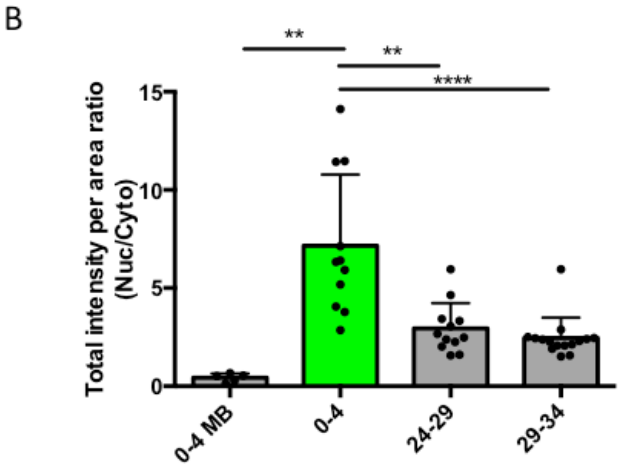
B
**
**
****
Total intensity per area ratio (Nuc/Cyto)
15
10
5
0
0-4 MB
0-4
24-29
29-34

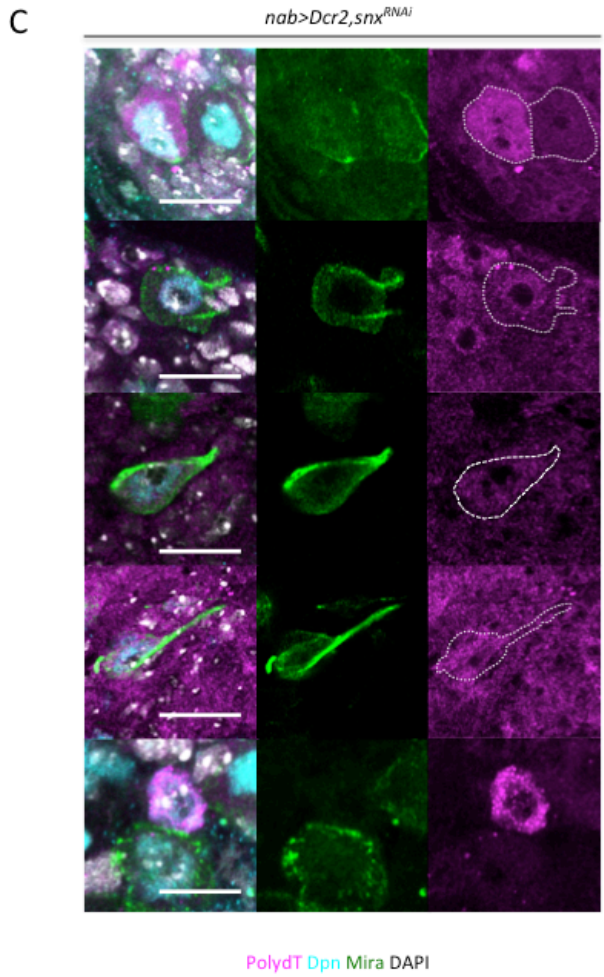

FIGURE 4.3. *IN SITU* HYBRIDIZATION OF POLYDT PROBES SHOWS A DIFFERENCE IN LEVELS AND LOCALIZATION OF RNA IN QUIESCENT VERSUS ACTIVE *DROSOPHILA* NSCS.

(A) MB stained at 0-4 hr ALH, NSCs stained at 0-4 hr ALH, 24-29 hr ALH 29-34 hr ALH in *grh>insc::GFP* background. (Magenta) PolydT, (Green) *insc>GFP* and (Grey) DAPI. (B) NSCs stained at wL3 in *nab>Dcr2,snxRNAi*. PolydT (Magenta), Dpn (Cyan), Mira (Green) and DAPI (Grey). (C) Quantification of nucleocytoplasmic ratio of PolydT intensity per cell in *grh>insc::GFP* background (n=11). Scale bars: 10 *μ*m.

4.6 RNA-BINDING PROTEINS LEVELS AND LOCALIZATION ARE ALTERED IN QUIESCENT *DROSOPHILA* NSCS

Following on the observation of altered RNA segregation in quiescent *Drosophila* NSCs, focus was drawn to target proteins potentially involved in RNA transport and/or stability. DEAD-Box Helicase 6 (DDX6) and T-cell restricted intracellular antigen 1-related protein (TIAR) are RNA-binding and stress-related proteins; RAs-related Nuclear protein (Ran), or GTP-binding nuclear protein Ran, is involved in most active transport through the NPC; RNA-binding protein Fox 1 (Rbfox1) regulates nuclear tissue specific alternative splicing and cytoplasmic mRNA translation; Unkempt (Unk) is an RNA-binding protein acting downstream of Megator.

In all targets, total intensity per volume and nuclear to cytoplasmic ratio of intensity per volume was quantified in NSCs from 0-4 hr ALH and 24-29 hr ALH CNSs. DDX6 ratio appeared similar in both conditions while quiescent NSCs presented a lower total intensity with active cells presenting more puncta-like stain (Figure 4.4A). TIAR ratio was higher in quiescent cells while total intensity was similar in both conditions, interestingly, TIAR localized mainly to the fiber in active NSCs (Figure 4.4B). Ran ratio and total intensity appeared similar in quiescent and active NSCs, stains did not show any significant difference either (Figure 4.4C). Rbfox1 ratio appeared lower in quiescent NSCs while total intensity appeared higher, overall stain in both conditions appeared to be very low compared to adjacent glia, leading me to consider that quantifications might not be relevant (Figure 4.4D). Finally, Unk ratio was similar in both conditions while total intensity was lower in quiescent NSCs with active cells presenting more puncta-like stain (Figure 4.4E).

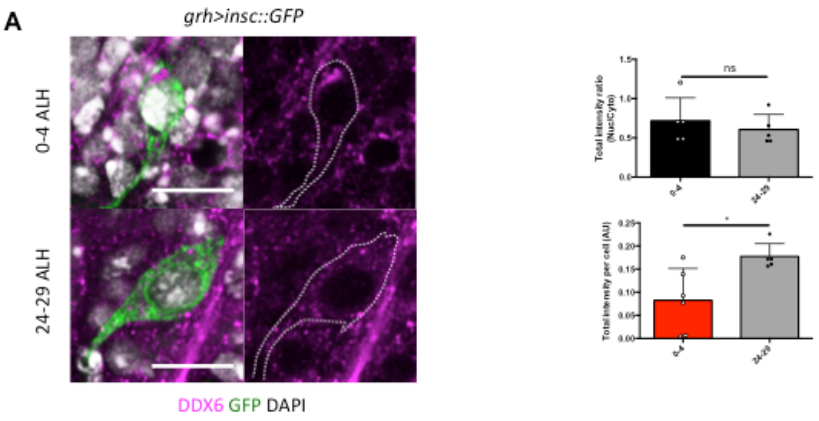
A
grh>insc::GFP
0-4 ALH
24-29 ALH
DDX6 GFP DAPI
Total Intensity ratio (Nuc/Cyto)
ns
Total Intensity per cell (AU)
*
0-4
24-29

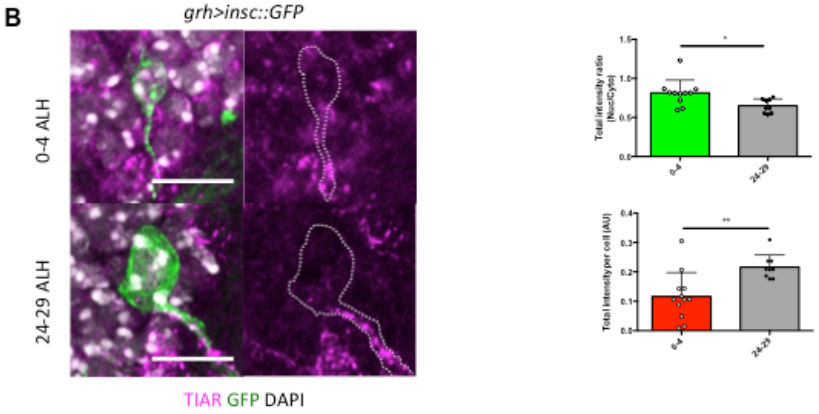
B
grh>insc::GFP
0-4 ALH
24-29 ALH
TIAR GFP DAPI
Total Intensity ratio (Nuc/Cyto)
*
Total Intensity per cell (AU)
**
0-4
24-29

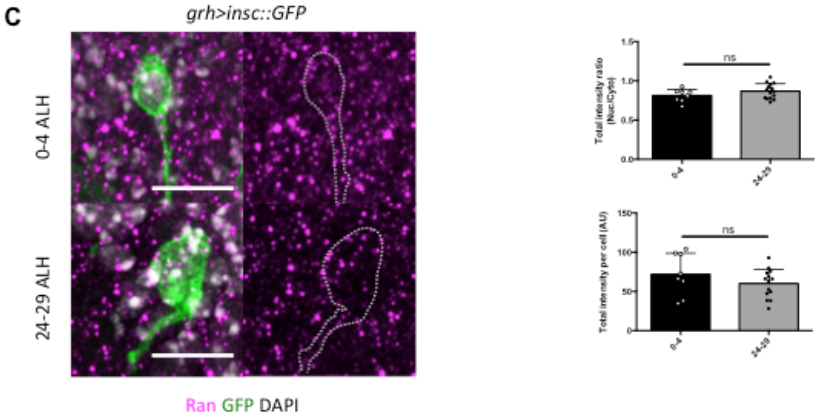
C
grh>insc::GFP
0-4 ALH
24-29 ALH
Ran GFP DAPI
Total Intensity ratio (Nuc/Cyto)
ns
Total Intensity per cell (AU)
ns
0-4
24-29

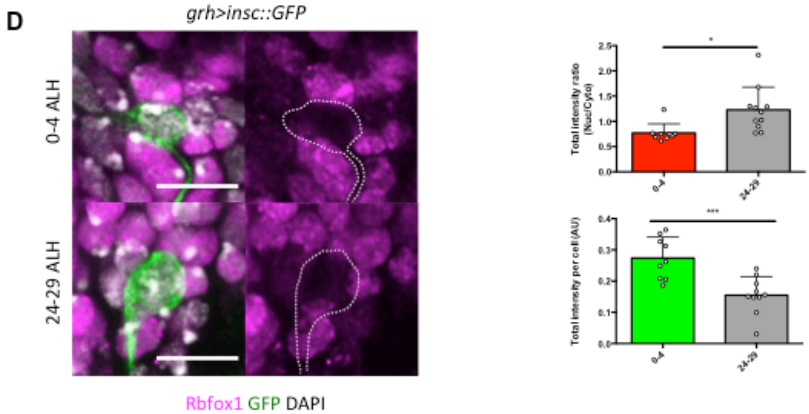
D
grh>insc::GFP
0-4 ALH
24-29 ALH
Rbfox1 GFP DAPI
Total Intensity ratio (Nuc/Cyto)
*
Total Intensity per cell (AU)
***
0-4
24-29

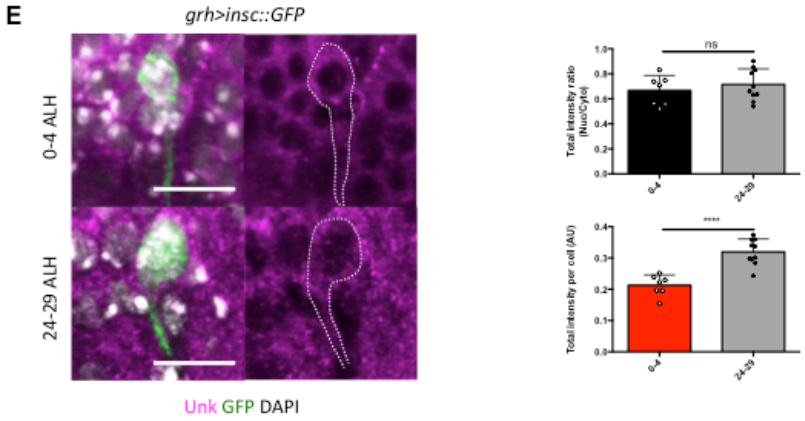

FIGURE 4.4. QUIESCENT *DROSOPHILA* NSCS SHOW DIFFERENCES IN LEVELS AND LOCALIZATION OF SEVERAL STRESS-RELATED OR RNA-BINDING PROTEINS WHEN COMPARED TO ACTIVE NSCS.

NSCs were stained 0-4 hr and 24-29 hr ALH, (Green) insc::GFP, (Grey) DAPI and (Magenta) (A) DDX6, (B) TIAR, (C) Ran, (D) Unk, (E) Rbfox. Quantification of nucleocytoplasmic ratio of target protein per cell (n=9) was carried out, as well as quantification of total intensity of target protein per cell (n=9). Scale bars: 10 μm.

4.7 DISCUSSION

In this chapter:

- I showed that Nup composition is altered in quiescent *Drosophila* NSCs when compared to active.
- I showed there was no difference in compartmentalization of classical NLSs in quiescent and active *Drosophila* NSCs.
- I showed that compartmentalization and/or levels of RNA, RNA-binding proteins, and stress-related proteins in quiescent and active *Drosophila* NSCs are altered.

4.7.1 QUIESCENT NSCS PRESENT ALTERED NUP LEVELS

I hypothesized that if Nup downregulation leads to NSC quiescence in *Drosophila*, Nup levels should be altered in quiescent NSCs. As isolating quiescent NSCs to quantify their Nup levels would prove a difficult and time-consuming enterprise, I

relied on available antibodies to stain and quantify Nups in both active and quiescent NSCs. The data gathered on the four working antibodies I obtained were not clear-cut. While Nup62 appeared to be downregulated at the protein level in quiescent NSCs, which fit with my hypothesis, both Nup98 and Nup96 appeared to be upregulated in quiescent NSCs, and Nup358 appeared to be unaltered between the two conditions (this result might be explained to the lack of specificity of the antibody which is known to also recognize Nup62, Nup153, and Nup214).

Hence, quiescence might not be easily described by an overall downregulation of Nups, or the downregulation of a particular subset of Nups, but by an altered stoichiometry of the NPC. Characterization of the actual NPC stoichiometry would require the availability of antibodies for every Nup in *Drosophila*, or the use of high-resolution microscopy. It is at the moment impossible to conclude on the potential leakiness of the pores in quiescence and the diffusion of proteins that would follow. It would be interesting to map all the Nups and their level in quiescent NSCs and correlate the results to the RNAi screen: are the positive hits actually downregulated or not in physiological quiescence? I already brought part of the answer as I showed that Nup98 is actually upregulated in quiescence.

4.7.2 Classical NLSs localization is unaltered in quiescence

Classical NLSs have been characterized and studied at length, which is not the case of other non-classical NLSs. Both monopartite and bipartite classical NLSs have been shown to belong in transcription factors and some RNA-binding proteins (Boulikas, 1994; Cokol, Nair, & Rost, 2000; Lange et al., 2007; Soniat & Chook, 2015). In an attempt to narrow down the RNA-related targets for quiescence regulation, I decided to assess the compartmentalization of a monopartite and a bipartite classical NLSs in quiescent and active NSCs. Both NLSs appeared to be segregated in the nucleus no matter the condition, hence it appears that NLS

compartmentalization is the same in active and quiescent NSCs. Nevertheless, this experiment did not asses the rate of import of the two NLSs, it is thus possible that if both NLSs are imported, one of the two might be imported faster or more efficiently than the other. This would be interesting to look at and could be assessed through fluorescence loss in photobleaching (FLIP) or fluorescence recovery after photobleaching (FRAP) experiments.

4.7.3 RNA SEGREGATION IN QUIESCENT DROSOPHILA *NSCS*

I showed that quiescent *Drosophila* NSCs accumulate polyA RNA in their nucleus while active NSCs present a higher concentration in their cytoplasm. This observation fits with the previous data showing that a majority of Nups and karyopherins involved in RNA export lead to a quiescent phenotype when downregulated in NSCs. Nuclear accumulation of polyA RNA has previously been reported in Kaposi-s sarcoma-associated herpesvirus (Massimelli, Majerciak, Kruhlak, & Zheng, 2013) and in saccharomyces cerevisiae following NUP133 downregulation (O. Li et al., 1995), but has not been reported in quiescent SCs. Interestingly, I observed nuclear polyA RNA accumulation in NSCs after Snx downregulation, thus drawing the quiescent phenotype closer to physiological quiescence.

I then decided to look at stress-related proteins, with the rationale that if RNA accumulates, it needs to be stabilized, and that quiescence might be a state of stress for the SCs; as plant cells have for example been shown to aggregate RNA in their nucleus during hypoxia (Niedojadło, Dełeńko, & Niedojadło, 2016). DDX6 is an RNA helicase found in P-bodies and stress granules, and functions in translation suppression and mRNA degradation, it has also been implicated in different types of cancer (Cho et al., 2016; Tajirika et al., 2018). TIAR, also called Rox8 in *Drosophila* melanogaster, is a stress granule RNA-binding protein, which regulates various

activities including translational control, splicing and apoptosis (Kedersha, Gupta, Li, Miller, & Anderson, 1999; Kim et al., 2013; Lafarga et al., 2018; Taupin, Tian, Kedersha, Robertson, & Anderson, 1995). Both concentrations of DDX6 and TIAR appeared to be lower overall in quiescent NSCs, which might disprove the hypothesis that quiescence is a state of stress. Nevertheless, TIAR appears to be more present in the nucleus of quiescent NSCs compared to active, suggesting that TIAR might indeed be binding to the polyA RNA accumulated in the nucleus. It is also interesting to note that TIAR appeared to localize in the fiber of reactivating NSCs, which might help to understand the yet to be described role of the fibers in quiescent *Drosophila* NSCs.

Ran concentration and ratio were unaltered in quiescent NSCs. Ran is a small GTP binding protein belonging to the RAS superfamily that is essential for the translocation of RNA and proteins through the nuclear pore complex, and is also involved in control of DNA synthesis and cell cycle progression (Kurisaki et al., 2006; Lowe et al., 2015; Steggerda & Paschal, 2002). This result was to be expected considering the broad involvement of Ran in different mechanisms. This suggests that nucleocytoplasmic transport might not be regulated in a homogeneous manner, but in a specific manner.

Rbfox1 is part of the Fox-1 family of RNA-binding proteins, which is evolutionarily conserved and regulates tissue-specific alternative splicing (Fogel et al., 2012; S. Sun, Zhang, Fregoso, & Krainer, 2012). Concentration of Rbfox1 appeared to be higher and more cytoplasmic in quiescent NSCs, nevertheless, the low intensity obtained lead me to be wary of the results. Moreover, it appears clearly that the levels of Rbfox are much higher and almost exclusively nuclear in surrounding cells. The results would be considered for discussion if I were able to isolate the NSCs

without the surrounding glia, allowing me to bring out a visible signal in the NSCs. But as of now, I would refrain from concluding anything from the obtained results.

Unk is an evolutionarily conserved RNA-binding protein that regulates translation of its target genes and is required for the establishment of the early bipolar neuronal morphology (Murn et al., 2015). Unk has been shown to be negatively regulated by mTOR (Avet-Rochex et al., 2014), which in turn has been shown to regulate quiescence (Sousa-Nunes et al., 2011a). Hence, the lower concentration of Unk observed in quiescent NSCs fits with the TOR upregulation during quiescence.

5 NUCLEOCYTOPLASMIC REGULATION OF QUIESCENCE IS CONSERVED IN MURINE AHNSCS

5.1 CHAPTER AIM

This chapter will:

- Introduce models of mouse AHNSCs and MSCs.
- Describe data obtained by collaborators and colleagues.
- Assess passive transport in quiescent and active AHNSCs.
- Assess differential compartmentalization and levels of RNA, RNA-binding proteins, and stress-related proteins in quiescent and active mouse AHNSCs.
- Assess differential compartmentalization and levels of RNA in quiescent and active mouse MSCs.

5.2 INTRODUCTION: MOUSE MODELS TO STUDY CONSERVATION IN MAMMALS

Mouse AHNSCs were obtained from Noelia Urbán, in our collaborator Dr François Guillemot's Lab. Adult neurogenesis occurs in the sub-granular zone of the dentate gyrus of mammals (Eriksson et al., 1998; Spalding et al., 2013), where a heterogeneous pool of NSCs exists with a radial glia-like morphology (Gebara et al., 2013). Adult neurogenesis and maturation of new neurons in the adult CNS are involved in learning and memory, stress responses, and mood regulation (Kempermann, Krebs, & Fabel, 2008; Sahay et al., 2010; Zhou et al., 2013). In contrast to embryonic neurogenesis, adult neurogenesis is regulated by neuronal activity as represented by parvalbumin interneurons regulating adult NSCs within the dentate gyrus (Kriegstein & Alvarez-buylla, 2011). Many niche signals have been

identified, but it is unclear how they influence the choice of stem cells to remain quiescent or divide (Ming & Song, 2011). The Guillemot Lab NSC quiescence was modeled in culture by replacing the mitogen EGF with BMP4 in the culture medium of AHNSCs (Martynoga et al., 2013; Urbán et al., 2017).

Isabelle Blomfield, from Dr François Guillemot's Lab, carried out a transcriptome analysis of active versus quiescent mAHNSCs (unpublished, personal communication). Interestingly, 30 different Nups appeared to be significantly downregulated at the RNA level in quiescent mAHNSCs, out of which 11 were homologs of *Drosophila* Nups leading to quiescent NSC phenotypes (Nup98, Nup62, Nup107, Nup205, Sec13, Seh1l, Nup85, Nup93, Nup133, Nup214, and Nup153); and 16 different karyopherins (and associated proteins) appeared to be significantly downregulated at the RNA level in quiescent mAHNSCs, out of which 7 were homologs of *Drosophila* karyopherins leading to quiescent NSC phenotypes (Ran, RanGap1, Rcc1, Ranbp3, Kpnb1, Tnpo1, and Tnpo3). These first observations suggest that quiescence regulation, or at least characteristics of quiescent NSCs, might similarly be related to nucleocytoplasmic transport machinery in both the *in vivo* and the *in vitro* models.

Additionally, 19 proteins involved in RNA binding, transport and processing also appeared to be downregulated at the RNA level in quiescent mAHNSCs (Thoc3, Thoc5, Thoc7, Ddx39b, Ddx39, Alyref, Iws1, Fyttd1, Nxt1, Ncbp1, Magoh, Rbm8a, Eif4a3, U2af2, U2af1, Cetn2, Ddx19a, Slbp, and Mbnl1); while proteins involved in positive regulation of transcription from RNA polymerase II promoter and positive regulation of RNA metabolic process appeared upregulated at the RNA level in quiescent mAHNSCs (e.g. Elf1, Sox2, TgfB3, Sox4, Nfix, Sox8, Fos, and Ascl1). This suggests that transcription still happens in quiescent mAHNSCs, but that export of RNA out of the nucleus might be altered.

MSCs were obtained from the extensor digitorum longus (EDL) muscle of mice by Nicolas Figeac, from Dr Peter Zammit's Lab. Satellite cell differentiation is essential to provide newly formed myofibers while satellite cell self-renewal is also essential to replenish the satellite cell pool. Maintenance of this balance between satellite cell differentiation and self-renewal is required for muscle homeostasis. Satellite cells are characterized by the expression of the paired type homeobox transcription factor, Pax7, identified as the first quantifiable marker for both the quiescent and activated satellite cells and essential for their development and survival (Lepper, Conway, & Fan, 2009; Seale & Rudnicki, 2000); nevertheless, MSCs have been shown to be a very heterogeneous population (Beauchamp et al., 2000; Cornelison, Filla, Stanley, Rapraeger, & Olwin, 2001; Cornelison & Wold, 1997; Fukada et al., 2007b; Gnocchi, White, Ono, Ellis, & Zammit, 2009; Irintchev, Zeschnigk, Starzinski-Powitz, & Wernig, 1994). Heterogeneity has also been reported in MSCs from different muscles, e.g. gene expression differences as well as the distinct stem cell abilities in satellite cells from EDL and masseter muscle (Ono, Boldrin, Knopp, Morgan, & Zammit, 2010).

5.3 PRELIMINARY DATA

Alina Miedzik, technician in the Sousa-Nunes Lab, carried out western blotting of Nups in active and quiescent AHNSCSs (Appendix Figure 5.1A). Results show a Downregulation of Nup93, Nup210, Pom121, Nup50, and Nup62 in quiescent mAHNSCs, while Nup37 and Nup98 appear to be upregulated (Appendix Figure 5.1B). If downregulation of Nup93 and Nup62 corroborates the results obtained in the *Drosophila* RNAi screen, upregulation of Nup98 would appear to go against the previous results. Alina M. also carried out ICC of Nups in active and quiescent mAHNSCs (Appendix Figure 5.1C). Quantification of total intensity per cell showed downregulation of Sec13, Nup43, Ndc1, Nup50, and Nup54, in agreement of previous results in *Drosophila*; but upregulation of Nup93, Nup160, Nup37, Nup188,

Nup53, Nupl1, Nupl2, Pom121, Nup358, Rae1, and Nup98 in quiescent mAHNSCs would appear to go against the previous results (Appendix Figure 5.1D). Through these experiments, Alina M. showed that quiescent mAHNSCs present an altered Nup stoichiometry when compared to active mAHNSCs, which is similar to the results I obtained in *Drosophila* NSCs. Even though the exact stoichiometry cannot be characterized yet, and even tough the results obtained are not identical to what was seen in *Drosophila*, the data gathered by Alina M. suggests a conservation of quiescent characteristics in mammals.

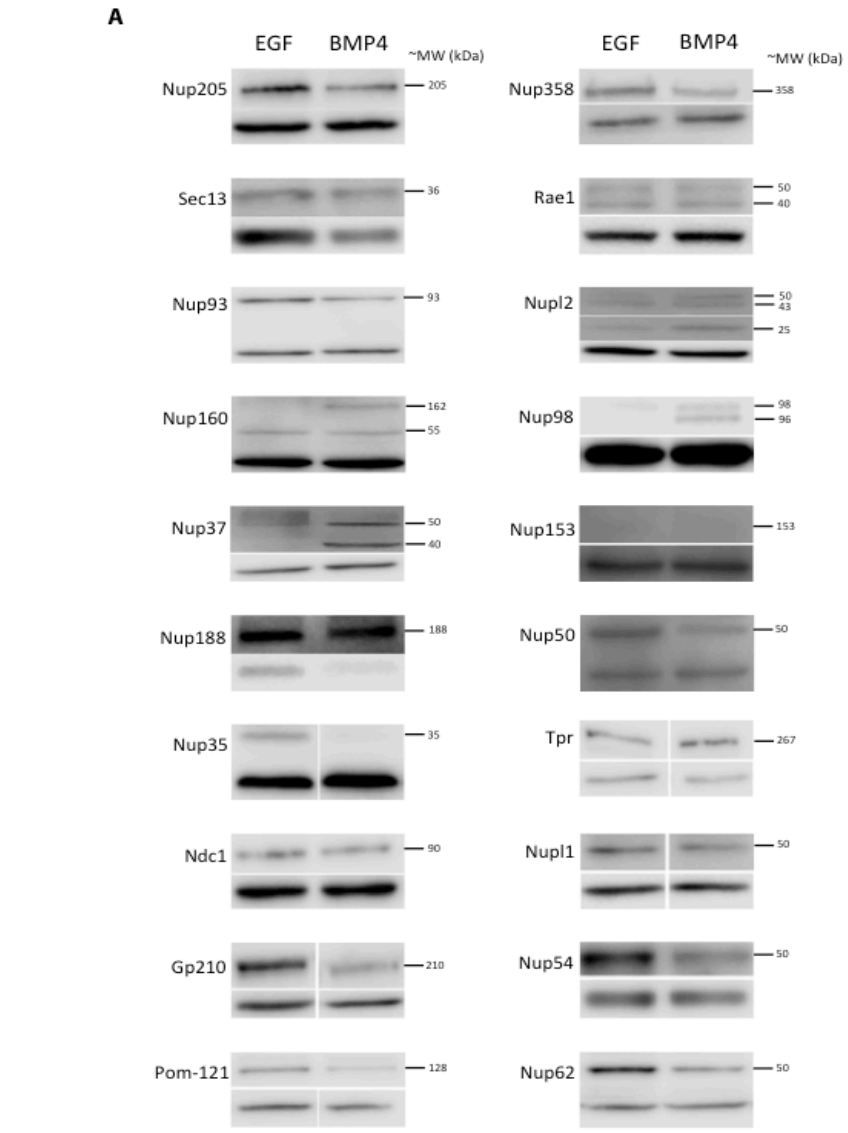
A
EGF
BMP4
~MW (kDa)
Nup205
205
Sec13
36
Nup93
93
Nup160
162
55
Nup37
50
40
Nup188
188
Nup35
35
Ndc1
90
Gp210
210
Pom-121
128
Nup358
358
Rae1
50
40
Nupl2
50
43
25
Nup98
98
96
Nup153
153
Nup50
50
Tpr
267
Nupl1
50
Nup54
50
Nup62
50

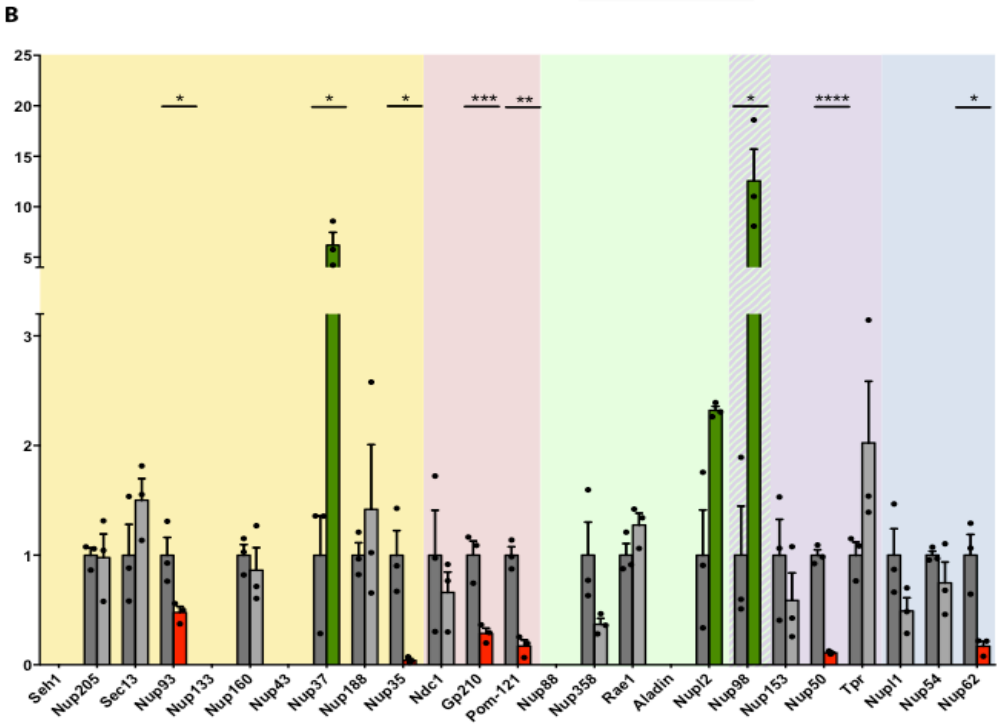
B
25
20
15
10
5
3
2
1
0
*
*
*
***
**
*
****
*
Seh1
Nup205
Sec13
Nup93
Nup133
Nup160
Nup43
Nup37
Nup188
Nup35
Ndc1
Gp210
Pom-121
Nup88
Nup358
Rae1
Aladin
Nupl2
Nup98
Nup153
Nup50
Tpr
Nupl1
Nup54
Nup62

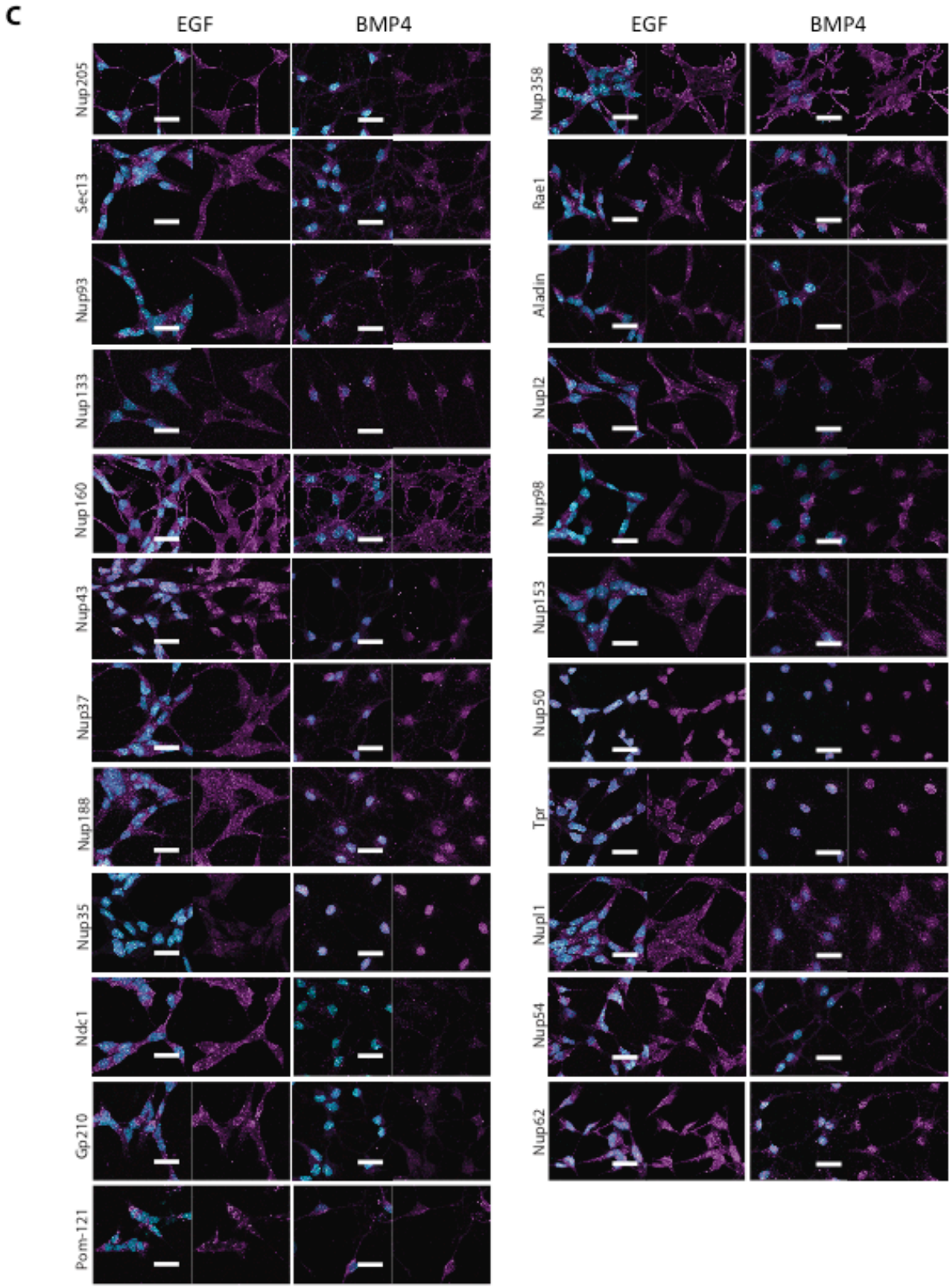
C
EGF
BMP4
EGF
BMP4
Nup205
Sec13
Nup93
Nup133
Nup160
Nup43
Nup37
Nup188
Nup35
Ndc1
Gp210
Pom-121
Nup358
Rae1
Aladin
Nupl2
Nup98
Nup153
Nup50
Tpr
Nupl1
Nup54
Nup62

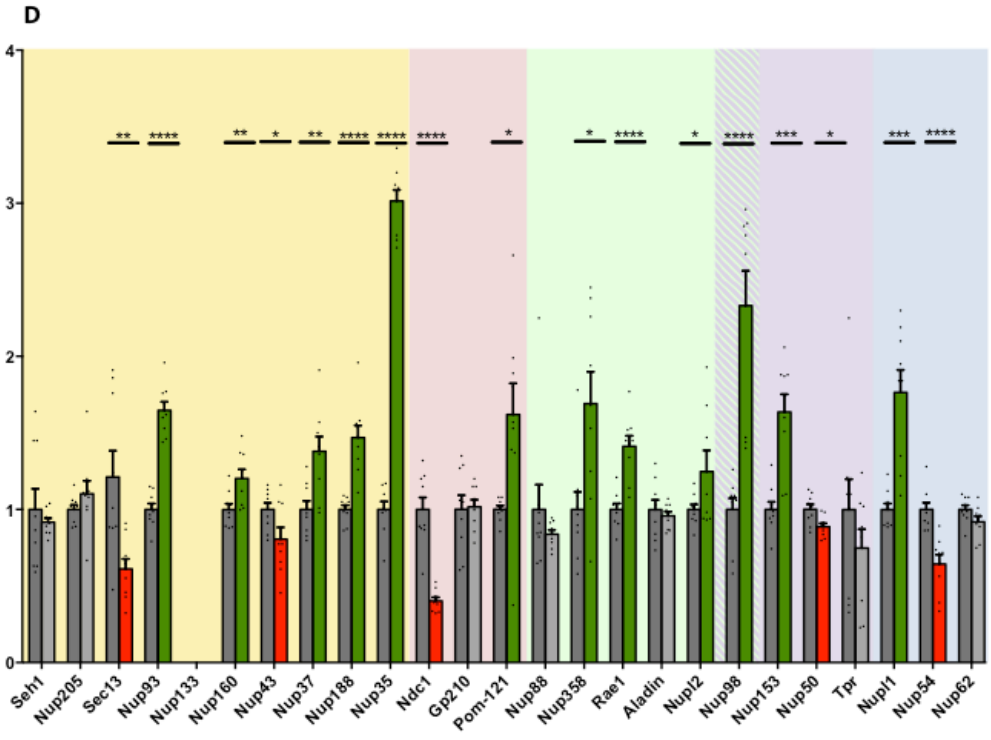

APPENDIX FIGURE 5.1: NUP COMPOSITION OF ACTIVE VERSUS QUIESCENT AHNSCS.

(A) Western Blot bands obtained in active versus quiescent AHNSCs. (B) Quantification of band intensity. For each Nup, left histogram corresponds to active cells while right histogram corresponds to quiescent cells. (C) IHC stains of active and quiescent mAHNSCs. (Magenta) Nups, (Cyan) DAPI. (D) Quantification of total intensity per cell for each Nup. For each Nup, left histogram corresponds to active cells while right histogram corresponds to quiescent cells. Scale bars: 20 μm.

5.4 PASSIVE TRANSPORT IS ALTERED IN ACTIVE VERSUS QUIESCENT AHNSCS

An altered Nup composition in quiescent versus active mAHNSCs might lead to an altered NPC permeability before an altered active transport of targets. mAHNSCs were incubated with FITC conjugated dextrans for 2, 14 or 24 hr; nuclear to cytoplasmic ratio of intensity per area was quantified and plotted. 20 kDa FITC-dextran incubation (Figure 5.2A) lead to an increased ratio in quiescent mAHNSCs, suggesting an increased passive permeability of NPCs for proteins around 20 kDa (Figure 5.2B). 40 kDa FITC-dextran incubation (Figure 5.2C) did not lead to any significantly different ratio, suggesting no altered permeability for proteins 40 kDa and up (Figure 5.2D).

A

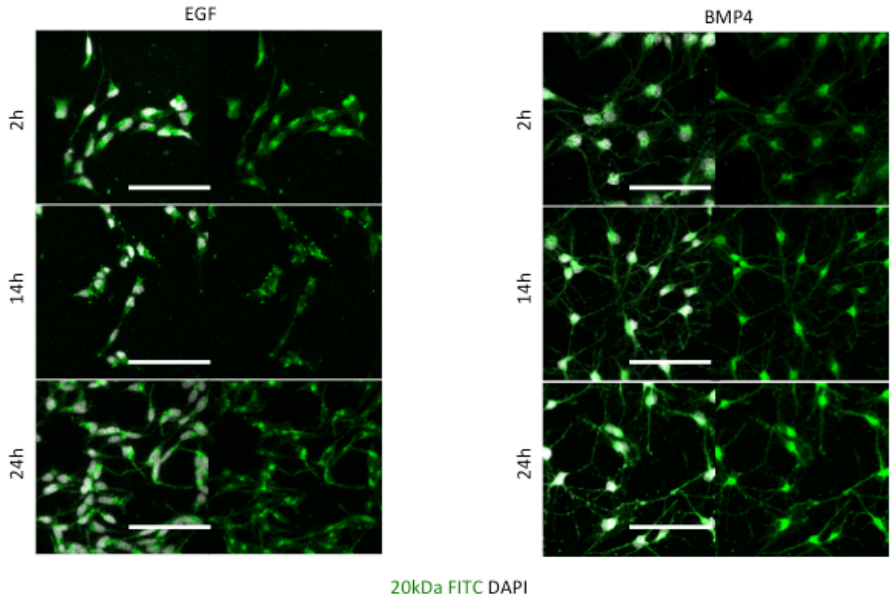
EGF
BMP4
2h
14h
24h
2h
14h
24h
20kDa FITC DAPI

B

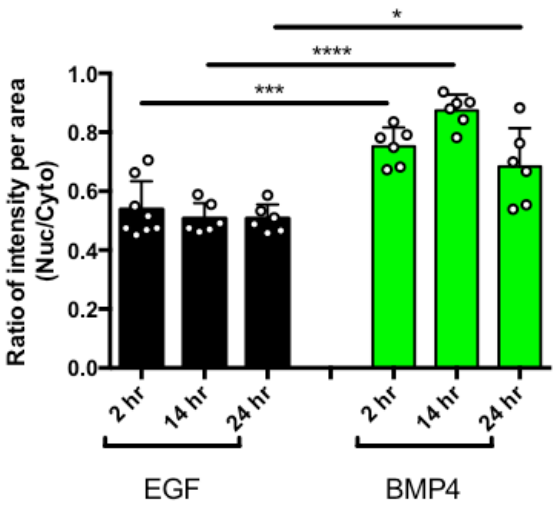
*
****
***
Ratio of intensity per area (Nuc/Cyto)
1.0
0.8
0.6
0.4
0.2
0.0
2 hr
14 hr
24 hr
2 hr
14 hr
24 hr
EGF
BMP4

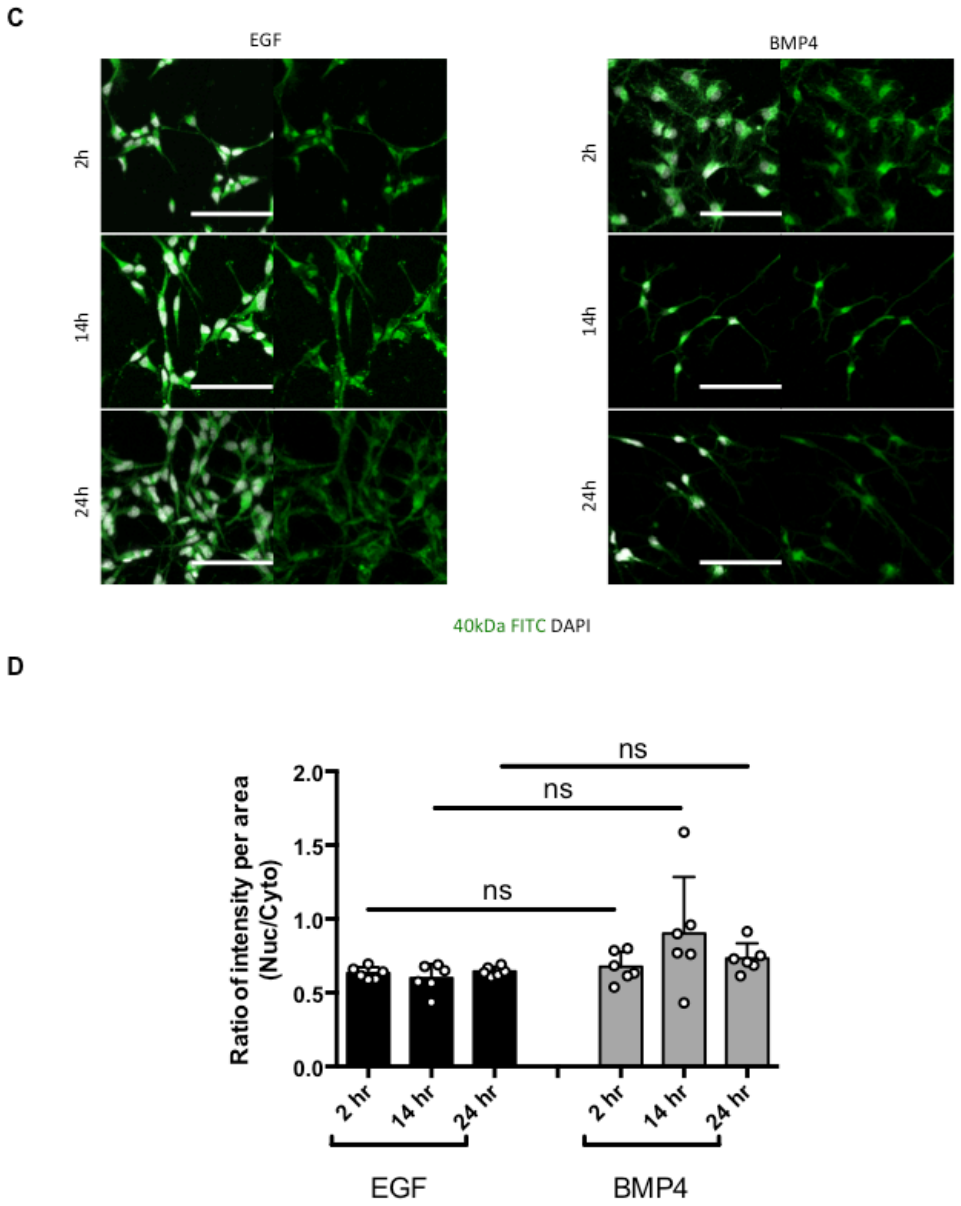

FIGURE 5.2. LONG EXPOSURE OF MAHNSCS TO FITC-DEXTRANS SHOWS AN INCREASED LEAKINESS OF THE NPC FOR 20 KDA FITC-DEXTRANS.

mAHNSCs were exposed for 2, 14 and 24 hr to 20 or 40 kDa dextrans. (A) IHC of active and quiescent mAHNSCs, (Grey) DAPI, (Green) 20 kDa FITC-dextran. (B) Quantification of nucleocytoplasmic ratio of 20 kDa FITC-dextran intensity per area. (A) IHC of active and quiescent mAHNSCs, (Grey) DAPI, (Green) 40 kDa FITC-dextran. (B) Quantification of nucleocytoplasmic ratio of 40 kDa FITC-dextran intensity per area. Scale bars: 40 μm.

The incubation times of the previous experiment brought concerns about FITC-dextran nuclear to cytoplasm ratios to be altered in both conditions by mitosis; nuclear membrane breakdown would homogenize FITC-dextran concentrations in both compartments rendering quantifications irrelevant. Hence the experiment was repeated on quiescent and active mAHNSCs with different molecular weights (4, 20, 40 and 70 kDa Figure 5.3A-D) and a shorter incubation time of 20 min. Nuclear to cytoplasmic ratio of intensity per area was higher in quiescent mAHNSCs for all four different molecular weights (1.84, 2.43, 1.80 and 1.36 times respectively). These results suggested a higher NPC permeability for all protein up to 70 kDa in quiescent mAHNSCs.

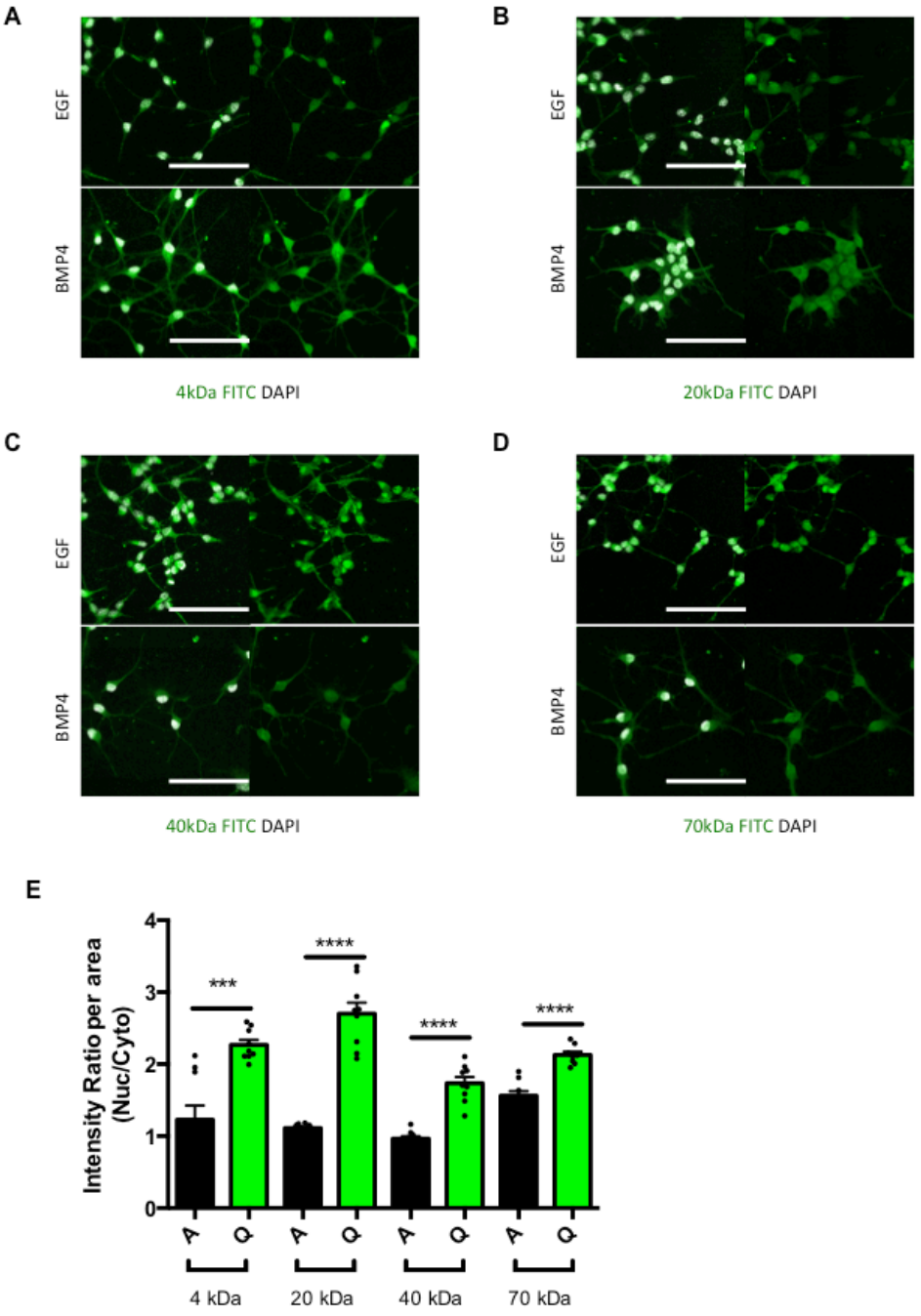

FIGURE 5.3. QUIESCENT MAHNSCS PRESENT A DECREASED NPC LEAKINESS FOR FITC-DEXTRAN BETWEEN 20 AND 70 KDA WHEN COMPARED TO ACTIVE MAHNSCS.

Active and Quiescent mAHNSCs were exposed to (A) 7kDa (B) 20kDa (C) 40kDa (D) 70 kDa FITC-dextrans for 20 minutes. (Green) FITC-dextran, (Grey) DAPI. (E) Quantification of nucleocytoplasmic ratio of FITC-dextran intensity per area. Scale bars: 40 μm.

5.5 RNA LEVELS AND LOCALIZATION ARE ALTERED IN MOUSE AHNSCS

To mirror results obtained in *Drosophila*, *in situ* hybridization of PolydT probes was carried out in quiescent and active mAHNSCs. EGF stimulated mAHNSCs were cultured in parallel to BMP4 stimulated mAHNSCs for 0.5, 1, 2 and 3 days to assess polyA RNA localization during quiescence entry (Figure 5.4A-B). BMP4 stimulated mAHNSCs were also cultured for 7, 14 and 21 days to observe the behavior of polyA RNA through long quiescence (Figure 5.4C). Nuclear to cytoplasmic ratio of PolydT probe intensity per area was quantified for every time-point. Ratio did not appear significantly different at 0.5, 1 or 2 days but ratio for 3-day BMP4-stimulated mAHNSCs was 2.09 times higher than in EGF-stimulated mAHNSCs. Nuclear retention of polyA RNA appeared to increase with time in quiescent mAHNSCs, as ratio appeared 3.02, 2.84, and 4.39 times higher in 7, 14, and 21-day BMP4-stimulated mAHNSCs respectively (Figure 5.4D). Nuclear retention of RNA is thus higher in quiescent mAHNSCs than in active mAHNSCs, and increases the longer cells are in a quiescent state. Total intensity of PolydT probe per cell was quantified in 3-day EGF-stimulated as well as in 3, 14, and 21-day BMP4-stimulated mAHNSCs (Figure 5.4E). Total PolydT probe intensity was lower in quiescent compared to active mAHNSCs (0.55 times) suggesting that poly RNA levels are lower in quiescent mAHNSCs.

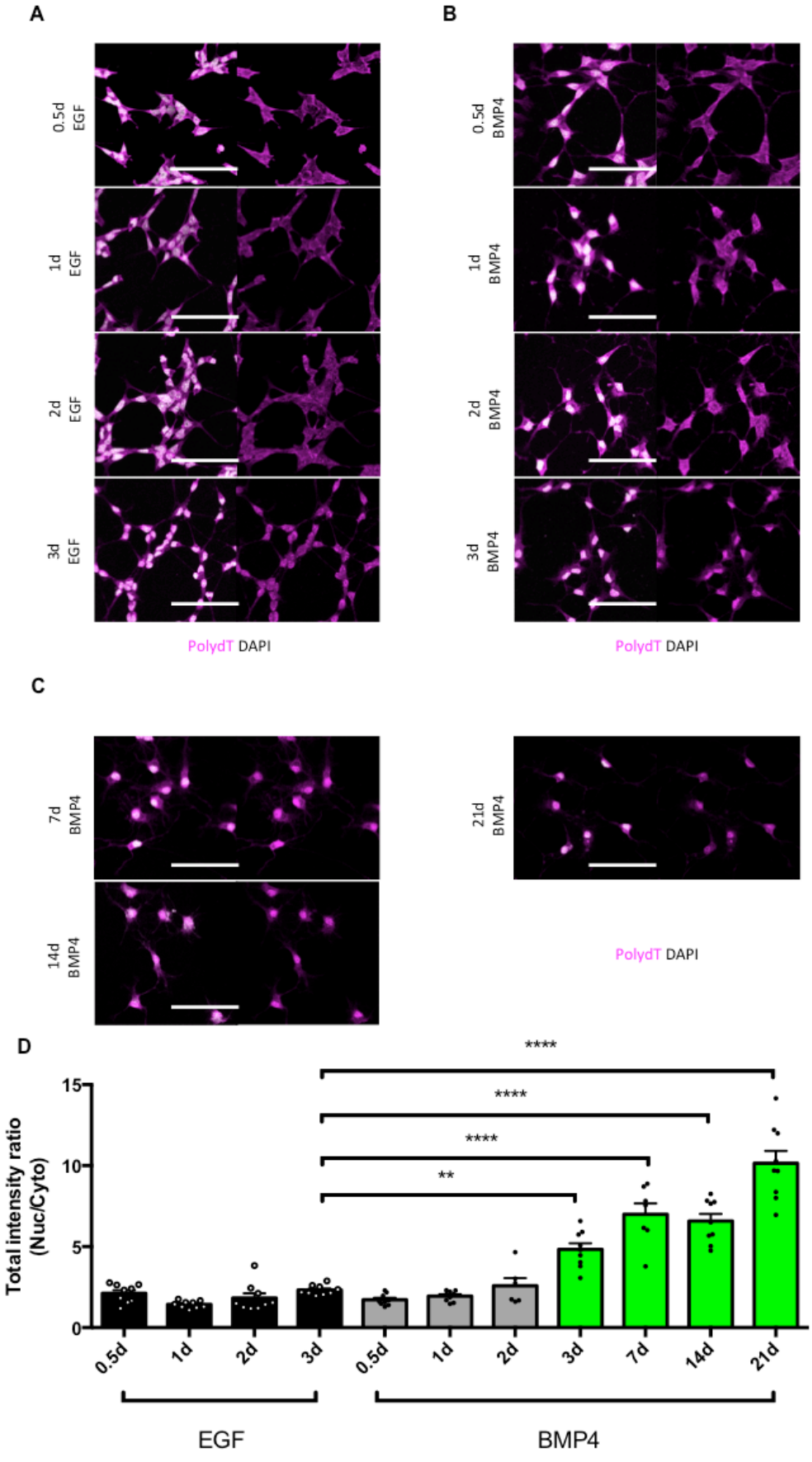
A
0.5d EGF
1d EGF
2d EGF
3d EGF
PolydT DAPI
B
0.5d BMP4
1d BMP4
2d BMP4
3d BMP4
PolydT DAPI
C
7d BMP4
14d BMP4
21d BMP4
PolydT DAPI
D
Total intensity ratio (Nuc/Cyto)
15
10
5
0
****
****
****
**
0.5d
1d
2d
3d
0.5d
1d
2d
3d
7d
14d
21d
EGF
BMP4

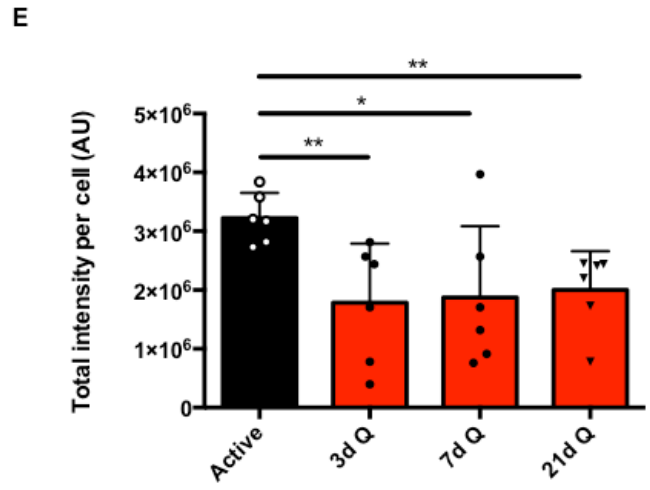

FIGURE 5.4. MAHNSCS GRADUALLY CONCENTRATE RNA TO THEIR NUCLEUS WHEN ENTERING QUIESCENCE.

When compared to (A) active mAHNSCs, (B) mAHNSCs show RNA retention in their nucleus after BMP4 stimulation for 3 d. Nuclear accumulation of RNA keep increasing after (C) 7, 14 and 21 d of BMP4 stimulation. (Magenta) PolydT probe, (Grey) DAPI. (D) Quantification of nucleocytoplasmic ratio of PolydT probe intensity per area. (E) Quantification of total intensity of PolydT probe per cell. Scale bars: 40 μm.

5.6 RNA-BINDING PROTEINS LEVELS AND LOCALIZATION ARE ALTERED IN MOUSE AHNSCS

Following on the observation that RNA is indeed segregated to the nucleus in quiescent mAHNSCs as observed in quiescent *Drosophila* NSCs, focus was drawn to target proteins potentially involved in RNA transport and/or stability: DDX6, TIAR, Rbfox1, Rbfox2, Rbfox3 and Unk. Focus was also drawn to Snuportin-1 (Snupn), a small nuclear ribonucleoprotein (snRNP)-specific nuclear import adapter. In all targets, total intensity per area and nuclear to cytoplasmic ratio of intensity per area was quantified in BMP4 or EGF-stimulated mAHNSCs. DDX6 ratio appeared lower in quiescent mAHNSCs by 0.51 times, but their total intensity was 1.29 times higher (Figure 5.5A). TIAR ratio was 0.62 times lower in quiescent mAHNSCs while their total intensity was 5.37 times higher (Figure 5.5B). Both ratio and total intensity were

similar in Snupn (Figure 5.5C) and Rbfox1 (Figure 5.5D). Rbfox2 ratio was 0.84 times lower in quiescent mAHNSCs, and total intensity was 0.85 times lower (Figure 5.5E). Rbfox3 ratio was 0,87 times lower in quiescent mAHNSCs, but total intensity was similar in both conditions (Figure 5.5F). Finally, Unk ratio was lower by 0.55 times in quiescent mAHNSCs while their total intensity was 1.40 times higher (Figure 5.5G).

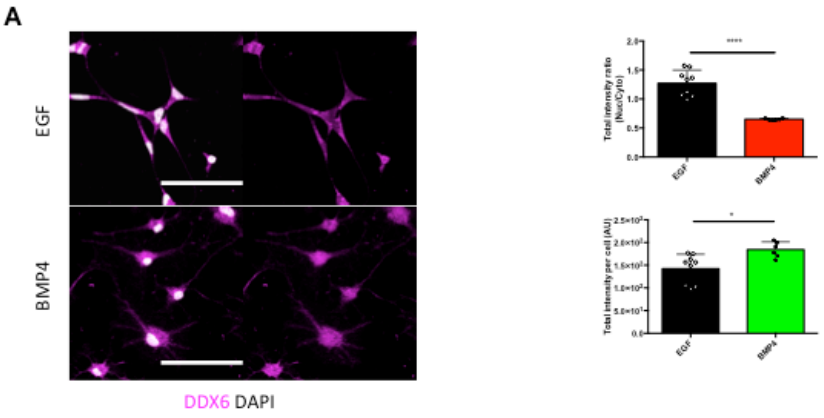
A
EGF
BMP4
DDX6 DAPI
B
EGF
BMP4
TIAR DAPI
C
EGF
BMP4
Snupn DAPI
D
EGF
BMP4
Rbfox1 DAPI

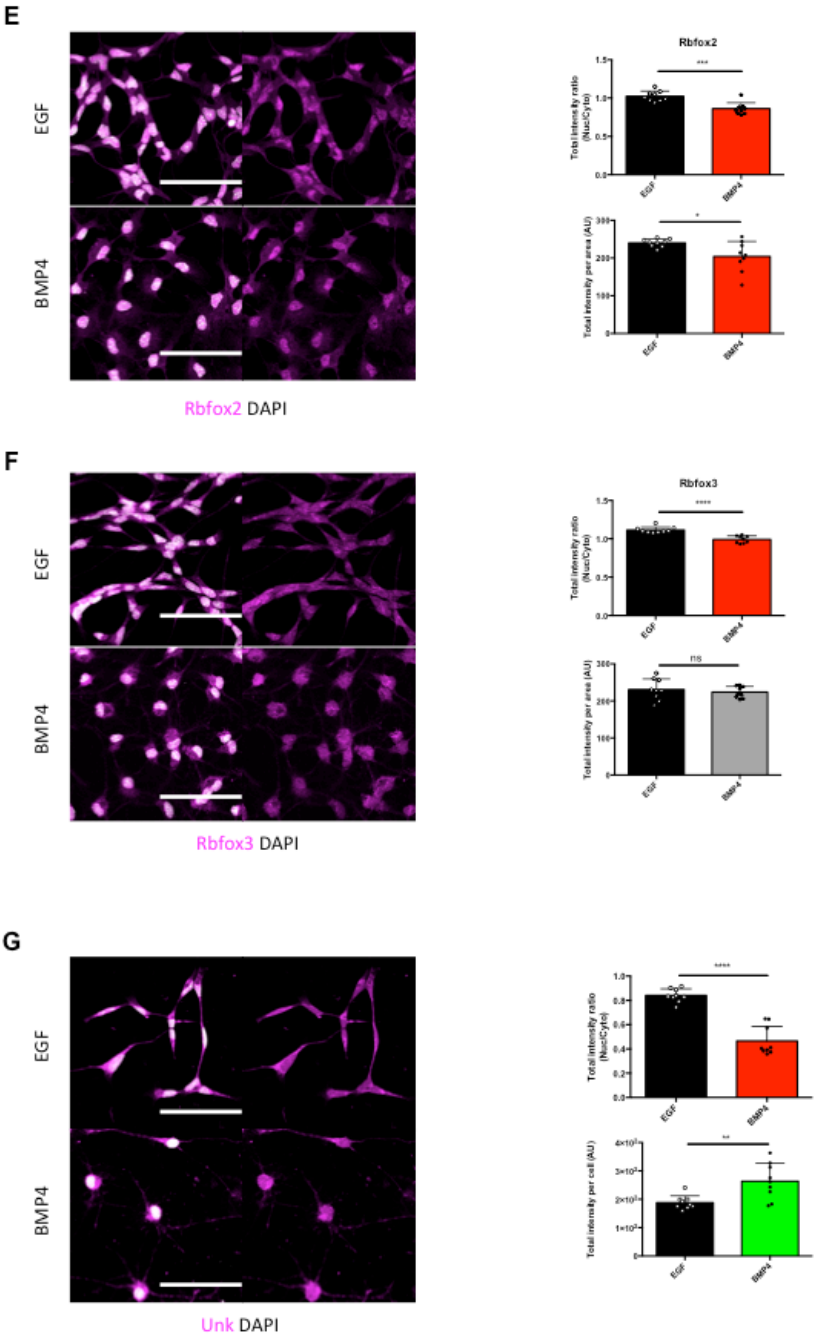

FIGURE 5.5. QUIESCENT MAHNSCS SHOW DIFFERENCES IN LEVELS AND LOCALIZATION OF SEVERAL STRESS-RELATED OR RNA-BINDING PROTEINS WHEN COMPARED TO ACTIVE MAHNSCS.

Active and quiescent (BMP4 3 d) mAHNSCs were stained, (Grey) DAPI and (Magenta) (A) DDX6, (B) TIAR, (C) Snupn, (D) Rbfox1, (E) Rbfox2, (F) Rbfox3, (G) Unk. Quantification of nucleocytoplasmic ratio of intensity of target protein per area (n=9) was carried out, as well as quantification of total intensity of target protein per area (n=9). Scale bars: 40 μm.

5.7 RNA LEVELS AND LOCALIZATION ARE ALTERED IN MOUSE MSCS

In an attempt to assess if results observed in *Drosophila* NSCs and mAHNSCs could potentially be universal in SCs, mMSCs were obtained from Dr Peter Zammit's Group. *In situ* hybridization of PolydT probes was carried out and ratio of nuclear to cytoplasmic intensity per area as well as total intensity per area were quantified. PolydT probe ratio was 3.10 times higher in quiescent mMSCs while their total intensity was 0.62 times lower (Figure 5.6A-B).

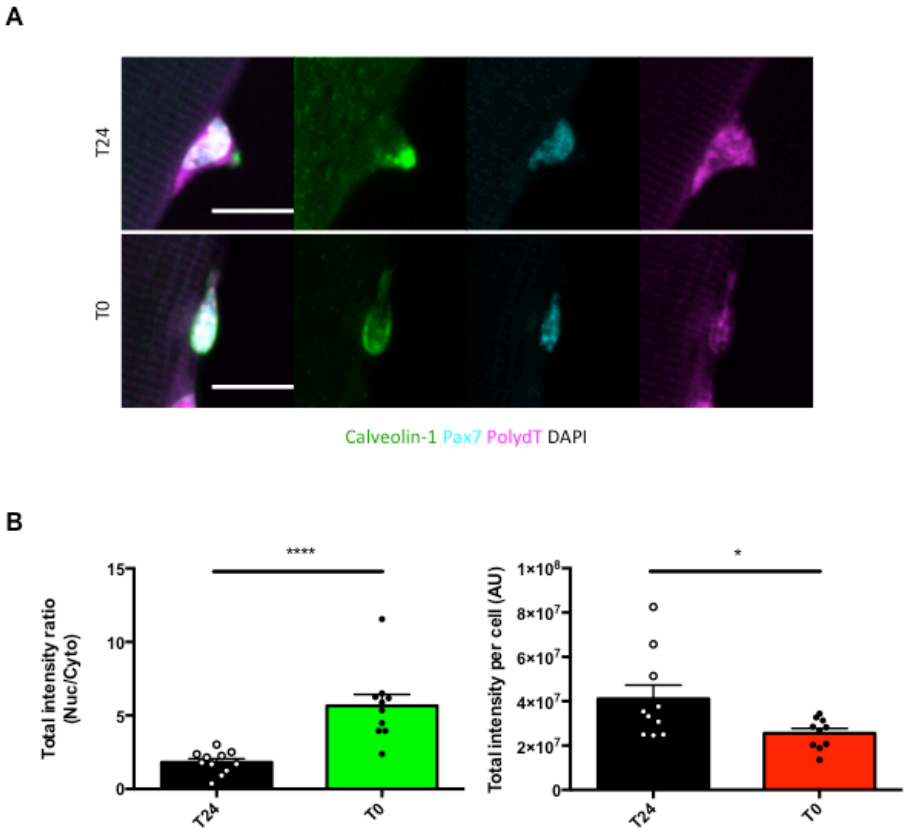

FIGURE 5.6. QUIESCENT MMSCS ACCUMULATE RNA IN THEIR NUCLEUS WHEN COMPARED TO ACTIVE MSCS.

MSCs were extracted from the EDL of adult mice and stained (A) at T24 and T0, (Green) Calveolin-1, (Cyan) Pax7, (Magenta) PolydT probe, (Grey) DAPI. (B) Quantification of nucleocytoplasmic ratio of intensity of PolydT probe per area (n=10) was carried out, as well as quantification of total intensity of PolydT probe per cell (n=10). Scale bars: 15 μm.

5.8 Discussion

The latent goal of my thesis is to compare regulation of NSC quiescence in *Drosophila* and a mammalian cell model. Both models have their advantages and drawbacks. The *Drosophila* model is convenient for genetic studies as tools like the UAS/GAL4 system are available, but *Drosophila* NSCs are not the best model of NSCs compared to mammalian ones. The mAHNSC model from our collaborator proves to be convenient for biochemistry as quiescence is easily induced, but it remains an in vitro model that is more artificial than an in vivo one. I hypothesize that, as Nups and karyopherins (Field, Koreny, & Rout, 2014; Peyro, Soheilypour, Lee, & Mofrad, 2015; Sampathkumar et al., 2013) as well as some aspects of NSC quiescence regulation (Ding et al., 2016; Paik et al., 2009; Renault et al., 2009; Sousa-Nunes, Yee, & Gould, 2011b; Yanagida, 2009) are highly conserved through evolution, implication of nucleocytoplasmic transport and NPC components in quiescence might be comparable in both models. Analogies can already be found in NSCs morphology. As described previously, *Drosophila* NSCs present a fiber when quiescent which disappears upon activation. While AHNSCs present cellular extensions in both quiescent and proliferating states, these extensions appear quantitatively longer during quiescence (Martynoga et al., 2013). While it is probable that results will not be the same in both models (O'Farrell, 2011), the goal is to try to find analogies, possibly homology, or eventually explain what brings differences in the regulation processes.

5.8.1 Nup levels appear altered in quiescent mAHNSCs

Both data sets from Isabelle Blomfield and Alina Miedzik show that Nup levels are altered in quiescent mAHNSCs at RNA and protein levels. Isabelle Blomfield also showed that quiescent mAHNSCs present downregulation of several karyopherins and RNA-binding protein at the RNA level. These observations resonate with the results obtained in *Drosophila* NSCs, indeed, Nups and karyopherins are altered in a

similar way in mouse quiescent mAHNSCs: NPC stoichiometry appears to be altered, and components involved in RNA export are downregulated.

5.8.2 PASSIVE TRANSPORT IS ALTERED IN MAHNSCS

In an attempt to assess NPC leakiness in quiescent mAHNSCs, I carried out dextran loading experiments. The first experiment involved loading mAHNSCs for different amounts of time and observing the nuclear to cytoplasmic ratio of dextran obtained. This experiment showed a higher leakiness for 20 kDa dextrans and no difference for 40 kDa dextrans. The design of this first experiment was flawed, as proliferating mAHNSCs would keep on dividing through the loading, homogenizing the dextran levels at each division. Hence I decided to repeat the experiment by loading mAHNSCs for a shorter time during which proliferation would be negligible. This experiment suggested an overall higher leakiness of NPCs in quiescent mAHNSCs for all dextrans tested. While this result is interesting, it does not tell us anything about NPC composition, NPC number, or dynamics of dextran diffusion through the pores. It would thus be important to assess NPC composition and number through high-resolution microscopy and IHC (Beck & Medalia, 2008; Hurt & Beck, 2015), while diffusion kinetics could be assessed through FRAP or FLIP (Bancaud, Huet, Rabut, & Ellenberg, 2010; Köster, Frahm, & Hauser, 2005).

5.8.3 RNA SEGREGATION IN MAHNSCS

I showed that quiescent mAHNSCs accumulate polyA RNA in their nucleus while active NSCs present a higher concentration in their cytoplasm, and that the longer the mAHNSCs are quiescent the more polyA RNA are accumulated in their nucleus. While the overall level of polyA RNA is lower in quiescent than in active mAHNSCs, it appears that RNA biogenesis is not arrested during quiescence, which does not mean that protein translation is happening. Nuclear retention of RNA strongly suggests that protein synthesis does not occur, but another convenient and direct

way to show the lack of protein translation would be an o-propargyl-puromycin stain (J. Liu, Xu, Stoleru, & Salic, 2012). Interestingly, overall levels of polyA RNA do not appear to decrease through quiescence, suggesting that, if cytoplasmic polyA RNA is degraded through time, nuclear polyA RNA might be stabilized or polyA RNA degradation rate might be lower than RNA biosynthesis rate. All observations were made mAHNSCs quiescent from 3 to 21 days; I was unable to observe results on older quiescent mAHNSCs as the SCs still showed a low rate of proliferation leading to overcrowded flasks. I attempted to split quiescent mAHNSCs and seed them to new flasks, but EdU stains showed that de-attaching quiescent mAHNSCs induced their reactivation (data not shown). Hence, I am unable to tell if nuclear polyA RNA concentration reaches a plateau, or if polyA RNA eventually starts degrading.

Nevertheless, the apparent stability of nuclear polyA RNA led me to assess the presence of potential stabilizing proteins in quiescent mAHNSCs. I carried out DDX6 and TIAR stainings as previously done in *Drosophila* NSCs. Both stress-related proteins showed a lower overall level in quiescent mAHNSCs, with a higher nuclear to cytoplasmic ratio. Interestingly, TIAR stain in *Drosophila* showed similar results, and TIAR has been associated with RNA binding and translational repression (Dember, Kim, Liu, & Anderson, 1996; Mazan-mamczarz, Lal, Martindale, Kawai, & Gorospe, 2006; Waris, Wilce, & Wilce, 2014). This observation could suggest that if quiescence might not be an overall state of stress for mAHNSCs, there might be a stress response segregated to the nucleus in order to stabilize polyA RNA and repress translation. A way to induce RNA segregation to the nucleus without relying on Nup or karyopherin downregulation would be to altered the levels of Snupn, which functions as a snRNP-specific nuclear import receptor (Natalizio & Matera, 2013). snRNPs are RNA-protein complexes that combine with unmodified pre-mRNA and various other proteins to form a spliceosome, a large RNA-protein molecular complex

upon which splicing of pre-mRNA occurs (Will & Lührmann, 2001). Hence, an altered level of Snupn would lead to an altered import of snRNPs, leading to an altered splicing of pre-mRNA, which would thus not be exported from the nucleus. This hypothesis is disproved by the unaltered levels of Snupn in quiescent mAHNSCs, suggesting that polyA RNA segregation relies mainly on Nups and karyopherins alteration. Rbfox stains were more reliable than in *Drosophila*. While Rbfox1 appeared unaltered, both Rbfox2 and Rbfox3 showed an overall lower concentration in quiescent mAHNSCs, with Rbfox2 showing a lower nuclear to cytoplasmic ratio in quiescent mAHNSCs. Finally, Unk levels appeared lower in quiescent mAHNSCs, as observed in *Drosophila*, while the nuclear to cytoplasmic ratio appeared higher. As previously stated, Unk is negatively regulated by mTOR, which in turn is upregulated in quiescent NSCs (Avet-Rochex et al., 2014; Yanagida, 2009), which explains the overall lower levels of Unk in quiescent mAHNSCs. While Unk did not show a higher nuclear to cytoplasmic ratio in *Drosophila*, Unk is a RNA-binding protein thus its concentration to the nucleus in quiescent mAHNSCs might not be surprising.

Even though all results are not exactly identical between the *Drosophila* and the mammalian NSC models, the similarities in Nup and karyopherin alteration, RNA segregation and RNA-binding proteins expression strongly suggest a conserved mechanism of NSC quiescence regulation.

5.8.4 RNA SEGREGATION IN MMSCS

As a preamble to broadening the results obtained in *Drosophila* NSCs and mAHNSCs, I observed polyA RNA segregation in mMSCs. Quiescent mMSCs presented a lower overall level of polyA RNA, which was strongly accumulated in their nucleus. While this experiment was carried out only once and needs to be repeated, and potentially modified to limit the reactivation of the quiescent mMSCs during dissection (Moyle & Zammit, 2014), it is an encouraging observation that the

RNA segregation uncovered through my thesis might be conserved not only between species, but also between SC types.

6 GENERAL CONCLUSION

In this thesis, I present a new cell metabolism mechanism linked to SC quiescence in *Drosophila* CNS, mAHNSCs and mMSC. Through these three models, I studied the role of nucleocytoplasmic transport in regulating SC quiescence and showed that downregulation of several nucleocytoplasmic transport components, Nups and karyopherins, leads to quiescence in *Drosophila* NSCs. This observation needs to be strengthened in the mAHNSC model to show its conservation in mammals. I started to design shRNA probes in order to downregulate Nup and/or karyopherin expression though lentivirus transfection. Adding an inducible expression actor to virus transfection would allow me to modulate shRNA expression, hence letting me show reversibility of any phenotype observed. Nevertheless, these experiments would not allow me to describe downregulation of nucleocytoplasmic transport components as either a cause or a consequence of NSC quiescence. Designing an experiment to this end would prove challenging, all the more as it is possible that both mechanisms are concurrent.

NPC composition study in *Drosophila* NSCs, coupled with work on mAHNSCs done by A. Miedzik, suggested a different Nup stoichiometry in quiescent NSCs when compared to proliferating NSCs. This difference in stoichiometry is most probably the cause of the altered passive transport observed in quiescent mAHNSCs. Even though results obtained though WB and IHC suggest the opposite, passive transport alteration could also be due to the presence of a lower number of nuclear pores on the nuclear membrane. Nuclear pores could be quantified through high-resolution imaging. Another important characteristic to assess, as previously stated, is kinetics of passive transport through NPCs, which could be described through FLIP or FRAP experiments. I also considered studying passive transport in *Drosophila* NSCs

through temperature-controlled expression of GFP different fusions –1x, 2x or 3xGFP- followed by quantifications, FLIP and/or FRAP experiments.

I then described nuclear RNA segregation in all three models and presented it as characteristic of SC quiescence. While RNA segregation needs to be described in all other types of SCs, the conservation observed in *Drosophila* NSCs, mAHNSCs, and mMSCs suggest that nuclear RNA segregation might indeed be common to all quiescent SCs. A screen compiling *in situ* hybridization through different species and SC types would need the use of tissue banks or global collaborations, but would present little technical challenge. The current lack of knowledge about a quiescence marker as well as the absence of observed nuclear RNA segregation in a physiological context would legitimize such an initiative. A marker of SC quiescence would open a world of possibilities in the filed of quiescence studies, which has heavy implications in regeneration and cancer studies and treatment.

To further characterize and understand the rationale of RNA segregation during quiescence, I decided to extract nuclear and cytoplasmic RNA from active and quiescent cells in order to carry out RNA-seq. Indeed, while *in situ* hybridization shows nuclear segregation of polyA RNA in quiescent cells, it lacks information on the exact RNA being segregated. RNA-seq would allow me to describe which RNA is segregated in the nucleus: are all RNA subtypes segregated to the nucleus of quiescent NSCs, or do quiescent NSCs segregate only particular subtypes of RNA? Unfortunately, cell fractionation is known to lead to poor RNA quality, and I did not manage to obtain samples for RNA-seq. This experiment needs to be carried out and optimized in the future as it holds key information in understanding the segregation mechanism.

Another interesting path to follow would involve the study of quiescence as a state of stress for SCs. I showed that DDX6 and TIAR appeared to localize preferably in the nucleus of quiescent *Drosophila* NSCs and mAHNSCs, suggesting that they are involved RNA stabilization, and that quiescent SCs might appear in a state of 'nuclear stress' rather than generalized stress. Hence studying the presence and localization of other stress-related markers –e.g. heat shock factors, heat shock proteins, inositol-requiring protein-1, caspases, NF-kappaB, p53, JNK, …- could prove interesting and useful in understanding the state of quiescence.

In light of the observations and discoveries previously presented, I believe this thesis is helping in advancing the field of NSC and SC quiescence and will help sparking new, valuable, and innovative discoveries.

7 BIBLIOGRAPHY

Allemand, E., Dokudovskaya, S., Bordonné, R., & Tazi, J. (2002). A Conserved Drosophila Transportin-Serine/Arginine- rich (SR) Protein Permits Nuclear Import of Drosophila SR Protein Splicing Factors and Their Antagonist Repressor Splicing Factor 1. *Molecular Biology of the Cell*, *13*, 2436–2447. http://doi.org/10.1091/mbc.E02

Ashburner, M., Ball, C. A., Blake, J. A., Botstein, D., Butler, H., Cherry, J. M., … Sherlock, G. (2000). Gene Ontology : tool for the unification of biology. The Gene Ontology Consortium. *Nature Genetics*, *25*(1), 25–29. http://doi.org/10.1038/75556.Gene

Avet-Rochex, A., Carvajal, N., Christoforou, C. P., Yeung, K., Maierbrugger, K. T., Hobbs, C., … Bateman, J. M. (2014). Unkempt Is Negatively Regulated by mTOR and Uncouples Neuronal Differentiation from Growth Control. *PLoS Genetics*, *10*(9). http://doi.org/10.1371/journal.pgen.1004624

Baeg, G. H., Zhou, R., & Perrimon, N. (2005). Genome-wide RNAi analysis of JAK/STAT signaling components in Drosophila. *Genes and Development*, *19*(16), 1861–1870. http://doi.org/10.1101/gad.1320705

Bancaud, A., Huet, S., Rabut, G., & Ellenberg, J. (2010). Fluorescence perturbation techniques to study mobility and molecular dynamics of proteins in live cells: FRAP, Photoactivation, Photoconversion, and FLIP. *Cold Spring Harbor Protocols*, *5*(12). http://doi.org/10.1101/pdb.top90

Beauchamp, J. R., Heslop, L., Yu, D. S. W., Tajbakhsh, S., Kelly, R. G., Wernig, A., … Zammit, P. S. (2000). Expression of CD34 and Myf5 defines the majority of

quiescent adult skeletal muscle satellite cells. *Journal of Cell Biology*, *151*(6), 1221–1233. http://doi.org/10.1083/jcb.151.6.1221

Beck, M., & Medalia, O. (2008). Structural and functional insights into nucleocytoplasmic transport. *Histology and Histopathology*, *23*(8), 1025–1033.

Bergmann, O., Spalding, K. L., & Frisén, J. (2015). Adult neurogenesis in humans. *Cold Spring Harbor Perspectives in Medicine*, *5*(8), 1–13. http://doi.org/10.1101/cshperspect.a018994

Bernad, R., van der Velde, H., Fornerod, M., & Pickersgill, H. (2004). Nup358/RanBP2 Attaches to the Nuclear Pore Complex via Association with Nup88 and Nup214/CAN and Plays a Supporting Role in CRM1-Mediated Nuclear Protein Export. *Molecular and Cellular Biology*, *24*(6), 2373–2384. http://doi.org/10.1128/MCB.24.6.2373-2384.2004

Betschinger, J., & Knoblich, J. a. (2004). Dare to be different: Asymmetric cell division in Drosophila, C. elegans and vertebrates. *Current Biology*, *14*(16), 674–685. http://doi.org/10.1016/j.cub.2004.08.017

Bi, X., Jones, T., Abbasi, F., Lee, H., Stultz, B., Hursh, D. A., & Mortin, M. A. (2005). Drosophila caliban, a nuclear export mediator, can function as a tumor suppressor in human lung cancer cells. *Oncogene*, *24*(56), 8229–8239. http://doi.org/10.1038/sj.onc.1208962

Bjornson, C. R. R., Cheung, T. H., Liu, L., Tripathi, P. V., Steeper, K. M., & Rando, T. A. (2012). Notch signaling is necessary to maintain quiescence in adult muscle stem cells. *Stem Cells*, *30*(2), 232–242. http://doi.org/10.1002/stem.773

Blanpain, C., Lowry, W. E., Geoghegan, A., Polak, L., & Fuchs, E. (2004). Self-renewal, multipotency, and the existence of two cell populations within an

epithelial stem cell niche. *Cell*, *118*(5), 635–648. http://doi.org/10.1016/j.cell.2004.08.012

Bonifaci, N., Moroianu, J., Radu, A., & Blobel, G. (1997). Karyopherin beta2 mediates nuclear import of a mRNA binding protein. *PNAS*, *94*, 5055–5060. http://doi.org/10.1073/pnas.94.10.5055

Boulikas, T. (1994). Putative nuclear localization signals (NLS) in protein transcription factors. *Journal of Cellular Biochemistry*, *55*(1), 32–58. http://doi.org/10.1002/jcb.240550106

Brand, A. H., & Perrimon, N. (1993). Targeted gene expression as a means of altering cell fates and generating dominant phenotypes. *Development (Cambridge, England)*, *118*(2), 401–415. http://doi.org/10.1101/lm.1331809

Brinkmann, U., Brinkmann, E., Gallo, M., Scherf, U., & Pastan, I. (1996). Role of CAS, a human homologue to the yeast chromosome segregation gene CSE1, in toxin and tumor necrosis factor mediated apoptosis. *Biochemistry*, *35*(21), 6891–6899. http://doi.org/10.1021/bi952829+

Brochta, D. A. O., Sheilachu, P. G., & Handler, A. M. (1991). P element excision in Drosophila melanogaster and related drosophilids. *Molecular Genetics and Genomics*, *225*, 387–394.

Carvalhal, S., Ribeiro, S. A., Arocena, M., Kasciukovic, T., Temme, A., Koehler, K., … Griffis, E. R. (2015). The nucleoporin ALADIN regulates Aurora A localization to ensure robust mitotic spindle formation. *Molecular Biology of the Cell*, *26*(19), 3424–38. http://doi.org/10.1091/mbc.E15-02-0113

Cautain, B., Hill, R., de Pedro, N., & Link, W. (2015). Components and regulation of nuclear transport processes. *FEBS Journal*, *282*(3), 445–462.

http://doi.org/10.1111/febs.13163

Chakraborty, P., Wang, Y., Wei, J. H., van Deursen, J., Yu, H., Malureanu, L., … Fontoura, B. M. a. (2008). Nucleoporin Levels Regulate Cell Cycle Progression and Phase-Specific Gene Expression. *Developmental Cell*, *15*(5), 657–667. http://doi.org/10.1016/j.devcel.2008.08.020

Chapouton, P., Skupien, P., Hesl, B., Coolen, M., Moore, J., Madelaine, R., … Bally-cuif, L. (2010). Notch Activity Levels Control the Balance between Quiescence and Recruitment of Adult Neural Stem Cells Running title : Notch in Adult Neural Stem Cell Quiescence Abstract The limited generation of neurons during adulthood is controlled by a balance betwe. *Journal of Neuroscience*, *30*(23), 7961–7974. http://doi.org/10.1523/JNEUROSCI.6170-09.2010

Chen, X., & Xu, L. (2010). Specific Nucleoporin Requirement for Smad Nuclear Translocation. *Molecular and Cellular Biology*, *30*(16), 4022–4034. http://doi.org/10.1128/MCB.00124-10

Cheung, T. H., & Rando, T. a. (2013). Molecular regulation of stem cell quiescence. *Nature Reviews. Molecular Cell Biology*, *14*(6), 329–40. http://doi.org/10.1038/nrm3591

Cho, Y. J., Kang, W., Kim, S. H., Sa, J. K., Kim, N., Paddison, P. J., … Nam, D. H. (2016). Involvement of DDX6 gene in radio- and chemoresistance in glioblastoma. *International Journal of Oncology*, *48*(3), 1053–1062. http://doi.org/10.3892/ijo.2016.3328

Codega, P., Silva-Vargas, V., Paul, A., Maldonado-Soto, A. R., DeLeo, A. M., Pastrana, E., & Doetsch, F. (2014). Prospective Identification and Purification of Quiescent Adult Neural Stem Cells from Their In Vivo Niche. *Neuron*, *82*(3),

545–559. http://doi.org/10.1016/j.neuron.2014.02.039

Cokol, M., Nair, R., & Rost, B. (2000). Finding nuclear localization signals Murat. *EMBO Reports*, *1*(5), 411–415. http://doi.org/10.1136/jech.2007.068551

Colledge, W. H., Richardson, W. D., Edge, M. D., & Smith, A. E. (1986). Extensive mutagenesis of the nuclear location signal of simian virus 40 large-T antigen. *Molecular and Cellular Biology*, *6*(11), 4136–9.

Coller, H. A., Sang, L., & Roberts, J. M. (2006). A new description of cellular quiescence. *PLoS Biology*, *4*(3), 0329–0349. http://doi.org/10.1371/journal.pbio.0040083

Colozza, G., Montembault, E., Quénerch'du, E., Riparbelli, M. G., D'Avino, P. P., & Callaini, G. (2011). Drosophila nucleoporin Nup154 controls cell viability, proliferation and nuclear accumulation of Mad transcription factor. *Tissue and Cell*, *43*(4), 254–261. http://doi.org/10.1016/j.tice.2011.05.001

Conover, J. C., & Notti, R. Q. (2008). The neural stem cell niche. *Cell and Tissue Research*, *331*(1), 211–224. http://doi.org/10.1007/s00441-007-0503-6

Cornelison, D. D. W., Filla, M. S., Stanley, H. M., Rapraeger, A. C., & Olwin, B. B. (2001). Syndecan-3 and syndecan-4 specifically mark skeletal muscle satellite cells and are implicated in satellite cell maintenance and muscle regeneration. *Developmental Biology*, *239*(1), 79–94. http://doi.org/10.1006/dbio.2001.0416

Cornelison, D. D. W., & Wold, B. J. (1997). Single-Cell Analysis of Regulatory Gene Expression in Quiescent and Activated Mouse Skeletal Muscle Satellite Cells. *Developmental Biology*, *191*, 270–283. http://doi.org/10.1111/j.1365-2478.2009.00831.x

D'Angelo, M. a., & Hetzer, M. W. (2008). Structure, dynamics and function of nuclear pore complexes. *Trends Cell Biol*, *18*(10), 456–466. http://doi.org/10.1016/j.tcb.2008.07.009.Structure

Dai, F., Lin, X., Chang, C., & Feng, X.-H. (2009). Nuclear export of Smad2 and Smad3 by RanBP3 facilitates termination of TGF-β signaling. *Developmental Cell*, *16*(3), 345–357. http://doi.org/10.1016/j.neuroimage.2013.08.045.The

Dember, L. M., Kim, N. D., Liu, K. Q., & Anderson, P. (1996). Individual RNA recognition motifs of TIA-1 and TIAR have different RNA binding specificities. *Journal of Biological Chemistry*, *271*(5), 2783–2788. http://doi.org/10.1074/jbc.271.5.2783

Devos, D., Dokudovskaya, S., Williams, R., Alber, F., Eswar, N., Chait, B. T., … Sali, A. (2006). Simple fold composition and modular architecture of the nuclear pore complex. *Proceedings of the National Academy of Sciences of the United States of America*, *103*(7), 2172–2177. http://doi.org/10.1073/pnas.0506345103

Ding, R., Weynans, K., Bossing, T., Barros, C. S., & Berger, C. (2016). The Hippo signalling pathway maintains quiescence in Drosophila neural stem cells. *Nature Communications*, *7*, 10510. http://doi.org/10.1038/ncomms10510

Dottori, M., & Pera, M. F. (2008). *Methods in Molecular Biology 438: Neural Stem Cells. Methods and Protocols. Neural Differentiation of Human Embryonic Stem Cells*.

Ebisuya, M., Kondoh, K., & Nishida, E. (2005). The duration, magnitude and compartmentalization of ERK MAP kinase activity: mechanisms for providing signaling specificity. *Journal of Cell Science*, *118*(Pt 14), 2997–3002. http://doi.org/10.1242/jcs.02505

Egger, B., Chell, J. M., & Brand, A. H. (2008). Insights into neural stem cell biology from flies. *Philosophical Transactions of the Royal Society of London. Series B, Biological Sciences*, *363*(1489), 39–56. http://doi.org/10.1098/rstb.2006.2011

Emery, P. (2007). Protein Extraction From Drosophila Heads. In *Circadian Rhythms* (Vol. 362, pp. 375–377). http://doi.org/10.3389/fcell.2016.00058

Encinas, J. M., Michurina, T. V., Peunova, N., Park, J. H., Tordo, J., Peterson, D. A., … Enikolopov, G. (2011). Division-coupled astrocytic differentiation and age-related depletion of neural stem cells in the adult hippocampus. *Cell Stem Cell*, *8*(5), 566–579. http://doi.org/10.1016/j.stem.2011.03.010

Eriksson, P. S., Perfilieva, E., Björk-Eriksson, T., Alborn, A. M., Nordborg, C., Peterson, D. A., & Gage, F. H. (1998). Neurogenesis in the adult human hippocampus. *Nature Medicine*, *4*(11), 1313–1317. http://doi.org/10.1038/3305

Fernández-Hernández, I., Rhiner, C., & Moreno, E. (2013). Adult Neurogenesis in Drosophila. *Cell Reports*, *3*(6), 1857–1865. http://doi.org/10.1016/j.celrep.2013.05.034

Field, M. C., Koreny, L., & Rout, M. P. (2014). Enriching the Pore: Splendid Complexity from Humble Origins. *Traffic*, *15*(2), 141–156. http://doi.org/10.1111/tra.12141

Fogel, B. L., Wexler, E., Wahnich, A., Friedrich, T., Vijayendran, C., Gao, F., … Geschwind, D. H. (2012). RBFOX1 regulates both splicing and transcriptional networks in human neuronal development. *Human Molecular Genetics*, *21*(19), 4171–4186. http://doi.org/10.1093/hmg/dds240

Forsberg, E. C., Passegué, E., Prohaska, S. S., Wagers, A. J., Koeva, M., Stuart, J. M., & Weissman, I. L. (2010). Molecular signatures of quiescent, mobilized and

leukemia-initiating hematopoietic stem cells. *PLoS ONE*, *5*(1), 1–11. http://doi.org/10.1371/journal.pone.0008785

Fukada, S., Uezumi, A., Ikemoto, M., Masuda, S., Segawa, M., Tanimura, N., … Takeda, S. (2007a). Molecular signature of quiescent satellite cells in adult skeletal muscle. *Stem Cells*, *25*(10), 2448–2459. http://doi.org/10.1634/stemcells.2007-0019

Fukada, S., Uezumi, A., Ikemoto, M., Masuda, S., Segawa, M., Tanimura, N., … Takeda, S. (2007b). Molecular Signature of Quiescent Satellite Cells in Adult Skeletal Muscle. *Stem Cells*, *25*(10), 2448–2459. http://doi.org/10.1634/stemcells.2007-0019

Furutachi, S., Matsumoto, A., Nakayama, K. I., & Gotoh, Y. (2013). P57 Controls Adult Neural Stem Cell Quiescence and Modulates the Pace of Lifelong Neurogenesis. *The EMBO Journal*, *32*(7), 970–81. http://doi.org/10.1038/emboj.2013.50

Galloway, A., Saveliev, A., Ukasiak, S., Hodson, D. J., Bolland, D., Balmanno, K., … Turner, M. (2016). RNA-binding proteins ZFP36L1 and ZFP36L2 promote cell quiescence. *Science*, *352*(6284), 453–459. http://doi.org/10.1126/science.aad5978

Gebara, E., Bonaguidi, M. A., Beckervordersandforth, R., Sultan, S., Udry, F., Gijs, P.-J., … Toni, N. (2013). Heterogeneity of Radial Glia-Like Cells in the Adult Hippocampus. *Stem Cells*, *31*(9), 1902–1909. http://doi.org/10.1002/stem.1435

Gerdes, J., Schwab, U., Lemke, H., & Stein, H. (1983). Production of a mouse monoclonal antibody reactive with a human nuclear antigen associated with cell proliferation. *International Journal of Cancer. Journal International Du Cancer*,

31(1), 13–20. http://doi.org/10.1002/ijc.2910310104

Gnocchi, V. F., White, R. B., Ono, Y., Ellis, J. A., & Zammit, P. S. (2009). Further characterisation of the molecular signature of quiescent and activated mouse muscle satellite cells. *PLoS ONE*, *4*(4). http://doi.org/10.1371/journal.pone.0005205

Gopinath, S. D., Webb, A. E., Brunet, A., & Rando, T. A. (2014). FOXO3 promotes quiescence in adult muscle stem cells during the process of self-renewal. *Stem Cell Reports*, *2*(4), 414–426. http://doi.org/10.1016/j.stemcr.2014.02.002

Götz, M., Nakafuku, M., & Petrik, D. (2016). Neurogenesis in the Developing and Adult. *Perspectives in Biology*, 1–24. http://doi.org/10.1101/cshperspect.a018853

Hao, S., Chen, C., & Cheng, T. (2016). Cell cycle regulation of hematopoietic stem or progenitor cells. *International Journal of Hematology*, *103*(5), 487–497. http://doi.org/10.1007/s12185-016-1984-4

Hashizume, C., Kobayashi, a, & Wong, R. W. (2013). Down-modulation of nucleoporin RanBP2/Nup358 impaired chromosomal alignment and induced mitotic catastrophe. *Cell Death & Disease*, *4*(10), e854. http://doi.org/10.1038/cddis.2013.370

Hashizume, C., Moyori, A., Kobayashi, A., Yamakoshi, N., Endo, A., & Wong, R. W. (2013). Nucleoporin Nup62 maintains centrosome homeostasis. *Cell Cycle*, *12*(24), 3804–3816. http://doi.org/10.4161/cc.26671

Heigwer, F., Port, F., & Boutros, M. (2018). RNA Interference (RNAi) Screening in Drosophila. In *Genetics* (Vol. 208, pp. 853–874).

Hosoyama, T., Nishijo, K., Prajapati, S. I., Li, G., & Keller, C. (2011). Rb1 gene inactivation expands satellite cell and postnatal myoblast pools. *Journal of Biological Chemistry*, *286*(22), 19556–19564. http://doi.org/10.1074/jbc.M111.229542

Hsieh, J. (2012). Orchestrating transcriptional control of adult neurogenesis. *Genes and Development*, *26*(10), 1010–1021. http://doi.org/10.1101/gad.187336.112

Hurt, E., & Beck, M. (2015). Towards understanding nuclear pore complex architecture and dynamics in the age of integrative structural analysis. *Current Opinion in Cell Biology*, *34*(i), 31–38. http://doi.org/10.1016/j.ceb.2015.04.009

Iatropoulos, M. J., & Williams, G. M. (1996). Proliferation markers. *Experimental and Toxicologic Pathology*, *48*(2–3), 175–181. http://doi.org/10.1016/S0940-2993(96)80039-X

Ibarra, A., & Hetzer, M. W. (2015). Nuclear pore proteins and the control of genome functions, 337–349. http://doi.org/10.1101/gad.256495.114.Cytoplasmic

Irintchev, A., Zeschnigk, M., Starzinski-Powitz, A., & Wernig, A. (1994). Expression pattern of M-cadherin in normal, denervated, and regenerating mouse muscles. *Developmental Dynamics*, *199*(4), 326–337. http://doi.org/10.1002/aja.1001990407

Isshiki, T., Pearson, B., Holbrook, S., & Doe, C. Q. (2001). Drosophila neuroblasts sequentially express transcription factors which specify the temporal identity of their neuronal progeny. *Cell*, *106*(4), 511–521. http://doi.org/10.1016/S0092-8674(01)00465-2

Itahana, K., Dimri, G. P., Hara, E., Itahana, Y., Zou, Y., Desprez, P. Y., & Campisi, J. (2002). A role for p53 in maintaining and establishing the quiescence growth

arrest in human cells. *Journal of Biological Chemistry*, *277*(20), 18206–18214. http://doi.org/10.1074/jbc.M201028200

Jacques, T. S., Swales, A., Brzozowski, M. J., Henriquez, N. V., Linehan, J. M., Mirzadeh, Z., … Brandner, S. (2010). Combinations of genetic mutations in the adult neural stem cell compartment determine brain tumour phenotypes. *EMBO Journal*, *29*(1), 222–235. http://doi.org/10.1038/emboj.2009.327

Januschke, J., & Gonzalez, C. (2008). Drosophila asymmetric division, polarity and cancer. *Oncogene*, *27*(55), 6994–7002. http://doi.org/10.1038/onc.2008.349

Jennings, B. H. (2011). Drosophila-a versatile model in biology & medicine. *Materials Today*, *14*(5), 190–195. http://doi.org/10.1016/S1369-7021(11)70113-4

Jessberger, S. (2016). Stem Cell-Mediated Regeneration of the Adult Brain. *Transfusion Medicine and Hemotherapy*, *43*(5), 321–326. http://doi.org/10.1159/000447646

Jin, X. (2016). The role of neurogenesis during development and in the adult brain. *European Journal of Neuroscience*, *44*(6), 2291–2299. http://doi.org/10.1111/ejn.13251

Joh, R. I., Khanduja, J. S., Calvo, I. A., Mistry, M., Palmieri, C. M., Savol, A. J., … Motamedi, M. (2016). Survival in quiescence requires the euchromatic deployment of Clr4/SUV39H by Argonaute-associated small RNAs. *Molecular Cell*, *64*(6), 1088–1101. http://doi.org/10.1016/j.pain.2014.05.025.Research

Jomon, J., & Mary, D. (2008). The nucleoporin Nup358 associates with and regulates interphase microtubules. *FEBS Lett*, *100*(2), 130–134. http://doi.org/10.1016/j.pestbp.2011.02.012.Investigations

Kalverda, B., Pickersgill, H., Shloma, V. V., & Fornerod, M. (2010). Nucleoporins Directly Stimulate Expression of Developmental and Cell-Cycle Genes Inside the Nucleoplasm. *Cell*, *140*(3), 360–371. http://doi.org/10.1016/j.cell.2010.01.011

Kanehisa, M., & Goto, S. (2000). KEGG : Kyoto Encyclopedia of Genes and Genomes. *Nucleic Acid Research*, *28*(1), 27–30.

Katz, S., Cussigh, D., Urbán, N., Blomfield, I., Guillemot, F., Bally-Cuif, L., & Coolen, M. (2016). A Nuclear Role for miR-9 and Argonaute Proteins in Balancing Quiescent and Activated Neural Stem Cell States. *Cell Reports*, *17*(5), 1383–1398. http://doi.org/10.1016/j.celrep.2016.09.088

Kedersha, Gupta, M., Li, W., Miller, I., & Anderson, P. (1999). RNA-binding Proteins TIA-1 and TIAR Link the Phosphorylation of eIF-2alpha to the Assembly of Mammalian Stress Granules. *The Journal of Cell Biology*, *147*(7), 1431–1441. http://doi.org/10.1083/jcb.147.7.1431

Kempermann, G., Krebs, J., & Fabel, K. (2008). The contribution of failing adult hippocampal neurogenesis to psychiatric disorders. *Current Opinion in Psychiatry*, *21*(3), 2990–295. http://doi.org/10.3779/j.issn.1009-3419.2016.07.05

Kheirbek, M. A., & Hen, R. (2011). Dorsal vs Ventral Hippocampal Neurogenesis: Implications for Cognition and Mood. *Neuropsychopharmacology*, *36*(1), 373–374. http://doi.org/10.1038/npp.2010.148

Kim, H. S., Headey, S. J., Yoga, Y. M. K., Scanlon, M. J., Gorospe, M., Wilce, M. C. J., & Wilce, J. A. (2013). Distinct binding properties of TIAR RRMs and linker region. *RNA Biology*, *10*(4), 579–589. http://doi.org/10.4161/rna.24341

Köhler, A., & Hurt, E. (2007). Exporting RNA from the nucleus to the cytoplasm.

Nature Reviews Molecular Cell Biology, *8*(10), 761–773. http://doi.org/10.1038/nrm2255

Kops, G. J. P. L., Dansen, T. B., Polderman, P. E., Saarloos, I., Wirtz, K. W. A., Coffer, P. J., … Burgering, B. M. T. (2002). Forkhead transcription factor FOXO3a protects quiescent cells from oxidative stress. *Nature*, *419*(6904), 316–321. http://doi.org/10.1038/nature01036

Köster, M., Frahm, T., & Hauser, H. (2005). Nucleocytoplasmic shuttling revealed by FRAP and FLIP technologies. *Current Opinion in Biotechnology*, *16*(1 SPEC. ISS.), 28–34. http://doi.org/10.1016/j.copbio.2004.11.002

Kraut, R., Chia, W., Yeh Jan, L., Nung Jan, Y., & Knoblich, J. A. (1996). Role of inscuteable in orienting asymmetric cell divisions in Drosophila. *Nature*. http://doi.org/10.1111/j.1600-0560.2008.01112.x

Kreso, A., & Dick, J. E. (2014). Evolution of the cancer stem cell model. *Cell Stem Cell*, *14*(3), 275–291. http://doi.org/10.1016/j.stem.2014.02.006

Kriegstein, A., & Alvarez-buylla, A. (2011). The Glial Nature of Embryonic and Adult Neural Stem Cells. *Annual Reviews of Neuroscience*, 149–184. http://doi.org/10.1146/annurev.neuro.051508.135600.The

Kurisaki, A., Kurisaki, K., Kowanetz, M., Sugino, H., Yoneda, Y., Heldin, C.-H., & Moustakas, A. (2006). The Mechanism of Nuclear Export of Smad3 Involves Exportin 4 and Ran. *Molecular and Cellular Biology*, *26*(4), 1318–1332. http://doi.org/10.1128/MCB.26.4.1318-1332.2006

Kusano, A., Staber, C., & Ganetzky, B. (2001). Nuclear Mislocalization of Enzymatically Active RanGAP Causes Segregation Distortion in Drosophila. *Developmental Cell*, *1*(3), 351–361. Retrieved from

http://www.ncbi.nlm.nih.gov/pubmed/11702947%0Apapers3://publication/uuid/110D7567-A85A-44D1-B36F-CA493EC58B86

Kutay, U., Ralf Bischoff, F., Kostka, S., Kraft, R., & Görlich, D. (1997). Export of importin α from the nucleus is mediated by a specific nuclear transport factor. *Cell*, *90*(6), 1061–1071. http://doi.org/10.1016/S0092-8674(00)80372-4

Kwon, J. S., Everetts, N. J., Wang, X., Wang, W., Della Croce, K., Xing, J., & Yao, G. (2017). Controlling Depth of Cellular Quiescence by an Rb-E2F Network Switch. *Cell Reports*, *20*(13), 3223–3235. http://doi.org/10.1016/j.celrep.2017.09.007

Ladha, M. H., Lee, K. Y., Upton, T. M., Reed, M. F., & Ewen, M. E. (1998). Regulation of exit from quiescence by p27 and cyclin D1-CDK4. *Molecular and Cellular Biology*, *18*(11), 6605–15. http://doi.org/10.1128/MCB.18.11.6605

Lafarga, V., Sung, H., Haneke, K., Roessig, L., Pauleau, A., Bruer, M., … Stoecklin, G. (2018). TIAR marks nuclear G2/M transition granules and restricts CDK1 activity under replication stress. *EMBO Reports*, 1–16. http://doi.org/10.15252/embr.201846224

Lai, M., Kuo, H., Chang, W., & Tarn, W. (2003). A novel splicing regulator shares a nuclear import pathway with SR proteins, *22*(6), 1359–1369.

Lai, S.-L., & Doe, C. Q. (2014). Transient nuclear Prospero induces neural progenitor quiescence. *ELife*, *3*, 1–12. http://doi.org/10.7554/eLife.03363

Lange, A., Mills, R. E., Lange, C. J., Stewart, M., Devine, S. E., & Corbett, A. H. (2007). Classical nuclear localization signals: Definition, function, and interaction with importin ?? *Journal of Biological Chemistry*, *282*(8), 5101–5105. http://doi.org/10.1074/jbc.R600026200

Laporte, D., Lebaudy, A., Sahin, A., Pinson, B., Ceschin, J., Daignan-Fornier, B., & Sagot, I. (2011). Metabolic status rather than cell cycle signals control quiescence entry and exit. *Journal of Cell Biology*, *192*(6), 949–957. http://doi.org/10.1083/jcb.201009028

Lee, T., & Luo, L. (1999). Mosaic analysis with a repressible cell marker for studies of gene function in neuronal morphogenesis. *Neuron*, *22*(3), 451–461. http://doi.org/10.1016/S0896-6273(00)80701-1

Lemke, E. A. (2016). The multiple faces of disordered nucleoporins. *Journal of Molecular Biology*, 1–14. http://doi.org/10.1016/j.jmb.2016.01.002

Lemons, J. M. S., Coller, H. A., Feng, X. J., Bennett, B. D., Legesse-Miller, A., Johnson, E. L., … Rabinowitz, J. D. (2010). Quiescent fibroblasts exhibit high metabolic activity. *PLoS Biology*, *8*(10). http://doi.org/10.1371/journal.pbio.1000514

Lepper, C., Conway, S. J., & Fan, C. (2009). Adult satellite cells and embryonic muscle progenitors have distinct genetic requirements, *460*(7255), 627–631. http://doi.org/10.1038/nature08209.Adult

Li, L., & Bhatia, R. (2011). Stem cell quiescence. *Clinical Cancer Research*, *17*(15), 4936–4941. http://doi.org/10.1158/1078-0432.CCR-10-1499

Li, O., Heath, C. V, Amberg, D. C., Dockendorff, T. C., Copeland, C. S., Snyder, M., & Cole, C. N. (1995). Mutation or Deletion of the Saccharomyces cerevisiae RAT3/NUP133 Gene Causes Temperature-dependent Nuclear Accumulation of Poly (A) + RNA and Constitutive Clustering of Nuclear Pore Complexes. *Molecular Biology of the Cell*, *6*(April), 401–417. http://doi.org/10.1083/jcb.131.6.1677

Lin, G. G., & Scott, J. G. (2012). A family business: stem cell progeny join the niche to regulate homeostasis, *100*(2), 130–134. http://doi.org/10.1016/j.pestbp.2011.02.012.Investigations

Liu, J., Xu, Y., Stoleru, D., & Salic, A. (2012). Imaging protein synthesis in cells and tissues with an alkyne analog of puromycin. *Proceedings of the National Academy of Sciences*, *109*(2), 413–418. http://doi.org/10.1073/pnas.1111561108

Liu, Q., Rand, T. A., Kalidas, S., Du, F., Kim, H.-E., Smith, D. P., & Wang, X. (2013). Initiation the a bridge and between effector steps pathway the of Drosophila RNAi. *Science*, *301*(5641), 1921–1925.

Lowe, A. R., Tang, J. H., Yassif, J., Graf, M., Huang, W. Y. C., Groves, J. T., … Liphardt, J. T. (2015). Importin-β modulates the permeability of the nuclear pore complex in a Ran-dependent manner. *ELife*, *4*, 1–24. http://doi.org/10.7554/eLife.04052

Martinez, I., Hayes, K. E., Barr, J. A., Harold, A. D., Xie, M., Bukhari, S. I. A., … DiMaio, D. (2017). An Exportin-1–dependent microRNA biogenesis pathway during human cell quiescence. *Proceedings of the National Academy of Sciences*, *114*(25), E4961–E4970. http://doi.org/10.1073/pnas.1618732114

Martynoga, B., Mateo, J. L., Zhou, B., Andersen, J., Achimastou, A., Urbán, N., … Guillemot, F. (2013). Epigenomic enhancer annotation reveals a key role for NFIX in neural stem cell quiescence. *Genes and Development*, *27*(16), 1769–1786. http://doi.org/10.1101/gad.216804.113

Massimelli, M. J., Majerciak, V., Kruhlak, M., & Zheng, Z.-M. (2013). Interplay between Polyadenylate-Binding Protein 1 and Kaposi's Sarcoma-Associated

Herpesvirus ORF57 in Accumulation of Polyadenylated Nuclear RNA, a Viral Long Noncoding RNA. *Journal of Virology*, *87*(1), 243–256. http://doi.org/10.1128/JVI.01693-12

Matsubayashi, Y., Fukuda, M., & Nishida, E. (2001). Evidence for Existence of a Nuclear Pore Complex-mediated, Cytosol-independent Pathway of Nuclear Translocation of ERK MAP Kinase in Permeabilized Cells. *Journal of Biological Chemistry*, *276*(45), 41755–41760. http://doi.org/10.1074/jbc.M106012200

Mazan-mamczarz, K., Lal, A., Martindale, J. L., Kawai, T., & Gorospe, M. (2006). Translational Repression by RNA-Binding Protein TIAR. *Molecular and Cellular Biology*, *26*(7), 1–32. http://doi.org/10.1128/MCB.26.7.2716

McConnell, A. M., Yao, C., Yeckes, A. R., Wang, Y., Selvaggio, A. S., Tang, J., … Stripp, B. R. (2016). p53 Regulates Progenitor Cell Quiescence and Differentiation in the Airway. *Cell Reports*, *17*(9), 2173–2182. http://doi.org/10.1016/j.celrep.2016.11.007

Meacham, C. E., & Morrison, S. J. (2013). Tumour heterogeneity and cancer cell plasticity. *Nature*, *501*(7467), 328–337. http://doi.org/10.1038/nature12624

Ming, G., & Song, H. (2011). Adult neurogenesis in the mammalian brain: significant answers and significant questions. *Neuron*, *70*(4), 687–702. http://doi.org/10.1016/j.neuron.2011.05.001.Adult

Mira, H., Andreu, Z., Suh, H., Chichung Lie, D., Jessberger, S., Consiglio, A., … Gage, F. H. (2010). Signaling through BMPR-IA regulates quiescence and long-term activity of neural stem cells in the adult hippocampus. *Cell Stem Cell*, *7*(1), 78–89. http://doi.org/10.1016/j.stem.2010.04.016

Moyle, L., & Zammit, P. (2014). Isolation, Culture and Immunostaining of Skeletal

Muscle Fibres to Study Myogenic Progression in Satellite Cells. *Methods in Molecular Biology*, *2*, 63–78.

Murn, J., Zarnack, K., Yang, Y. J., Durak, O., Murphy, E. A., Cheloufi, S., … Shi, Y. (2015). Control of a neuronal morphology program by an RNA-binding zinc finger protein, Unkempt. *Genes and Development*, *29*(5), 501–512. http://doi.org/10.1101/gad.258483.115

Nakamura-Ishizu, a., Takizawa, H., & Suda, T. (2014). The analysis, roles and regulation of quiescence in hematopoietic stem cells. *Development*, *141*(24), 4656–4666. http://doi.org/10.1242/dev.106575

Natalizio, A. H., & Matera, A. G. (2013). Identification and characterization of *Drosophila* Snurportin reveals a role for the import receptor Moleskin/importin-7 in snRNP biogenesis. *Molecular Biology of the Cell*, *24*(18), 2932–2942. http://doi.org/10.1091/mbc.e13-03-0118

Niedojadło, J., Dełeńko, K., & Niedojadło, K. (2016). Regulation of poly(A) RNA retention in the nucleus as a survival strategy of plants during hypoxia. *RNA Biology*, *13*(5), 531–543. http://doi.org/10.1080/15476286.2016.1166331

Nintendo. (1996). Pokemon. Tokyo: Game Freak.

O'Farrell, P. H. (2011). Quiescence: early evolutionary origins and universality do not imply uniformity. *Philosophical Transactions of the Royal Society B: Biological Sciences*, *366*(1584), 3498–3507. http://doi.org/10.1098/rstb.2011.0079

Ohtsubo, M., Kai, R., Furuno, N., Sekiguchi, T., Sekiguchi, M., Hayashida, H., … Murotsu, T. (1987). Isolation and characterization of the active cDNA of the human cell cycle gene (RCC1) involved in the regulation of onset of chromosome condensation. *Genes & Development*, *1*(6), 585–593.

http://doi.org/10.1101/gad.1.6.585

Ono, Y., Boldrin, L., Knopp, P., Morgan, J. E., & Zammit, P. S. (2010). Muscle satellite cells are a functionally heterogeneous population in both somite-derived and branchiomeric muscles. *Developmental Biology*, *337*(1), 29–41. http://doi.org/10.1016/j.ydbio.2009.10.005

Otsuki, L., & Brand, A. H. (2018). Cell cycle heterogeneity directs the timing of neural stem cell activation from quiescence. *Science*, *360*(6384), 99–102. http://doi.org/10.1126/science.aan8795

Ou, H. L. (2013). Gene knockout by inducing P-element transposition in Drosophila. *Genetics and Molecular Research*, *12*(3), 2852–2857.

Paik, J. H., Ding, Z., Narurkar, R., Ramkissoon, S., Muller, F., Kamoun, W. S., … DePinho, R. a. (2009). FoxOs Cooperatively Regulate Diverse Pathways Governing Neural Stem Cell Homeostasis. *Cell Stem Cell*, *5*(5), 540–553. http://doi.org/10.1016/j.stem.2009.09.013

Paliouras, G. N., Hamilton, L. K., Aumont, a., Joppe, S. E., Barnabe-Heider, F., & Fernandes, K. J. L. (2012). Mammalian Target of Rapamycin Signaling Is a Key Regulator of the Transit-Amplifying Progenitor Pool in the Adult and Aging Forebrain. *Journal of Neuroscience*, *32*(43), 15012–15026. http://doi.org/10.1523/JNEUROSCI.2248-12.2012

Park, Y., Filippov, V., Gill, S. S., & Adams, M. E. (2002). Deletion of the ecdysis-triggering hormone gene leads to lethal ecdysis deficiency. *Development (Cambridge, England)*, *129*(2), 493–503.

Parrott, B. B., Chiang, Y., Hudson, A., Sarkar, A., Guichet, A., & Schulz, C. (2011). Nucleoporin98-96 function is required for transit amplification divisions in the

germ line of Drosophila melanogaster. *PLoS ONE*, *6*(9). http://doi.org/10.1371/journal.pone.0025087

Patt, H. M., & Quastler, H. (1963). Radiation effects on cell renewal and related systems. *Physiological Reviews*, *77*(3).

Pearce, E., & Pearce, E. (2013). Metabolic pathways in immune cell activation and quiescence. *Immunity*, *38*(4), 633–643. http://doi.org/10.1016/j.immuni.2013.04.005

Peyro, M., Soheilypour, M., Lee, B. L., & Mofrad, M. R. K. (2015). Evolutionarily Conserved Sequence Features Regulate the Formation of the FG Network at the Center of the Nuclear Pore Complex. *Scientific Reports*, *5*(November), 15795. http://doi.org/10.1038/srep15795

Potter, C. J., Turenchalk, G. S., & Xu, T. (2000). Drosophila in cancer research. An expanding role. *Trends in Genetics : TIG*, *16*(1), 33–39. http://doi.org/10.1016/S0168-9525(99)01878-8

Renault, V. M., Rafalski, V. a., Morgan, A. a., Salih, D. a M., Brett, J. O., Webb, A. E., … Brunet, A. (2009). FoxO3 Regulates Neural Stem Cell Homeostasis. *Cell Stem Cell*, *5*(5), 527–539. http://doi.org/10.1016/j.stem.2009.09.014

Richardson, W. D., Mills, A. D., Dilworth, S. M., Laskey, R. A., & Dingwall, C. (1988). Nuclear protein migration involves two steps: Rapid binding at the nuclear envelope followed by slower translocation through nuclear pores. *Cell*, *52*(5), 655–664. http://doi.org/10.1016/0092-8674(88)90403-5

Rocheteau, P., Vinet, M., & Chretien, F. (2015). Dormancy and Quiescence of Skeletal Stem cells. In *Vertebrate Myogenesis: Stem Cells and Precursors* (pp. 215–236). Retrieved from http://www.springer.com/series/400

Roth, P., Xylourgidis, N., Sabri, N., Uv, A., Fornerod, M., & Samakovlis, C. (2003). The Drosophila nucleoporin DNup88 localizes DNup214 and CRM1 on the nuclear envelope and attenuates NES-mediated nuclear export. *Journal of Cell Biology*, *163*(4), 701–706. http://doi.org/10.1083/jcb.200304046

Sahay, A., Scobie, K., Hill, A., O'Carroll, C., Kheirbek, M., Burghardt, N., … Hen, R. (2010). Increasing adult hippocampal neurogenesis is sufficient to improve pattern separation. *Nature*, *472*(7344), 466–470. http://doi.org/10.1038/nature09817.Increasing

Saito, Y., Kitamura, H., Hijikata, A., Tomizawa-murasawa, M., Tanaka, S., Takagi, S., … Ishikawa, F. (2010). Identification of Therapeutic Targets for Quiescent, Chemotherapy-Resistant Human Leukemia Stem Cells. *Sci Transl Med*, *2*(17). http://doi.org/10.1126/scitranslmed.3000349.Identification

Sampathkumar, P., Kim, S. J., Upla, P., Rice, W. J., Phillips, J., Timney, B. L., … Almo, S. C. (2013). Structure, dynamics, evolution, and function of a major scaffold component in the nuclear pore complex. *Structure*, *21*(4), 560–571. http://doi.org/10.1016/j.str.2013.02.005

Sang, L., Coller, H. A., & Roberts, J. M. (2008). Control of the reversibility of cellular quiescence by the transcriptional repressor HES1. *Science*, *321*(5892), 1095–1100. http://doi.org/10.1126/science.1155998

Sarov, M., Barz, C., Jambor, H., Hein, M. Y., Schmied, C., Suchold, D., … Knust, E. (2016). A genome-wide resource for the analysis of protein localisation in Drosophila. *ELife*, 1–38. http://doi.org/10.7554/eLife.12068

Savas, J., Toyama, B., Xu, T., Yates, J., & Hetzer, M. (2012). Extremely Long-lived Nuclear Pore Proteins in the Rat Brain. *Science*, *1*(3), 233–245.

http://doi.org/10.1016/j.dcn.2011.01.002.The

Seale, P., & Rudnicki, M. A. (2000). A new look at the origin, function, and “stem-cell” status of muscle satellite cells. *Developmental Biology*, *218*(2), 115–124. http://doi.org/10.1006/dbio.1999.9565

Slack, C., Somers, W. G., Sousa-Nunes, R., Chia, W., & Overton, P. M. (2006). A mosaic genetic screen for novel mutations affecting Drosophila neuroblast divisions. *BMC Genetics*, *7*, 33. http://doi.org/10.1186/1471-2156-7-33

Sloan, K. E., Gleizes, P.-E., & Bohnsack, M. T. (2015). Nucleocytoplasmic transport of RNAs and RNA-protein complexes. *Journal of Molecular Biology*. http://doi.org/10.1016/j.jmb.2015.09.023

Smith, A. (2006). A glossary for stem-cell biology. *Nature*, *441*(7097), 1060. http://doi.org/10.1038/nature04954

Soniat, M., & Chook, Y. M. (2015). Nuclear localization signals for four distinct karyopherin-β nuclear import systems. *Biochemical Journal*, *468*(3), 353–362. http://doi.org/10.1042/BJ20150368

Sousa-Nunes, R., Cheng, L. Y., & Gould, A. P. (2010). Regulating neural proliferation in the Drosophila CNS. *Current Opinion in Neurobiology*, *20*(1), 50–57. http://doi.org/10.1016/j.conb.2009.12.005

Sousa-Nunes, R., Yee, L. L., & Gould, A. P. (2011a). Fat cells reactivate quiescent neuroblasts via TOR and glial insulin relays in Drosophila. *Nature*, *471*(7339), 508–512. http://doi.org/10.1038/nature09867

Sousa-Nunes, R., Yee, L. L., & Gould, A. P. (2011b). Fat cells reactivate quiescent neuroblasts via TOR and glial insulin relays in Drosophila. *Nature*, *471*(7339),

508–512. http://doi.org/10.1038/nature09867

Spalding, K. L., Bergmann, O., Alkass, K., Bernard, S., Salehpour, M., Huttner, H. B., … Frisen, J. (2013). Dynamics of hippocampal neurogenesis in adult humans. *Cell*, *153*(6), 1219–1227. http://doi.org/10.1016/j.cell.2013.05.002

Steggerda, S. M., & Paschal, B. M. (2002). Regulation of Nuclear Import and Export by the GTPase Ran, *217*, 41–91.

Stewart, M. (2007). Molecular mechanism of the nuclear protein import cycle. *Nature Reviews. Molecular Cell Biology*, *8*(3), 195–208. http://doi.org/10.1038/nrm2114

Stuwe, T., Bley, C. J., Thierbach, K., Petrovic, S., Schilbach, S., Mayo, D. J., … Hoelz, A. (2015). Architecture of the fungal nuclear pore inner ring complex. *Science*, *350*(6256), 56–64. http://doi.org/10.1126/science.aac9176

Subramaniam, S., Sreenivas, P., Cheedipudi, S., Reddy, V. R., Shashidhara, L. S., Chilukoti, R. K., … Dhawan, J. (2013). Distinct Transcriptional Networks in Quiescent Myoblasts: A Role for Wnt Signaling in Reversible vs. Irreversible Arrest. *PLoS ONE*, *8*(6). http://doi.org/10.1371/journal.pone.0065097

Suh, H., Consiglio, A., Ray, J., Sawai, T., D'Amour, K. A., & Gage, F. H. (2007). In Vivo Fate Analysis Reveals the Multipotent and Self-Renewal Capacities of Sox2+ Neural Stem Cells in the Adult Hippocampus. *Cell Stem Cell*, *1*(5), 515–528. http://doi.org/10.1016/j.stem.2007.09.002

Sun, S., Zhang, Z., Fregoso, O., & Krainer, A. R. (2012). Mechanisms of activation and repression by the alternative splicing factors RBFOX1/2. *Rna*, *18*(2), 274–283. http://doi.org/10.1261/rna.030486.111

Sun, Y., Hu, J., Zhou, L., Pollard, S. M., & Smith, A. (2011). Interplay between FGF2

and BMP controls the self-renewal, dormancy and differentiation of rat neural stem cells. *Journal of Cell Science*, *124*, 1867–1877. http://doi.org/10.1242/jcs.085506

Tajirika, T., Tokumaru, Y., Taniguchi, K., Sugito, N., Matsuhashi, N., Futamura, M., … Yoshida, K. (2018). DEAD-box protein RNA-helicase DDX6 regulates the expression of HER2 and FGFR2 at the post-transcriptional step in gastric cancer cells. *International Journal of Molecular Sciences*, *19*(7). http://doi.org/10.3390/ijms19072005

Taupin, J. L., Tian, Q., Kedersha, N., Robertson, M., & Anderson, P. (1995). The RNA-binding protein TIAR is translocated from the nucleus to the cytoplasm during Fas-mediated apoptotic cell death. *Proceedings of the National Academy of Sciences of the United States of America*, *92*(5), 1629–33. http://doi.org/10.1073/pnas.92.5.1629

Tekotte, H., Berdnik, D., Török, T., Buszczak, M., Jones, L. M., Cooley, L., … Davis, I. (2002). Dcas is required for importin-α3 nuclear export and mechano-sensory organ cell fate specification in Drosophila. *Developmental Biology*, *244*(2), 396–406. http://doi.org/10.1006/dbio.2002.0612

Terzi, M. Y., Izmirli, M., & Gogebakan, B. (2016). The cell fate: senescence or quiescence. *Molecular Biology Reports*, *43*(11), 1213–1220. http://doi.org/10.1007/s11033-016-4065-0

Truman, J. W., & Bate, M. (1988). Spatial and temporal patterns of neurogenesis in the central nervous system of Drosophila melanogaster. *Developmental Biology*, *125*(1), 145–157. http://doi.org/10.1016/0012-1606(88)90067-X

Urbán, N., Berg, D. L. C. Van Den, Forget, A., Andersen, J., Crick, F., & Cnrs, U. K. I.

C. (2017). Return to quiescence of murine neural stem cells by degradation of a pro-activation protein, *353*(6296), 292–295. http://doi.org/10.1126/science.aaf4802.Return

Valcourt, J. R., Lemons, J. M. S., Haley, E. M., Kojima, M., Demuren, O. O., & Coller, H. a. (2012). Staying alive: Metabolic adaptations to quiescence. *Cell Cycle*, *11*(9), 1680–1696. http://doi.org/10.4161/cc.19879

Vaquerizas, J. M., Suyama, R., Kind, J., Miura, K., & Luscombe, N. M. (2010). Nuclear Pore Proteins Nup153 and Megator Define Transcriptionally Active Regions in the Drosophila Genome, *6*(2). http://doi.org/10.1371/journal.pgen.1000846

Venezia, T. a., Merchant, A. a., Ramos, C. a., Whitehouse, N. L., Young, A. S., Shaw, C. a., & Goodell, M. a. (2004). Molecular signatures of proliferation and quiescence in hematopoietic stem cells. *PLoS Biology*, *2*(10). http://doi.org/10.1371/journal.pbio.0020301

Vidal, S. J., Rodriguez-Bravo, V., Galsky, M., Cordon-Cardo, C., & Domingo-Domenech, J. (2014). Targeting cancer stem cells to suppress acquired chemotherapy resistance. *Oncogene*, *33*(36), 4451–4463. http://doi.org/10.1038/onc.2013.411

Waris, S., Wilce, M. C. J., & Wilce, J. A. (2014). RNA recognition and stress granule formation by TIA proteins. *International Journal of Molecular Sciences*, *15*(12), 23377–23388. http://doi.org/10.3390/ijms151223377

Wells, A., Griffith, L., Wells, J. Z., & Taylor, D. P. (2013). The dormancy dilemma: Quiescence versus balanced proliferation. *Cancer Research*, *73*(13), 3811–3816. http://doi.org/10.1158/0008-5472.CAN-13-0356

Whitehurst, A. W., Wilsbacher, J. L., You, Y., Luby-Phelps, K., Moore, M. S., & Cobb, M. H. (2002). ERK2 enters the nucleus by a carrier-independent mechanism. *Proceedings of the National Academy of Sciences of the United States of America*, *99*(11), 7496–501. http://doi.org/10.1073/pnas.112495999

Whitfield, M. L., George, L. K., Grant, G. D., & Perou, C. M. (2006). Common markers of proliferation. *Nature Reviews Cancer*, *6*(2), 99–106. http://doi.org/10.1038/nrc1802

Wilder, E. L. (2000). Ectopic expression in Drosophila. *Methods Mol. Biol.*, *137*, 9–14. http://doi.org/10.1385/1-59259-066-7:9

Will, C. L., & Lührmann, R. (2001). Spliceosomal UsnRNP biogenesis, structure and function. *Current Opinion in Cell Biology*, *13*(3), 290–301. http://doi.org/10.1016/S0955-0674(00)00211-8

Xu, D., Farmer, A., & Chook, Y. M. (2011). Recognition of nuclear targeting signals by Karyopherin-ß proteins. *Curr Opin Struct Biol*, *20*(6), 782–790. http://doi.org/10.1016/j.sbi.2010.09.008.Recognition

Yanagida, M. (2009). Cellular quiescence: are controlling genes conserved? *Trends in Cell Biology*, *19*(12), 705–715. http://doi.org/10.1016/j.tcb.2009.09.006

Zhang, Y. (2008). I-TASSER server for protein 3D structure prediction. *BMC Bioinformatics*, *9*, 40. http://doi.org/10.1186/1471-2105-9-40

Zhou, M., Li, W., Huang, S., Song, J., Kim, J., Tian, X., … Silva, A. (2013). mTOR Inhibition ameliorates cognitive and affective deficits caused by Disc1 knockdown in adult-born dentate granule neurons. *NeuronNeuron*, *77*(4), 647–654. http://doi.org/10.1016/j.neuroimage.2013.08.045.The

Zismanov, V., Chichkov, V., Colangelo, V., Jamet, S., Wang, S., Syme, A., … Crist, C. (2016). Phosphorylation of eIF2α is a Translational Control Mechanism Regulating Muscle Stem Cell Quiescence and Self-Renewal. *Cell Stem Cell*, *18*(1), 79–90. http://doi.org/10.1016/j.stem.2015.09.020

Appendix Table 1. Drosophila Stocks

Genotype	Origin
UAS-CG14712[RNAi]	VRDC 18347 GD
UAS-CG14712[RNAi]	BL-35622 GL00466
UAS-CG14712[RNAi]/CyO	NIG HMJ21299
UAS-drongo[RNAi]	VDRC 43763 GD
UAS-drongo[RNAi]	VDRC 109801 KK
UAS-drongo[RNAi]	BL-38960 HMS01874
UAS-drongo[RNAi]	BL-60891 HMJ22758
UAS-drongo[RNAi]	NIG 3365R-1
UAS-drongo[RNAi]/TM6,Sb,Dfd-YFP	NIG 3365R-2; Rebalanced
UAS-Nup50[RNAi]	VDRC 20824 GD
UAS-Nup50[RNAi]	VDRC 100564 KK
UAS-Nup50[RNAi]	BL-34580 HMS01054
UAS-Nup54[RNAi]	VDRC 42153 GD
UAS-Nup54[RNAi]	VDRC 42154 GD
UAS-Nup54[RNAi]	VDRC 103724 KK
UAS-Nup54[RNAi]	BL-57426 HMC04733
UAS-Nup58[RNAi]/TM6,Sb,Dfd-YFP	VDRC 40773 GD; Rebalanced
UAS-Nup58[RNAi]	VDRC 108016 KK
UAS-Nup58[RNAi]	BL-60110 HMC05104
UAS-Nup62[RNAi]/TM6,Sb,Dfd-YFP	VDRC 44806 GD; Rebalanced
UAS-Nup62[RNAi]	VDRC 44808 GD
UAS-Nup62[RNAi]	VDRC 100588 KK
UAS-Nup62[RNAi]	BL-35695 GLV21060
UAS-Nup62[RNAi]	BL-43189 GL01533
UAS-Nup62[RNAi]	BL-52927 HMC03668
UAS-Nup62[RNAi]	NIG 6251R-1
UAS-Nup62[RNAi]	NIG 6251R-2
UAS-Nup98-96[RNAi]	VDRC 31198 GD
UAS-Nup98-96[RNAi]	VDRC 31199 GD
UAS-Nup98-96[RNAi]	VDRC 109279 KK
UAS-Nup98-96[RNAi]/TM6,Sb,Dfd-YFP	BL-28562 HM05048; Rebalanced
UAS-Nup98-96[RNAi]/CyO,Dfd-YFP	NIG 10198R-1; Rebalanced
UAS-Nup98-96[RNAi]	NIG 10198R-3
UAS-Nup153[RNAi]	VDRC 47155 GD
UAS-Nup153[RNAi]	VDRC 107750 KK
UAS-Nup153[RNAi]	BL-30504 HM05248
UAS-Nup153[RNAi]	BL-32837 HMS00527
UAS-Nup214[RNAi]	VDRC 41964 GD
UAS-Nup214[RNAi]	BL-33897 HMS00837

UAS-Nup214[RNAi]	VDRC 330104
UAS-Nup358[RNAi]/CyO,Dfd-YFP	VDRC 38581 GD; Rebalanced
UAS-Nup358[RNAi]	VDRC 38583 GD
UAS-Nup358[RNAi]/TM6,Sb,Dfd-YFP	BL-33003 HMS00803; Rebalanced
UAS-Nup358[RNAi]	BL-34967 HMS00865
UAS-Nup358[RNAi]	NIG 11856R-1
UAS-CG16892[RNAi]	VDRC 23844 GD
UAS-CG16892[RNAi]	VDRC 101415 KK
UAS-CG16892[RNAi]	BL-51938 HMC03342
UAS-CG16892[RNAi]	BL-62286 HMJ23643
UAS-Ndc1[RNAi]	VDRC 3408 GD
UAS-Ndc1[RNAi]	VDRC 101264 KK
UAS-CG14215[RNAi]	VDRC 103547 KK
UAS-Rae1[RNAi]	VDRC 29302 GD
UAS-Rae1[RNAi]	VDRC 29303 GD
UAS-Rae1[RNAi]	VDRC 101338 KK
UAS-Rae1[RNAi]	BL-32882 HMS00670
UAS-Rae1[RNAi]	BL-57832 HMJ21842
UAS-Rae1[RNAi]	NIG 9862R-2
UAS-Rae1[RNAi]	NIG 9862R-3
UAS-Sec13[RNAi]	VDRC 50367 GD
UAS-Sec13[RNAi]	VDRC 110428 KK
UAS-Sec13[RNAi]	BL-32468 HMS00468
UAS-Sec13[RNAi]/CyO,Dfd-YFP	NIG 6773R-1; Rebalanced
UAS-sec13[RNAi]	NIG 6773R-3
UAS-Nup44A[RNAi]/TM6,Sb,Dfd-YFP	VDRC 40717 GD; Rebalanced
UAS-Nup44A[RNAi]/CyO,Dfd-YFP	VDRC 106489 KK; Rabalanced
UAS-Nup44A[RNAi]	BL-32942 HMS00736
UAS-Nup44A[RNAi]	BL-38357 HMS01825
UAS-Nup44A[RNAi]/CyO,Dfd-YFP	NIG 8722R-1; Rebalanced
UAS-Nup44A[RNAi]/CyO,Dfd-YFP	NIG 8722R-3; Rebalanced
UAS-Mtor[RNAi]	VDRC 24265 GD
UAS-Mtor[RNAi]	VDRC 110218 KK
UAS-Mtor[RNAi]	BL-32941 HMS00735
UAS-Mtor[RNAi]/CyO,Dfd-YFP	NIG 8274R-2; Rebalanced
UAS-Mtor[RNAi]	Mendjan et al. 2006 Mol Cell 21:811-23
UAS-Nup35[RNAi]	NIG 6540R-1
UAS-Nup35[RNAi]/CyO,Dfd-YFP	NIG 6540R-4; Rebalanced
UAS-Nup37[RNAi]	VDRC 16342 GD
UAS-Nup37[RNAi]	VDRC 109814 KK
UAS-Nup37[RNAi]/CyO,Dfd-YFP	BL-62328 HMJ23685;

	Rebalanced
UAS-Nup37[RNAi]	NIG 11875R-2
UAS-Nup43[RNAi]/CyO,Dfd-YFP	VDRC 33645 GD; Rebalanced
UAS-Nup43[RNAi]	VDRC 108595 KK
UAS-Nup43[RNAi]/CyO,Dfd-YFP	NIG HMJ21643; Rebalanced
UAS-Nup43[RNAi]	NIG 7671R-1
UAS-Nup43[RNAi]	NIG 7671R-4
UAS-Nup75[RNAi]	VDRC 27495 GD
UAS-Nup75[RNAi]	BL-28315 JF02946 TRiP (attP2)
UAS-Nup75[RNAi]/TM6,Sb,Dfd-YFP	NIG 5733R-1 Rebalanced
UAS-Nup75[RNAi]/CyO,Dfd-YFP	NIG 5733R-2; Rebalanced
UAS-mbo[RNAi]	VDRC 22446 GD
UAS-mbo[RNAi]	VDRC 47691 GD
UAS-mbo[RNAi]	VDRC 47692 GD
UAS-mbo[RNAi]	VDRC 47693 GD
UAS-mbo[RNAi]/CyO,Dfd-YFP	NIG 6819R-2; Rabalanced
UAS-mbo[RNAi]	NIG 6819R-3
UAS-Nup93-1[RNAi]/TM6,Sb,Dfd-YFP	VDRC 16189 GD; Rebalanced
UAS-Nup93-1[RNAi]	VDRC 100315 KK
UAS-Nup93-1[RNAi]	BL-33908 HMS00850
UAS-Nup93-1[RNAi]	TRiP (attP2)
UAS-Nup93-1[RNAi]/TM6,Sb,Dfd-YFP	BL-31196 JF01712 (attP2)
UAS-Nup93-2[RNAi]	VDRC 22552 GD
UAS-Nup93-2[RNAi]	BL-51758 HMC03310
UAS-Nup107[RNAi]	VDRC 22407 GD
UAS-Nup107[RNAi]	VDRC 110759 KK
UAS-Nup133[RNAi]	VDRC 110194 KK
UAS-Nup133[RNAi]/CyO;Dfd-YFP	BL-58290 HMJ22393; Rebalanced
UAS-Nup154[RNAi]	VDRC 21878 GD
UAS-Nup154[RNAi]	VDRC 106136 KK
UAS-Nup154[RNAi]	BL-34710 HMS01189
UAS-Nup154[RNAi]	NIG 4579R-2
UAS-Nup154[RNAi]/CyO,Dfd-YFP	NIG 4579R-3; Rebalanced
UAS-Nup160[RNAi]	VDRC 21937 GD
UAS-Nup160[RNAi]	VDRC 109318 KK
UAS-Nup160[RNAi]	BL-32391 HMS00385
UAS-Nup160[RNAi]	NIG 4738R-2
UAS-Nup160[RNAi]	NIG 4738R-3
UAS-Nup188[RNAi]	VDRC 102650 KK
UAS-Nup188[RNAi]	VDRC 36023 GD
UAS-Nup188[RNAi]/CyO,Dfd-YFP	NIG HMJ22993 TRiP; Rebalanced

UAS-Nup188[RNAi]	NIG 8771R-3
UAS-Nup188[RNAi]	NIG 8771R-4
UAS-Nup205[RNAi]	VDRC 38608 GD
UAS-Nup205[RNAi]	VDRC 38610 GD
UAS-Nup205[RNAi]	NIG 11943R-1
UAS-Nup205[RNAi]/CyO,Dfd-YFP	NIG 11943R-2; Rebalanced
UAS-ran[RNAi]/TM6,Sb,Dfd-YFP	BL-44587 HMS02885; Rebalanced
UAS-ran[RNAi]/CyO,Dfd-YFP	BL-42482 GL01341; Rebalanced
UAS-ran[RNAi]	BL-31392 JF01381
UAS-ran[RNAi]	NIG 1404R-2
UAS-ran[RNAi]/TM6,Sb,Dfd-YFP	NIG 1404R-5; Rebalanced
UAS-ran[RNAi]	VDRC 24835 GD
UAS-ran[RNAi]/CyO,Dfd-YFP	VDRC 104417 KK; Rebalanced
UAS-ranGAP[RNAi]/TM6,Sb,Dfd-YFP	BL-29565 JF03244; Rebalanced
UAS-ranGAP[RNAi]/TM6,Sb,Dfd-YFP	VDRC 30568 GD; Rebalanced
UAS-ranGAP[RNAi]	VDRC 108264 KK
UAS-ranGAP[RNAi]/TM6,Sb,Dfd-YFP	NIG 9999R-1; Rebalanced
UAS-Rcc1[RNAi]/CyO,Dfd-YFP	NIG HMJ21881
UAS-Rcc1[RNAi]	BL-36067 GL00485
UAS-Rcc1[RNAi]/TM6,Sb,Dfd-YFP	VDRC 38388 GD; Rebalanced
UAS-Rcc1[RNAi]	VDRC 38389 GD
UAS-Rcc1[RNAi]	VDRC 110321 KK
UAS-Rcc1[RNAi]	NIG 10480R-1
UAS-Rcc1[RNAi]/TM6,Sb,Dfd-YFP	NIG 10480R-2; Rebalanced
UAS-tamo[RNAi]	VDRC 21780 GD
UAS-tamo[RNAi]	VDRC 106015 KK
UAS-tamo[RNAi]	NIG 4057R-2
UAS-tamo[RNAi]	NIG 4057R-3
UAS-CG14718[RNAi]/TM6,Sb,Dfd-YFP	BL-38331 HMS01798; Rebalanced
UAS-CG14718[RNAi]/CyO,Dfd-YFP	BL-39018 HMS01936; Rebalanced
UAS-CG14718[RNAi	VDRC 32311 GD
UAS-CG14718[RNAi]/TM6,Sb,Dfd-YFP	VDRC 32312 GD; Rebalanced
UAS-CG14718[RNAi]	VDRC 39702 GD
UAS-CG14718[RNAi]	VDRC 105543 KK
UAS-CG14718[RNAi]/TM6,Sb,Dfd-YFP	NIG 14718R-1; Rebalanced
UAS-CG14718[RNAi]/CyO,Dfd-YFP	NIG 14718R-2; Rebalance
UAS-RanBP3[RNAi]	BL-40948 HMS02196
UAS-RanBP3[RNAi]	VDRC 38363 GD

UAS-RanBP3[RNAi]	VDRC 104432 KK
UAS-RanBP3[RNAi]	NIG 10225R-4
UAS-Kap-α1[RNAi]	BL-27523 JF02673
UAS-Kap-α1[RNAi]/CyO,Dfd-YFP	VDRC 28920 GD; Rebalanced
UAS-Kap-α1[RNAi]/CyO,Dfd-YFP	VDRC 28921 GD; Rebalanced
UAS-Kap-α1[RNAi]	VDRC 108741 KK
UAS-Kap-α1[RNAi]/CyO,Dfd-YFP	NIG 8548R-2; Rebalanced
UAS-Kap-α1[RNAi]	NIG 8548R-3
UAS-Kap-α4[RNAi]	BL-31640 JF01429
UAS-Kap-α4[RNAi]	VDRC 27265 GD
UAS-Kap-α4[RNAi]	VDRC 27266 GD
UAS-Kap-α4[RNAi]	VDRC 108143 KK
UAS-Kap-α4[RNAi]	NIG 10478R-1
UAS-Kap-α4[RNAi]	NIG 10478R-4
UAS-pen[RNAi]	BL-43142 GL01483
UAS-Pen[RNAi]	BL-27692 JF02772
UAS-Pen[RNAi]	VDRC 34265 GD
UAS-Pen[RNAi]	VDRC 34266 GD
UAS-Pen[RNAi]	VDRC 102627 KK
UAS-Pen[RNAi]	NIG 4799R-1
UAS-Pen[RNAi]	NIG 4799R-3
UAS-Kap-α3[RNAi]	BL-27535 JF02686
UAS-Kap-α3[RNAi]	VDRC 36103 GD
UAS-Kap-α3[RNAi]	VDRC 36104 GD
UAS-Kap-α3[RNAi]	VDRC 106249 KK
UAS-Karyβ3[RNAi]/CyO,Dfd-YFP	VDRC 39713 GD; Rebalanced
UAS-Karyβ3[RNAi]	VDRC 105602 KK
UAS-Karyβ3[RNAi]/TM6,Sb,Dfd-YFP	NIG 1059R-2; Rebalanced
UAS-Karyβ3[RNAi]/CyO,Dfd-YFP	NIG 1059R-4; Rebalanced
UAS-cse[RNAi]	BL-28337 JF02972
UAS-cse[RNAi]	BL-31195 JF01711
UAS-cse[RNAi]	VDRC 12647 GD
UAS-cse[RNAi]	VDRC 12648 GD
UAS-cse[RNAi]	VDRC 110215 KK
UAS-Ket[RNAi]	BL-27567 JF02721
UAS-Ket[RNAi]	BL-31242 JF01755
UAS-Ket[RNAi]/TM6,Sb,Dfd-YFP	BL-41845 GL01273; Rebalanced
UAS-Ket[RNAi]/TM6,Sb,Dfd-YFP	BL-44576 HMS02872; Rebalanced
UAS-Ket[RNAi]	VDRC 22348 GD
UAS-Ket[RNAi]	VDRC 107622 KK
UAS-Ket[RNAi]/CyO,Dfd-YFP	NIG 2637R-1; Rebalanced

UAS-Ket[RNAi]/CyO,Dfd-YFP	NIG 2637R-3; Rebalanced
UAS-msk[RNAi]	BL-27572 JF02727
UAS-msk[RNAi]/TM6,Sb,Dfd-YFP	BL-33626 TRiP HMS00020; Rebalanced
UAS-msk[RNAi]	BL-34998 HMS01408
UAS-msk[RNAi]	BL-35598 GL00435
UAS-msk[RNAi]	VDRC 38963 GD
UAS-msk[RNAi]	VDRC 108415 KK
UAS-cdm[RNAi]	BL-31639 JF01428
UAS-cdm[RNAi]	BL-44551 HMS02846
UAS-cdm[RNAi]	VDRC 40436 GD
UAS-cdm[RNAi]/CyO,Dfd-YFP	NIG 7212R-2; Rebalanced
UAS-CG32164[RNAi]	BL-28692 JF03108
UAS-CG32164[RNAi]	BL-60487 HMJ22881
UAS-CG32164[RNAi]	VDRC 34422 GD
UAS-CG32164[RNAi]	VDRC 109183 KK
UAS-CG32164[RNAi]/CyO,Dfd-YFP	NIG 32164R-1; Rebalanced
UAS-CG32164[RNAi]	NIG 32164R-2
UAS-CG32165[RNAi]	VDRC 49306 GD
UAS-CG32165[RNAi]	VDRC 49307 GD
UAS-CG32165[RNAi]	VDRC 109561 KK
UAS-RanBP9[RNAi]	BL-33004 HMS00804
UAS-RanBP9[RNAi]	BL-33005 HMS00805
UAS-RanBP9[RNAi]	VDRC 27383 GD
UAS-RanBP9[RNAi]/TM6,Sb,Dfd-YFP	VDRC 27384 GD; Rebalanced
UAS-RanBP9[RNAi]	VDRC 110236 KK
UAS-RanBP11[RNAi]/CyO,Dfd-YFP	BL-58311 HMJ22418; Rebalanced
UAS-RanBP11[RNAi]	BL-55142 HMC03738
UAS-RanBP11[RNAi]	VDRC 44731 GD
UAS-RanBP11[RNAi]	VDRC 110496 KK
UAS-RanBP16[RNAi]/CyO,Dfd-YFP	NIG HMJ21402; Rebalanced
UAS-RanBP16[RNAi]	VDRC 107391 KK
UAS-RanBP21[RNAi]	VDRC 31706 GD
UAS-RanBP21[RNAi]	VDRC 31707 GD
UAS-RanBPM[RNAi]	BL-61172 HMC05142
UAS-RanBPM[RNAi]	VDRC 45981 GD
UAS-emb[RNAi]	BL-31353 JF01311
UAS-emb[RNAi]	BL-34021 HMS00991
UAS-emb[RNAi]	VDRC 3347 GD
UAS-emb[RNAi]	VDRC 103767 KK
UAS-emb[RNAi]	NIG 13387R-1
UAS-emb[RNAi]	NIG 13387R-4
UAS-CG10950[RNAi]	VDRC 41460 GD

UAS-CG10950[RNAi]	VDRC 41462 GD
UAS-ebo[RNAi]	BL-32347 HMS00338
UAS-ebo[RNAi]	VDRC 34737 GD
UAS-TRN[RNAi]	BL-27546 JF02697
UAS-TRN[RNAi]	BL-61230 HMJ23009
UAS-TRN[RNAi]/TM6,Sb,Dfd-YFP	BL-50732 HMS02968; Rebalanced
UAS-TRN[RNAi]	VDRC 6543 GD
UAS-TRN[RNAi]	VDRC 6544 GD
UAS-TRN[RNAi]	VDRC 30066 GD
UAS-TRN[RNAi]	VDRC 105181 KK
UAS-TRN[RNAi]	NIG 7398R-1
UAS-CG8219[RNAi]	VDRC 24245 GD
UAS-CG8219[RNAi]	VDRC 103487 KK
UAS-CG8219[RNAi]	NIG 8219R-1
UAS-CG8219[RNAi]	NIG 8219R-2
UAS-Trn-SR[RNAi]	BL-25988 JF02010
UAS-Trn-SR[RNAi]	BL-56974 HMC04414
UAS-Trn-SR[RNAi]	VDRC 33569 GD
UAS-Trn-SR[RNAi]	VDRC 33571 GD
UAS-Trn-SR[RNAi]	NIG 2848R-1
UAS-Trn-SR[RNAi]	NIG 2848R-2
Df(3R)Exel6276/TM6B,Sb,Dfd-YFP	BL-7743; Rebalanced
FRT82B,2V327,nab-GAL4/TM6B,Sb,Dfd-YFP	R. Sousa Nunes
FRT82B?,2V327,nab-GAL4/TM6B,Sb,Dfd-YFP	A. Coum
FRT82B?,2V327,da-GAL4/TM6B,Sb,Dfd-YFP	A. Coum
UAS-CG14712/(CyO); +/(TM6B)	15467-2-2M
UAS-CG14712/(CyO); +/(TM6B)	15467-2-3M
+/(CyO); UAS-CG14712/TM6B	15467-2-5M
+/(CyO); UAS-CG14714/(TM6B)	15467-2-8M
UAS-V::CG14712 (CyO) (TM6B)	15467-1-1M
UAS-V::CG14712/(TM6B)	15467-1-2M
UAS-V::CG14712/(CyO); +/(TM6B)	15467-1-3M
UAS-V::CG14712 (CyO) (TM6B)	15467-1-6M
+/(CyO); UAS-V::CG14712/TM6B	15467-1-7M
UAS-V::CG14712/(CyO); +/(TM6B)	15467-1-8M
+/(CyO); UAS-V::CG14712/(TM6B)	15467-1-9M
UAS-V::CG14712/(CyO);+/(TM6B)	15467-1-10M
grh-GAL4	A. Brand
grh-GAL4,UAS-CD8::GFP	R. Sousa Nunes
nab-GAL4/(TM6B,Sb,Dfd-YFP)	NP4607; Rebalanced
nab-GAL4,UAS-CD8::GFP/(TM6B)	R. Sousa Nunes
w;tub-GAL80[ts];nab>CD8::GFP	R. Sousa Nunes
nab>Dcr-2	R. Sousa Nunes
tub-GAL80[ts];nab>Dcr2	R. Sousa Nunes

UAS-insc::GFP[2-1],UAS-insc::GFP[4-3];nabGAL4/(TM6B,Sb,Dfd-YFP)	R. Sousa Nunes
hs-FLP[1.22],UAS-GFP::Myc::NLS; tub-GAL4,FRT42D,tubP-GAL80[LL10]	G. Struhl
w;UAS-RedStinger-NLS/CyO,Fdf-YFP	BL-8546; Rebalanced
UAS-NLS2::RFP	BL-38425
UAS-NLS2::GFP	I. Salecker
UAS-NLS5::GFP	P. Pachnis
w;UAS-cycE[RNAi]	BL-29314 JF02473
UAS-cdk1[RNAi]	VDRC 41838 GD
UAS-cycA[RNAi]	VDRC 32421 GD